The Application of Symmetry Concepts
to
Physical Problems II (contd)
Analysis of Hyperfine structure in Crystals

B. G. Wybourne

The only questions worth asking are the unanswerable ones
— John Ciardi *Saturday Review-World (1973)*

■ Lecture 1

■ 1.1 Nature of the Problem

In this semester I want us to use the knowledge gained in earlier lectures to analyse a particular problem in solid state physics, namely the interpretation of nuclear hyperfine structure in a crystalline environment. The specific system we shall analyse will be the high resolution optical spectrum of a $LiYF_4 : Ho$ crystal. Extensive experimental work has been done on this system by M. N. Popova and her associates in the Institute of Spectroscopy, in the Russian Academy of Sciences, Troitsk, Moscow. The chief papers containing the data are:-

1. N. I. Agladze and M. N. Popova, *Hyperfine Structure in Optical Spectra of* $LiYF_4 : Ho$, Sol. St. Comm. **55** 1097-1100(1985)
2. N. I. Agladze, E. A. Vinogradov and M. N. Popova, *Manifestation of quadrupole hyperfine interaction and of interlevel interaction in the optical spectrum of the* $LiYF_4 : Ho$ *crystal* Sov. Phys. JETP **64** 716-720 (1986)
3. N. I. Agladze etal, *Isotope Structure in Optical Spectra of* $LiYF_4 : Ho^{3+}$ Phys. Rev. Lett. **66** 477-480 (1991)
4. N. I. Adgladze etal, *Study of isotope composition in crystals by high resolution spectroscopy of monoisotope impurity* JETP **76** 1110-1113 (1993)
5. N. I. Agladze etal, *Isotope effects in the lattice structure and vibrational and optical spectra of* ${}^6Li_x^7Li_{1-x}YF_4 : Ho$ *crystals* JETP **77** 1021-1033 (1993)

Holmium occurs in nature as a single stable isotope, ${}^{165}_{67}Ho$, with a groundstate nuclear angular momentum of $I = \frac{7}{2}$. The trivalent ion, Ho^{3+} substitutes for the Y^{3+} ion at sites of tetragonal symmetry (S_4 point group) in $LiYF_4$ crystals. The Holmium nucleus interacts with the electrons via the nuclear magnetic dipole and electric quadrupole moments. For a holmium ion in free space the total angular momentum F is the vector sum of the nuclear angular momentum I and the electron angular momentum J and is a conserved quantity. The coupling of the angular momentum is

$$\mathbf{F} = \mathbf{J} + \mathbf{I} \tag{1.1}$$

with

$$F = J + I, J + I - 1, \ldots, |J - I| \tag{1.2}$$

and as a result for those states with $J \geq I$ we obtain $(2I + 1)$ hyperfine sublevels associated with each

level of the atom with electronic angular momentum J and for states with $I > J$ $2J+1$ sublevels. Thus for an electronic state with $J = 8$ and a nucleus with angular momentum $I = \frac{7}{2}$ we would expect a hyperfine pattern for a free ion to be like below

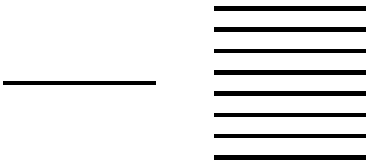

In free space the total angular momentum F is a conserved quantity but the electronic angular momentum J need not be. For a nucleus with $I = 0$ the electronic angular momentum J remains a conserved quantity as there is then no coupling between the nuclear and electronic moments.

Placing the ion in a crystalline environment changes things considerably. Ignoring the hyperfine interaction for the moment, the electronic angular momentum J and its projection M_J are no longer good quantum numbers. The $2J+1$-fold degeneracy of the free ion levels is lifted and the levels are seen to split due to the electric fields in the crystalline environment. The number of sub-levels (Stark levels) and their residual degeneracies are determined from a knowledge of the appropriate $SO(3) \rightarrow G$ branching rules where G is the point group symmetry of the ion site in the crystal, in our case S_4. The various sub-levels can be labelled by the irreducible representations of the group G.

Including the interaction of the nuclear moments with the electronic moments leads to the appearance of hyperfine structure superimposed on the Stark sub-levels. The quantum numbers F and M_F are no longer conserved. The multitude of hyperfine sub-levels will have degeneracies appropriate to the irreducible representations of the group G. If J is an integer and I a half-integer then the irreducible representations will be appropriate to the spin or double group of G. This further means that selection rules deduced for transitions between Stark sub-levels neglecting the hyperfine interaction will be different from those deduced by there inclusion.

The problem we shall tackle in this course will be to understand the experimental data relating to the observations given in the five papers referenced earlier. We would like to understand the splittings of the hyperfine structure and the relative intensities of transitions. To that end we will follow a definite plan of action - solving problems as they arise.

■ 1.2 Outline of the proposed plan of action

My approach to the problem will involve the following steps:-

A. **The zero-order problem**

B. **The spectroscopic terms for** Ho^{3+}

C. **Properties of the Hund's rule groundstate**

D. **Calculation of the Stark splittings**

E. **Calculation of hyperfine interactions**

F. **Calculation of intensities of transitions**

■ 1.3 The zero-order problem

Only in very special cases can we write down a Hamiltonian for a system and solve the quantum equations exactly. Examples of these special cases include one-electron hydrogenic atoms. Note even when we say "*an exact solution*" we really mean an exact solution of a model system. For any real system our solutions can only be approximate. In some cases the solutions may apply to a system, such as, for example, a relativistic hydrogen atom with astonishing precision while for a rare earth atom with ~ 60 electrons we cannot expect to attain anything like the same precision.

For an $N-$electron atom we may write the Hamiltonian, H, as

$$\mathrm{H} = \sum_{i=1}^{N} \left[\mathbf{p}_i^2 - \frac{Ze^2}{r_i} + \zeta(r_i)(\mathbf{s}\cdot\mathbf{l})_i \right] + \sum_{i>j} \frac{e^2}{r_{ij}} + \ldots \tag{1.3}$$

The first term represents the kinetic energy of the electrons, the second the Coulomb attraction between

the positively charge nucleus of atomic number Z and the $i-th$ electron, the third the spin-orbit coupling, and the fourth term the Coulomb repulsion between pairs of electrons. The ... are there to remind us that there may be many other terms such as internal, or external, magnetic or electric fields, hyperfine interactions coupling the nuclear magnetic or electric quadrupole moments to the electrons, crystal fields and a multitude of relativistic effects etc. Furthermore, we are assuming, for the moment that the nucleus is an infinitely massive point object which means that we ignore mass isotope effects and finite nuclear size effects.

Given the above Hamiltonian we wish to solve the eigenvalue equation

$$\mathrm{H}\Psi = \mathrm{E}\Psi \tag{1.4}$$

This deceptively simple equation is incapable of exact solution, or even near exact solution for nearly all atoms. We seek to solve a simpler problem and then proceed to use perturbation theory.

■ 1.4 Central Field approximation

In order to simplify our problem let us assume each electron moves independently of the other electrons in a spherically averaged central field potential $-\mathrm{U}(r_i)/e$ with a zero-order Hamiltonian, H_0,

$$\mathrm{H}_0 = \sum_{i=1}^{N} \left[\frac{\mathbf{p}_i^2}{2m} + \mathrm{U}(r_i) \right] \tag{1.5}$$

with

$$\mathrm{H}' = \sum_i \left[-\frac{Ze^2}{r_i} - \mathrm{U}(r_i) \right] + \sum_{i>j} \frac{e^2}{r_{ij}} + \sum_i \zeta(r_i)(\mathbf{s}\cdot\mathbf{l})_i + \ldots \tag{1.6}$$

To proceed we first solve the much simpler central field equation

$$\mathrm{H}_0\Psi_0 = \mathrm{E}_0\Psi_0 \tag{1.7}$$

This equation can be separated using a set of functions $\psi(\alpha_i)$ such that

$$\Psi_0 = \prod_{i=1}^{N} \psi_i(\alpha_i) \quad \text{and} \quad \mathrm{E}_0 = \sum_{i=1}^{N} \varepsilon_i(\alpha_i) \tag{1.8}$$

leading to equations of the general form

$$\left[\frac{\mathbf{p}^2}{2m} + U(r) \right] \psi(\alpha) = \varepsilon(\alpha)\psi(\alpha) \tag{1.9}$$

This equation may be separated in spherical coordinates (r, θ, ϕ) by writing

$$\psi(\alpha) = \frac{\mathrm{R}_{n\ell}(r)\mathrm{Y}_{\ell m_\ell}(\theta,\phi)}{r} \tag{1.10}$$

with the usual definition of the spherical harmonics as

$$Y_{\ell m_\ell}(\theta,\phi) = (-1)^{m_\ell} \sqrt{\frac{2\ell+1)(l-m_\ell)!}{4\pi(\ell+m_\ell)!}} \mathrm{P}_\ell^{m_\ell}(cos\theta) \exp^{im_\ell\phi} \tag{1.11}$$

with

$$P_\ell^{m_\ell}(z) = \frac{(1-z^2)^{\frac{m_\ell}{2}}}{2^\ell \ell!} \frac{d^{\ell+m_\ell}}{dz^{\ell+m_\ell}} (z^2-1)^\ell \tag{1.12}$$

Whereas the radial function $\mathrm{R}_{n\ell}(r)$ depends explicitly upon the central field potential $\mathrm{U}(r)$ the angular part $\mathrm{Y}_{\ell m_\ell}(\theta,\phi)$ is exactly the same as that for a hydrogenic atom. Each electron carries a spin $s = \frac{1}{2}$ with spin projection $m_s = \pm\frac{1}{2}$ and hence we should augment the orbital eigenfunctions of Eq.(1-8) with a two-component spinor $\chi(s, m_s)$ to give a complete spin-orbital eigenfunction

$$\psi(\alpha) = \frac{\mathrm{R}_{n\ell}(r)\mathrm{Y}_{\ell m_\ell}(\theta,\phi)}{r} \chi(s, m_s) \tag{1.13}$$

where now

$$\alpha \equiv (n\ell m_\ell s m_s) \tag{1.14}$$

describes a set of five quantum numbers associated with the state of a particular electron in the central field approximation (for the moment we suspend discussion of the identity of electrons).

■ 1.5 Electron Configurations

Note that the one-electron energies $\varepsilon_{n\ell}$ depend only on the quantum number pair $n\ell$ and hence the sequence of quantum numbers

$$n_1\ell_1, n_2\ell_2, \ldots, n_N\ell_N \tag{1.15}$$

define an *electron configuration*. Within the central field approximation the states associated with the same sequence of $n\ell$ quantum numbers, and hence electron configuration, are degenerate in energy. Different electron configurations have different energy eigenvalues. As is usual in designating a particular electron configuration we will normally suppress the quantum numbers associated with closed shells and will thus often refer to configurations giving just such as are necessary for clarity e.g. $3d^x$ (the 3d transition ions) or $4f^x$ (the lanthanide ions) with multiple occupation of an orbital being indicated by a superscript.

■ 1.6 Single Configuration Approximation

The lowest energy configuration is the *ground configuration*. In neutral atoms there are often several electron configurations competing for lowest energy. Thus in the neutral $3d$ transition metal atoms the $3d^N$, $3d^{N-1}4s$ and $3d^{N-2}4s^2$ are usually energetically close and strongly interacting. In that case we have *configuration mixing* occurring. A similar situation arises in the neutral lanthanides. As the ionisation of atoms increases the low lying electron configurations tend to become energetically separated from one another and the lowest states of the ion may be well characterised by those of a single configuration. Thus the low lying states of the doubly charged transition ions are well characterised by a single $3d^N$ ($N = 1, 2, \ldots, 10$) configuration and those of the triply ionised lanthanides by a single $4f^N$ ($N = 1, 2, \ldots, 14$). In much of our work we shall assume a single configuration approximation though, as we shall see later, there are important phenomena such as intensities of transitions in solid state materials where such an assumption must abandoned.

■ 1.7 Madelung's rules and the lanthanides

According to Madelung the electron orbitals associated with the ground configuration are filled in order of increasing $n + \ell$ and for a given value of $n + \ell$ in order of decreasing ℓ as indicated below.

$n + \ell$	orbitals $n\ell$	orbital degeneracy	total no. electrons
1	$1s$	2	2
2	$2s$	2	4
3	$2p, 3s$	8	12
4	$3p, 4s$	8	20
5	$3d, 4p, 5s$	18	38
6	$4d, 5p, 6s$	18	56
7	$4f, 5d, 6p, 7s$	32	88

Madelung's rules give a surprisingly accurate account of the broad features of the chemical periodic table. The lanthanides cover the elements from $Z = 57$ to 71 corresponding to the elements

57	58	59	60	61	62	63	64	65	66	67	68	69	70	71
La	Ce	Pr	Nd	Pm	Sm	Eu	Gd	Tb	Dy	Ho	Er	Tm	Yb	Lu

In solid state physics we usually encounter the lanthanides in the trivalent state and compared with the neutral lanthanide atoms have given up three electrons. Maria Goeppert-Mayer studied the behaviour of the $4f-$orbitals as a function of atomic number in terms of the Fermi wavefunction approximation and observed that the $4f-$orbitals exhibited a strong contraction with the result that the charge density of the $4f-$orbitals was concentrated inside the filled $5p^6 6s^2$ shell. This *lanthanide contraction* results in the $4f-$orbitals being largely shielded from external fields and hence their interaction with the environment is significantly reduced compared with that for the transition elements associated with the filling of $d-$orbitals. For the trivalent lanthanide ions we are led to the electron configurations $4f^N$ with $N = 0$

to 14, apart from closed shells, as indicated below

Lanthanide	Electron Configuration
Lanthanum	$4f^0$
Cerium	$4f^1$
Praseodymium	$4f^2$
Neodymium	$4f^3$
Promethium	$4f^4$
Samarium	$4f^5$
Europium	$4f^6$
Gadolinium	$4f^7$
Terbium	$4f^8$
Dysprosium	$4f^9$
Holmium	$4f^{10}$
Erbium	$4f^{11}$
Thulium	$4f^{12}$
Ytterbium	$4f^{13}$
Lutecium	$4f^{14}$

NB. The element Promethium has no stable isotopes and is a man-made element. Holmium is associated with the $4f^{10}$ configuration.

■ 1.8 Classification of the states of the $4f^N$ configurations

To proceed further it is necessary to determine the possible SL terms associated with a given $4f^N$ configuration. We first note that an orbital ℓ has $4\ell+2$ $m_s m_\ell$ states and they can be taken as a basis for spanning the vector irreducible representation $\{1\}$ of the unitary group in $4\ell+2$ dimensions, i.e. for the $f-$orbital the group U_{14}. The states of an $N-$equivalent electron configuration must be totally antisymmetric and span the representation $\{1^N\}$ of $U_{4\ell+2}$. The number of possible $SLM_S M_L$ states for the configuration ℓ^N will be just the dimension of the irreducible representation $\{1^N\}$ of $U_{4\ell+2}$. This number is just the binomial coefficient

$$\begin{pmatrix} 4\ell+2 \\ N \end{pmatrix} = \frac{4\ell+2!}{N!4\ell+2-N!} \tag{1.16}$$

We note that the binomial coefficient is symmetric with respect to $N \rightarrow 4\ell+2-N$ which leads to the conclusion that the number of $SLM_S M_L$ states for the configurations ℓ^N and $\ell^{4\ell+2-N}$ for $N \geq 2\ell+1$. Furthermore, we may show that the SL terms that arise in the configurations ℓ^N and $\ell^{4\ell+2-N}$ are identical. Figuratively speaking, this amounts to saying that SL terms associated with N holes in a shell of equivalent electrons are the same as for N electrons. Thus the SL terms for the ground configuration of triply ionised promethium $(4f^4)$ and holmium $(4f^{10})$ are identical and hence it suffices to enumerate just the SL terms associated with $N=1$ to $N=2\ell+1$. We shall refer to the special case of $N=2\ell+1$ as the *half-filled shell* and is associated with distinctive properties not shared by the other configurations of the given shell.

A deeper classification of the states of the $f-$shell follows by consideration of the subgroup structure of the group U_{14} and the branching rules for the decomposition of the antisymmetric irreducible representations $\{1^N\}$ under restriction to the transformations of these subgroups. The spin and orbital spaces can be split by considering the subgroup $U_{14} \supset SU_2 \times SU_7$ where we regard the spin states as spanning irreducible representations of the special unitary group SU_2 and the orbital states as spanning irreducible representations of the special unitary group SU_7. Recall that for a single $f-$orbital there are two spin states and seven orbital states.

Algorithms for the various group-subgroup branching rules required have been developed in the references given below:-

6. B. G. Wybourne, *Symmetry Principles in Atomic Spectroscopy*, New York: Wiley, (1970)
7. R. C. King, *Branching rules for the classical Lie groups using tensor and spinor methods*, J. Phys. A: Math. Gen. **8**, 429-449 (1975)

8. G. R. E. Black, R. C. King and B. G. Wybourne, *Kronecker produst for compact semisimple Lie groups*, J. Phys. A: Math. Gen. **16**, 1555-1589 (1983)

9. G. R. E. Black and B. G. Wybourne, *Branching rules and even-dimensional rotation groups*, J. Phys. A: Math. Gen. **16**, 2405-2421 (1983)

and have been implemented in SCHUR. A complete list of the branching rules available in SCHUR is given in Table 1.1 as shown on page 160 of the SCHUR User's Manual where complete instructions are given for using SCHUR. The branching rule we want is for $U_{14} \Rightarrow SU_2 \times SU_7$. We do not find this rule listed in Table 1.1 but we do see Rule No. 9 for $U_{mn} \Rightarrow U_m \times U_n$.

The following sequence of commands in SCHUR will produce the desired results:

```
  DP>
⇒gr u14
  Group is U(14)
  DP>
⇒br9,2,7gr1[1^]
  Groups are U(2)*U(7)
  {4}{1^4} + {31}{21^2} + {2^2}{2^2}
  DP>
⇒gr2su2su7
  Groups are SU(2) *SU(7)
⇒std last
  DP>
  {4}{1^4} + {2}{21^2} + {0}{2^2}
  DP>
```

Recall that the irreducible representations of U_n involve partitions in up to n parts. These irreducible representations remain irreducible upon restriction to SU_n except that irreducible representations involving n parts become equivalent to irreducible representations of SU_n involving at most $n-1$ parts such that

$$\{\lambda_1, \lambda_2, \ldots, \lambda_n\} \equiv \{\lambda_1 - \lambda_n, \lambda_2 - \lambda_n, \ldots, 0\} \tag{1.17}$$

Thus under $U_2 \Rightarrow SU_2$ we have

$$\{2^2\} \equiv \{0\}, \quad \{31\} \equiv \{2\}$$

Furthermore, the irreducible representations of SU_2 are locally isomorphic to those of SO_3 so that

$$\{a\} \sim [\frac{a}{2}] \tag{1.18}$$

The irreducible representations of SO_3 are termed *tensor* irreducible representations if a is *even* or *spin* irreducible representations if a is *odd*. The angular momentum associated with a SO_3 irreducible representation $[S]$ is just S where S is an integer or half-integer. The entire branching rule for $U_{14} \Rightarrow SO_3 \times SU_7$ can be accomplished in SCHUR by writing and running the following function where as usual input is indicated by an arrow $->$

Table 1.1 The branching rule table.

Rule No.	Group		Subgroup
1 :	U_n	$\Rightarrow$	O_n
2 :	U_n	$\Rightarrow$	Sp_n
3 :	U_n	R	U_{n-1}
4 :	O_n	$\Rightarrow$	S_n
5 :	O_n	$\Rightarrow$	S_{n+1}
6 :	U_n	$\Rightarrow$	SO_3
7 :	SO_n	$\Rightarrow$	SO_3 $\quad (n\ odd)$
8 :	Sp_n	$\Rightarrow$	SO_3 $\quad (n\ even)$
9 :	U_{mn}	$\Rightarrow$	$U_m \times U_n$
10 :	SO_{m+n}	$\Rightarrow$	$SO_m \times SO_n$
11 :	SO_n	$\Rightarrow$	$U_1 \times SU_k \quad n = 2k$
12 :	Sp_n	$\Rightarrow$	$U_1 \times SU_k \quad n = 2k$
13 :	Sp_n	$\Rightarrow$	$SU_2 \times SO_k \quad n = 2k$
14 :	S_{m+n}	$\Rightarrow$	$S_m \times S_n$
15 :	SO_4	$\Rightarrow$	$SU_2 \times SU_2$
16 :	SU_{m+n}	$\Rightarrow$	$U_1 \times SU_m \times SU_n$
17 :	$SU_{m/n}$	$\Rightarrow$	$U_1 \times SU_m \times SU_n$
18 :	$SU_{m+n/p+q}$	$\Rightarrow$	$U_1 \times SU_{m/p} \times SU_{n/q}$
19 :	$U_{mn+pq/mq+np}$	$\Rightarrow$	$U_{m/p} \times U_{n/q}$
20 :	$OSp_{m/n}$	$\Rightarrow$	$O_m \times Sp_n$
21 :	O_n	$\Rightarrow$	U_n
22 :	Sp_n	$\Rightarrow$	U_n $\quad (n\ even)$
23 :	SO_7	$\Rightarrow$	G_2
24 :	SO_7	$\Rightarrow$	SO_3
25 :	G_2	$\Rightarrow$	SU_3
26 :	G_2	$\Rightarrow$	SO_3
27 :	G_2	$\Rightarrow$	SO_7
28 :	F_4	$\Rightarrow$	SO_9
29 :	E_6	$\Rightarrow$	$SU_2 \times SU_6$
30 :	E_6	$\Rightarrow$	$U_1 \times SO_{10}$
31 :	E_6	$\Rightarrow$	G_2
32 :	E_7	$\Rightarrow$	SU_8
33 :	E_7	$\Rightarrow$	$U_1 \times E_6$
34 :	E_8	$\Rightarrow$	SU_9
35 :	E_8	$\Rightarrow$	SO_{16}
36 :	E_8	$\Rightarrow$	$SU_2 \times E_7$
37 :	E_8	$\Rightarrow$	$SU_3 \times E_6$
38 :	SU_{27}	$\Rightarrow$	E_6
39 :	SU_{56}	$\Rightarrow$	E_7
40 :	SU_{248}	$\Rightarrow$	E_8
41 :	O_{mn}	$\Rightarrow$	$O_m \times O_n$
42 :	S_n	$\Rightarrow$	A_n

```
DP>
->setfn1
->gr u14
->enter rv1
->dim[rv1]
->br9,2,7gr1[rv1]
->gr2su2su7
->std last
->auto gr1so3,last
->stop
DP>
->fn1
Group is U(14)
->1^4
Dimension = 1001
Groups are   U(2) * U(7)
Groups are   SU(2) * SU(7)
Groups are   SO(3) * SU(7)
      [2]{1^4 } + [1]{21^2 } + [0]{2^2 }
```

In this case we have run the decomposition relevant to the f^4 configuration. The irreducible representations of SO_3 give us the *spin*, S, of the states. Recall that the *spin multiplicity* is $2S+1$. The irreducible representations of SU_7 are associated with the orbital states.

■ **Exercise**

1 Use SCHUR to calculate the decomposition $U_{14} \Rightarrow SO_3 \times SU_7$ for each of the irreducible representations $\{1^N\}$ for $N = 0, 1, \ldots, 7$.

To pursue the classification of the orbital states it is necessary to look further at the subgroups of SU_7. The special unitary group SU_7 can be restricted to rotations in seven dimensions, that is the subgroup SO_7. We might then think that the classification might be complete if we now restrict $SO_7 \Rightarrow SO_3$. Remarkably there is a group that fits between SO_7 and SO_3, namely the exceptional group, G_2. This leads to a richer classification and the orbital states are described by the group chain

$$SU_7 \supset SO_7 \supset G_2 \supset SO_3 \tag{1.19}$$

as shown in Tables 1.2 to 1.5 given at the end of these notes.

■ **Exercises**

2. Use SCHUR to verify some of the entries in Tables 1.2 to 1.5.
3. Use SCHUR to construct a function that will give the number of terms associated with a given J for any f^N configuration. Hint: you will need to make use of the command ContractGroups described on page 134 of the manual.

■ 1.9 Hund's rules and the ground state of Ho^{3+}

Table 1.2 gives the SL terms associated with the configuration f^4. Precisely the same SL terms occur in the f^{10} configuration. States of total angular momentum J may be found by noting the familar angular momentum addition rule

$$J = L+S, L+S-1, \ldots, |L-S| \tag{1.20}$$

The next problem is to determine the SLJ quantum numbers associated with the ground state of Ho^{3+}. Here we may use the Hund's rules as follows:-

1. Select the SL terms associated with the highest spin S. i.e. $S = 2$ and the terms ${}^5SDFGI$.
2. From the terms found in 1. select the term of highest L i.e. $L = 6$ corresponding to ${}^5I$.

3. If $N \leq 2\ell + 1$ choose the smallest value of J while for $N \geq 2\ell + 2$ choose the largest value of J. Thus we deduce that the groundstate for the free ion, Ho^{3+}, is

$$\boxed{Ho^{3+} \quad 4f^{10} \quad {}^5I_8}$$

in agreement with experiment. The five spectroscopic terms

$${}^5I_4, \quad {}^5I_5, \quad {}^5I_6, \quad {}^5I_7, \quad {}^5I_8$$

form the *ground multiplet* of Ho^{3+} and the next problem we must tackle is to calculate the spin-orbit splitting in the ground multiplet, the subject of our next lecture.

Table 1.2 LS multiplets of the f^N (N = 1 to 4) configurations

# of states	U_{14}	$SU_2^S \times SU_7^L$	SO_7	G_2	^{2S+1}L
1	$\{0\}$	$\{0\} \times \{0\}$	[000]	(00)	^1S
14	$\{1\}$	$\{1\} \times \{1\}$	[100]	(10)	^2F
45	$\{1^2\}$	$\{2\} \times \{1^2\}$	[110]	(11)	^3PH
				(10)	^3F
		$\{0\} \times \{2\}$	[200]	(20)	^1DGI
			[000]	(00)	^{S}
364	$\{1^3\}$	$\{3\} \times \{1^3\}$	[111]	(20)	^4DGI
				(10)	^4F
				(00)	^4S
		$\{1\} \times \{21\}$	[210]	(21)	^2DFGHKL
				(20)	^2DGI
				(11)	^2PH
			[100]	(10)	^2F
1001	$\{1^4\}$	$\{4\} \times \{1^4\}$	[111]	(20)	^5DGI
				(10)	^5F
				(00)	^5S
		$\{2\} \times \{211\}$	[211]	(30)	$^3PFGHIKM$
				(21)	^3DFGHKL
				(20)	^3DGI
				(11)	^3PH
				(10)	^3F
		$\{0\} \times \{2^2\}$	[220]	(22)	$^1SDGHILN$
				(21)	^1DFGHKL
				(20)	^1DGI
			[200]	(20)	^1DGI
			[000]	(00)	^1S

Table 1.3 LS multiplets of the f^5 configuration

# of states	U_{14}	$SU_2^S \times SU_7^L$	SO_7	G_2	^{2S+1}L
2002	$\{1^5\}$	$\{5\} \times \{1^5\}$	[110]	(11)	^6PH
				(10)	^6F
		$\{3\} \times \{21^3\}$	[211]	(30)	$^4PFGHIKM$
				(21)	^4DFGHKL
				(20)	^4DGI
				(11)	^4PH
				(10)	^4F
			[111]	(20)	^4DGI
				(10)	^4F
				(00)	^4S
		$\{1\} \times \{2^21\}$	[221]	(31)	$^2PDFFGHHIIKKLMNO$
				(30)	$^2PFGHIKM$
				(21)	^2DFGHKL
				(20)	^2DGI
				(11)	^2PH
				(10)	^2F
			[210]	(21)	$^2DFGHIKL$
				(20)	^2DGI
				(11)	^2PH
			[100]	(10)	^2F

Table 1.4 LS multiplets of the f^6 configuration

# of states	U_{14}	$SU_2^S \times SU_7^L$	SO_7	G_2	^{2S+1}L
3003	$\{1^6\}$	$\{6\} \times \{1^6\}$	[100]	(10)	^7F
		$\{4\} \times \{21^4\}$	[210]	(21)	$^5DFGHIKL$
				(20)	^5DGI
				(11)	^5PH
			[111]	(20)	^5DGI
				(10)	^5F
				(00)	^5S
		$\{2\} \times \{2^21^2\}$	[221]	(31)	$^3PDFFGHHIIKKLMNO$
				(30)	$^3PFGHIKM$
				(21)	^3DFGHKL
				(20)	^3DGI
				(11)	^3PH
				(10)	^3F
			[211]	(30)	$^3PFGHIKM$
				(21)	^3DFGHKL
				(20)	^3DGI
				(11)	^3PH
				(10)	^3F
			[110]	(11)	^3PH
				(10)	^3F
		$\{0\} \times \{2^3\}$	[222]	(40)	$^1SDFGGHIIKLLMNQ$
				(30)	$^1PFGHIKM$
				(20)	^1DGI
				(10)	^1F
				(00)	^1S
			[220]	(22)	$^1SDGHILN$
				(21)	^1DFGHKL
				(20)	^1DGI
			[200]	(20)	^1DGI
			[000]	(00)	^1S

Table 1.5 LS multiplets of the f^7 configuration

# of states	U_{14}	$SU_2^S \times SU_7^L$	SO_7	G_2	^{2S+1}L
3432	$\{1^7\}$	$\{7\} \times \{1^7\}$	[000]	(00)	^8S
		$\{5\} \times \{21^5\}$	[200]	(20)	^6DGI
			[110]	(11)	^6PH
				(10)	^6F
		$\{3\} \times \{2^21^3\}$	[220]	(22)	$^4SDGHILN$
				(21)	^4DFGHKL
				(20)	^4DGI
			[211]	(30)	$^4PFGHIKM$
				(21)	^4DFGHKL
				(20)	^4DGI
				(11)	^4PH
				(10)	^4F
			[111]	(20)	^4DGI
				(10)	^4F
				(00)	^4S
		$\{1\} \times \{2^31\}$	[222]	(40)	$^2SDFGGHIIKLLMNQ$
				(30)	$^2PFGHIKM$
				(20)	^2DGI
				(10)	^2F
				(00)	^2S
			[221]	(31)	$^2PDFFGHHIIKKLMNO$
				(30)	$^2PFGHIKM$
				(21)	^2DFGHKL
				(20)	^2DGI
				(11)	^2PH
				(10)	^2F
			[210]	(21)	$^2DFGHIKL$
				(20)	^2DGI
				(11)	^2PH
			[100]	(10)	^2F

Table 1.8 Total angular momenta for $\frac{5}{2}^{N_1}\frac{7}{2}^{N_2}$ with $N_1 + N_2 = 4$

N_1, N_2	SO_3^J
0, 4	[0] + 2[2] + 2[4] + [5] + [6] + [8]
1, 3	[0] + 3[1] + 4[2] + 5[3] + 5[4] + 5[5] + 4[6] + 3[7] + 2[8] + [9] + [10]
2, 2	3[0] + 2[1] + 7[2] + 5[3] + 8[4] + 5[5] + 6[6] + 3[7] + 3[8] + [9] + [10]
3, 1	2[1] + 3[2] + 3[3] + 3[4] + 3[5] + 2[6] + [7] + [8]
4, 0	[0] + [2] + [4]

The Application of Symmetry Concepts
to
Physical Problems II (contd)
Analysis of Hyperfine structure in Crystals

B. G. Wybourne

The scientist does not study nature because it is useful to do so He studies it because he takes pleasure in it, and he takes pleasure in it because it is beautiful
— Henri Poincaré

■ Lecture 2

■ 2.1 Introduction

In our previous lecture we stated the problem and as a first step established our zero-order Hamiltonian, gave a group-theoretical account of the states of the $f-$shell and determined the ground state for the trivalent holmium ion. Our next step is to give an account of the free ion levels of Ho^{3+} and specifically to compute the energies of the levels of the ${}^5I$ multiplet for the $4f^{10}$ configuration. To that end we primarily need to compute the relevant electrostatic and spin-orbit matrix elements, construct the energy matrices for the $J = 4..8$ states of $4f^{10}$ and then diagonalise them to obtain the energy eigenvalues. The corresponding eigenvectors will then allow us to express the eigenfunctions for each level as particular linear combinations of the zero-order eigenfunctions.

■ 2.2 The zero-order state labelling

We have determined the ${}^{2S+1}L$ multiplets in terms of the group-subgroup chain

$$U_{14} \supset SU_2^S \times \{SU_7 \supset SO_7 \supset G_2 \supset SO_3^L\} \tag{2.1}$$

This means that a given zero-order basis state in f^N could be fully specified by the labelling

$$|WU\alpha SLJM\rangle \tag{2.2}$$

Where we have suppressed the U_{14} label as been common to the complete set of states of a given f^N configuration. In addition we suppress the SU_7 label since as noted earlier specifying, for a given N the spin S uniquely fixes the corresponding SU_7 label. W stands for the partition label [λ] of the group SO_7

and U for the partition label $(u_1 u_2)$ of the group G_2. The label α is reserved to distinguish those pairs of L irreducible representations of SO_3 that occur twice in the $G_2 \Rightarrow SO_3$ decomposition. The total angular momentum J is found by addition of the spin S and orbital L angular momenta. Finally, M is the projection of J on the chosen $z-$axis. For a free ion, in the absence of external fields, we may suppress the M quantum number.

■ 2.3 The Coulomb interaction

The two-particle Coulomb interaction

$$H_C = e^2 \sum_{i<j\leq N} \frac{1}{r_{ij}} \tag{2.3}$$

commutes with the angular momentum operators S^2, L^2, J^2, J_z and hence its matrix elements in the $|SLJM\rangle$ basis is diagonal in the quantum numbers S, L, J, M and are independent of JM. If the term ^{2S+1}L occurs in the f^N configuration x times then the electrostatic matrix will be of rank x. The calculation of the matrix elements of H_C starts with the expansion

$$\begin{aligned}\frac{1}{r_{ij}} &= \frac{1}{\sqrt{r_i^2 + r_j^2 - 2r_i r_j \cos\omega}} \\ &= \sum_k \frac{r_<^k}{r_>^{k+1}} P_k(\cos\omega)\end{aligned} \tag{2.4}$$

where $r_<$ is the lesser of $\{r_i, r_j\}$ and $r_>$ the greater. The spherical harmonic addition theorem gives

$$\begin{aligned}P_k(\cos\omega) &= \frac{4\pi}{2k+1} \sum_q Y^*_{kq}(\theta_i, \phi_i) Y_{kq}(\theta_j, \phi_j) \\ &= \sum_q (-1)^q (C^{(k)}_{-q})_i (C^{(k)}_q)_j \\ &= (\mathbf{C}^{(k)}_i \cdot \mathbf{C}^{(k)}_j)\end{aligned} \tag{2.6}$$

where

$$C^{(k)}_q = \left(\frac{4\pi}{2k+1}\right)^{\frac{1}{2}} Y^*_{kq}(\theta, \phi) \tag{2.7}$$

and

$$H_C = e^2 \sum_k \frac{r_<^k}{r_>^{k+1}} (\mathbf{C}^{(k)}_i \cdot \mathbf{C}^{(k)}_j) \tag{2.8}$$

For full details see:-

2.1 G. Racah, *Theory of Complex Spectra IV*, Phys. Rev. **76**, 1352 (1949).

2.2 B. R. Judd, *Operator Techniques in Atomic Spectroscopy*, New York: McGraw-Hill (1963).

The calculation of the matrix elements of H_C involves the product of purely angular terms and radial integrals. The latter are commonly termed *Slater* radial integrals and for equivalent electrons $n\ell$

$$F^{(k)} = e^2 \int_0^\infty \int_0^\infty \frac{r_<^k}{r_>^{k+1}} \left[R_{n\ell}(r_i) R_{n\ell}(r_j)\right]^2 dr_i dr_j \tag{2.9}$$

The values of k are restricted by the symmetry of the angular matrix elements to the *even* integers $k = 0, 2, \ldots, 2\ell$. To avoid the appearance of fractions it is usual to make the replacements (for the $f-$shell)

$$F_0 = F^{(0)}, \quad F_2 = \frac{F^{(2)}}{225}, \quad F_4 = \frac{F^{(4)}}{1089}, \quad F_6 = \frac{25F^{(6)}}{184041} \tag{2.10}$$

Thence the matrix elements of the Coulomb interaction are of the form:-

$$f_0 F_0 + f_2 F_2 + f_4 F_4 + f_6 F_6 \tag{2.11}$$

where the f_k are purely angular matrix elements.

■ 2.4 The Racah E^k Parameters

The terms in Eq.(2.11) take no advantage of the group structure used to classify the states of the $f-$shell. Racah suggested that Eq.(2.11) should be transformed in such a way as to yield operators that had well

defined transformation properties with respect to the groups used in the state classification scheme. In particular he chose the following linear combinations of the Slater radial integrals:-

$$\begin{aligned} E^0 &= F_0 - 10F_2 - 33F_4 - 286F_6 \\ E^1 &= \frac{70F_2 + 231F_4 + 2002F_6}{9} \\ E^2 &= \frac{F_2 - 3F_4 + 7F_6}{9} \\ E^3 &= \frac{5F_2 + 6F_4 - 91F_6}{3} \end{aligned} \tag{2.12}$$

with the analogue of Eq.(2.11) becoming

$$e_0E^0 + e_1E^1 + e_2E^2 + e_3E^3 \tag{2.13}$$

The angular operators $e_k \quad k = 0, 1, 2, 3$ transformed under $SO_7 \supset G_2 \supset SO_3$ as [000](00)0, [000](00)0, [400](40)0 and [220](22)0 respectively. The eigenvalues of e_0 all evaluated to $\frac{1}{2}N(N-1)$ for a given f^N configuration and hence may be ignored if we are only interested in relative term energies. Racah gave systematic tables of quantities required to calculate the e_k making use of the general Wigner-Eckart theorem.

Edith Reilly has tabulated the necessary matrix elements for the f^4 configuration. An independent calculation for all the f^N configurations has been made by Nielson and Koster.

2.3 E. F. Reilly, Phys. Rev. **91**, 876 (1953).

2.4 C. W. Nielson and G. F. Koster, *Spectroscopic Coefficients for the p^n, d^n and f^n Configurations*, Cambridge, Mass: The M. I. T. Press (1963).

For the purposes of these lectures the electrostatic matrix elements for the f^4 configuration have been entered into a MAPLE procedure to be discussed later.

The Racah approach gives an interesting insight into terms of maximum spin multiplicity in the f^N configurations. The contribution to the electrostatic energy of these terms of $e_0E^0 + e_1E^1$ is the same, while that of e_2E^2 is null. Thus the energy spacings of terms of maximum spin multiplcity are expressible in terms of just E^3. Indeed for these terms

$$\langle f^{N\ N+1}L|e_3|f^{N\ N+1}L\rangle = 36G(G_2)(u_1u_2) - \frac{3}{2}L(L+1) \tag{2.14}$$

where

$$G(G_2)(u_1u_2) = \frac{u_1^2 + u_2^2 + u_1u_2 + 5u_1 + 4u_2}{12} \tag{2.15}$$

is the eigenvalue of the Casimir operator for the relevant irreducible representation (u_1u_2) of the exceptional group G_2. Throughout these notes we use Racah's notation (u_1u_2) notation for labelling irreducible representations of G_2. SCHUR uses the labelling (a, b) based upon the SU_3 subgroup of G_2. The SCHUR labels are related to the Racah labels by the correspondance

$$(a,b)_{SCHUR}Rightarrow(a-b,b)_{RACAH} \tag{2.16}$$

■ **Exercise**

2.1 Determine the relative spacings of the terms of maximum multiplicity for the f^4 configuration due to the Coulomb interaction.

■ **2.5 Spin-orbit interaction matrix elements**

The spin-orbit interaction term H_{so}in the Hamiltonian is of the form

$$H_{so} = \sum_{i=1}^{N} \zeta_{n\ell}(r)(\mathbf{s}\cdot\ell)_i \tag{2.17}$$

and commutes with the operators J^2 and J_z and hence is diagonal in JM and independent of M. However, it does not commute with S^2 or L^2 and hence there can be non-zero matrix elements among states with

$$\Delta S, \Delta L = 0, \ \pm 1 \tag{2.18}$$

The spin-orbit interaction matrices for a given J will be of rank equal to the number number of SL terms yielding that value of J. This means that in f^4 the matrices for $J = 4..8$ will be of ranks $19, 14, 13, 7, 7$ respectively. The matrix elements of H_{so} may be calculated in the same basis as for H_C using the group classified states. These have been calculated by Crozier and Runciman while Nielson and Koster have given tables of reduced matrix elements from which the spin-orbit matrices may be derived.

2.5 M. H. Crozier and W. A. Runciman, J. Chem. Phys. **35**, 1392 (1962);

The methods of calculating the matrix elements of the spin-orbit interaction for the $f-$shell are well covered in Judd's book. As with the Coulomb matrices, the spin-orbit matrices are necessarily symmetric.

■ 2.6 Checking the spin-orbit matrices

It is always important to have checking procedures to ensure that matrix elements have been correctly computed and entered. In the case of the spin-orbit interaction a good check is to diagonalise the matrix for a given J and see if the resulting eigenvalues are those appropriate to $jj-$coupling where the spin-orbit interaction is necessarily diagonal. For a single electron $\mathbf{j} = \ell + \mathbf{s}$ and we have

$$\mathbf{s} \cdot \ell = \frac{1}{2}[j(j+1) - \ell(\ell+1) - s(s+1)] \tag{2.19}$$

Within a $jj-$coupled configuration j^N the spin-orbit term is multiplied by N. As noted on page 14 the states of the f^N configuration in $jj-$coupling derive from those of the sub-configurations $\frac{5}{2}^{N_1} 7/2^{N_2}$ where $N_1 + N_2 = N$. The total angular momentum states J for such configurations with $N = 4$ were given in Table 1.8. For $f_{\frac{5}{2}}$ Eq. (2.19) evaluates to -2 and for $f_{7/2}$ to $\frac{3}{2}$ and hence the spin-orbit interaction for any state of the sub-configuration $\frac{5}{2}^{N_1} \frac{7}{2}^{N_2}$ must be

$$\frac{3}{2}N_2 - 2N_1 \tag{2.20}$$

For example inspection of Table 1.8 shows that if we have correctly calculated the 7×7 spin-orbit interaction matrix for $J = 8$ then diagonalisation of the matrix, with the spin-orbit interaction coupling constant $\zeta_{n\ell} = 1$ should yield the followin eigenvalues, with multiplicities bracketed,

$$-8(1), \quad -\frac{9}{2}(2), \quad -1(3), \quad \frac{5}{2}(1) \tag{2.21}$$

■ 2.7 Ordering of Zero-order States for f^4

In setting up the energy matrices it is essential to specify carefully the ordering of the zero-order basis states for each value of J and to ensure that the matrices for the electrostatic and spin-orbit matrices follow the same order and that the phase choices for both are compatible. Here we will follow the ordering used by Crozier and Runciman as given in Table 2.1.

■ 2.8 Spin-orbit Interaction in the ^5I multiplet

Judd (p82) has shown that within a multiplet ^{2S+1}L the matrix elements of the spin-orbit interaction can be written as

$$\mathbf{S} \cdot \mathbf{L} = \frac{\lambda}{2}[J(J+1) - L(L+1) - S(S+1)] \tag{2.22}$$

where λ is a constant appropriate to the given multiplet. For a multiplet of maximum multiplicity in a ℓ^N configuration he finds

$$\lambda = \pm\frac{1}{2S} \tag{2.23}$$

where the $+$ sign is taken for $N \leq 2\ell$ and the $-$ sign for $N \geq 2\ell + 2$. Thus for Ho^{3+} we have for the ^5I multiplet

$$\mathbf{S} \cdot \mathbf{L} = -\frac{J(J+1)}{8} - 6 \tag{2.23}$$

and hence if $LS-$coupling holds in the ^5I multiplet we would expect

$$E_J - E_{J+1} = \frac{J+1}{4}\zeta_{4f} \tag{2.24}$$

$J=4$	$J=5$	$J=6$	$J=7$	$J=8$
$[111](20)^5D$	$[111](10)^5F$	$[111](20)^5G$	$[111](20)^5I$	$[111](20)^5I$
$[111](10)^5F$	$[111](20)^5G$	$[211](11)^3H$	$[211](20)^3I$	$[211](21)^3K$
$[211](10)^3F$	$[211](20)^3G$	$[211](21)^3H$	$[211](30)^3I$	$[211](30)^3K$
$[211](21)^3F$	$[211](21)^3G$	$[211](30)^3H$	$[211](21)^3K$	$[211](21)^3L$
$[211](30)^3F$	$[211](30)^3G$	$[110](11)^3H$	$[211](30)^3K$	$[220](21)^1L$
$[110](10)^3F$	$[211](11)^3H$	$[111](20)^5I$	$[220](21)^1K$	$[220](22)^1L$
$[111](20)^5G$	$[211](21)^3H$	$[211](20)^3I$	$[211](21)^3L$	$[211](30)^3M$
$[211](20)^3G$	$[211](30)^3H$	$[211](30)^3I$		
$[211](21)^3G$	$[110](11)^3H$	$[220](20)^1I$		
$[211](30)^3G$	$[220](21)^1H$	$[220](22)^1I$		
$[220](20)^1G$	$[220](22)^1H$	$[200](20)^1I$		
$[220](21)^1G$	$[111](20)^5I$	$[211](21)^3K$		
$[220](22)^1G$	$[211](20)^3I$	$[211](30)^3K$		
$[200](20)^1G$	$[211](30)^3I$			
$[211](11)^3H$				
$[211](21)^3H$				
$[211](30)^3H$				
$[110](11)^3H$				
$[111](20)^5I$				

Table 2.1 Ordering of the Zero-order States in f^4 Configurations

and hence

$$\frac{E_J - E_{J+1}}{J+1} = \frac{\zeta_{4f}}{4} \tag{2.25}$$

which gives us a test of the validity of $LS-$coupling in the ground multiplet of Ho^{3+}. Rajnak and Krupke

2.6 K. Rajnak and W. F. Krupke, *Energy levels of Ho^{3+} in $LaCl_3$*, J. Chem. Phys. **46**, 3532 (1967).

give the average positions of the ${}^5I_J$ levels in cm^-1 as

${}^5I_8$	108
${}^5I_7$	5155
${}^5I_6$	8657
${}^5I_5$	11219
${}^5I_4$	13284

Noting Eq.(2.25) we find

$\frac{{}^5I_7 - {}^5I_8}{15}$	336
$\frac{{}^5I_6 - {}^5I_7}{13}$	269
$\frac{{}^5I_5 - {}^5I_6}{11}$	233
$\frac{{}^5I_4 - {}^5I_5}{9}$	229

The lack of constancy in the second column shows clearly that there is a breakdown of $LS-$coupling which we may fully include only by diagonalising the complete combined electrostatic and spin-orbit matrices.

■ 2.9 Intermediate Coupling in Ho^{3+}

The complete construction of the energy matrices may be made into a set of MAPLE procedures using the electrostatic and spin-orbit matrices calculated, for example, by Reilly, and by Crozier and Runciman. The sections relevant to the $J=8$ states are given in the verbatim printout below:-

■ **2.10 Some MAPLE procedures**

■ **2.11 Running the MAPLE esof4 File**

The MAPLE code is available on a diskette as a single file *esof4* and may be read into a MAPLE session by entering in MAPLE the command *read‘eso4‘;*. Be sure to use backquotes (‘) and note that all MAPLE commands end with a semicolon (;). HELP may be brought to the screen by issuing the command *?esof4;*. As a starter try to run the two examples given in the HELP file. Use the eigenvectors produced in the second example to write the ground state of Ho^{3+} as a linear combination of the zero-order states given in Table 2.1.

■ **Exercises to be completed for the next lecture**

Take the parameters used in Example 2 and compute the energies of the five levels of the ^5I multiplet and their associated eigenvectors. Draw up a table of the calculated energies and the expansion of the free ion states as linear combinations of the zero order states keeping all expansion coefficients ≥ 0.1. Leave a column in your table to insert the experimental energies which will be given at the next lecture. These results will play an important role in the subsequent lectures.

The Application of Symmetry Concepts
to
Physical Problems II (contd)
Analysis of Hyperfine structure in Crystals

B. G. Wybourne

A good scientist is a person with original ideas. A good engineer is a person who makes a design that works, and prides himself on doing so with as few original ideas as possible
— Freeman Dyson, *New Yorker Magazine,* August 20, 1979, p54

■ **Lecture 3**

■ **3.1 Introduction**

In this lecture I shall first discuss the results of the intermediate coupling calculation for Ho^{3+} started in the previous lecture and then start on the question of calculating the effect of the crystal field on the "free ion" levels. This will require some review of the properties of angular momentum coupling coefficients and tensor operators - essential both for the calculation of crystal field and hyperfine perturbations.

■ **3.2 Intermediate Coupling in Ho^{3+}**

The effect of diagonalizing the energy matrices for the $J = 4, .., 8$ is to yield a set of energy eigenvalues and their associated eigenvectors. Thus the eigenstate $|E_J\rangle$ associated with the energy eigenvalue E_J is obtained as a linear combination of the zero-order states given in Table 2.1. Thus

$$|E_J M\rangle = \sum_{\alpha SL} a_{\alpha SLJ} |\alpha SLJM\rangle \tag{3.1}$$

Since the coefficients of the expansion are independent of M we will usually suppress the M quantum number. The α stands for any other labels required to distinguish states that occur with the same SL. In the case of our exercise it suffices, when necessary, to give just the G_2 irreducible representation label $(u_1 u_2)$ in Racah's notation. The normalised expansion coefficients are necessarily between 0 and 1 and the sum of their squares equal to unity. The square of a given coefficient is a measure of the significance of that particular zero-order state. If a coefficient is very close to unity then the state is very close to LS-coupling and a single zero-order state dominates. We shall choose to limit our attention to those zero-order states whose coefficients are ≥ 0.1 and thus contribute 1% or more to the eigenfunction. The relevant expansion coefficients for the five lowest states of Ho^{3+} are given in Table 3.1 along with the calculated and experimental averaged energy levels for $LiYF_4 : Ho^{3+}$.

Table 3.1 Energy levels and eigenvectors for the ^5I multiplet in $LiYF_4 : Ho^{3+}$.

J	E_{calc}	E_{expt}	Eigenvector
8	0	0	$0.9665\|^5I_8\rangle + 0.1189\|(20)^3K_8\rangle - 0.2221\|(30)^3K_8\rangle$
7	5097	5152	$0.9853\|^5I_7\rangle - 0.1462\|(30)^3K_7\rangle$
6	8672	8671	$0.9772\|^5I_6\rangle + 0.1352\|(30)^3H_6\rangle$
5	11281	11242	$0.9549\|^5I_5\rangle - 0.1377\|(21)^3H_5\rangle + 0.1944\|(30)^3H_5\rangle - 0.1067\|(11)^3H_5\rangle$
4	13350	13188	$0.9495\|^5I_4\rangle - 0.1620\|(21)^3H_4\rangle + 0.2247\|(30)^3H_4\rangle - 0.1186\|(11)^3H_4\rangle$

■ 3.3 Tensor operators in general

Consider a simple compact group G having elements g. Let U_g denote a unitary, not necessarily irreducible, representation of G on a Hilbert space $\mathcal{H}$. The various unitary representations will be distinguished, when necessary, by writing $U_g(\Lambda)$ or for brevity just as (Λ). Let $|\Lambda\lambda>$ be basis vectors of the representation (Λ), where λ labels individual basis vectors.

Let the complete set of basis vectors $|\Lambda\lambda>$ span the infinite Hilbert space $\mathcal{H}$ in which the linear operator R_g (or just R) corresponding to the element g of G is represented by the block-diagonal matrix $|<\Lambda\lambda|R|\Lambda\lambda'>|$. An individual matrix element will be designated as $<\Lambda\lambda|R|\Lambda\lambda'>$. The effect of the linear operator R acting on a basis vector $|\Lambda\lambda>$ will be to produce a linear combination of those basis vectors that span the representation (Λ), that is

$$R|\Lambda\lambda>=\sum_{\lambda'}<\Lambda\lambda'|R|\Lambda\lambda>|\Lambda\lambda'> \tag{3.4}$$

The set $\mathbf{T}(\Lambda)$ of $[\Lambda]$ linearly independent operators $T(\Lambda\lambda)$ is said to form a *tensor operator* under the group G belonging to the representation (Λ) of G if under the operations of the group it transforms according to the representation (Λ) i.e., if

$$RT(\Lambda\lambda)R^{-1}=<\Lambda\lambda'|R|\Lambda\lambda>T(\Lambda\lambda') \tag{3.5}$$

A tensor operator $\mathbf{T}(\Lambda)$ will be said to be *irreducible*, *reducible* or *equivalent* if the group representation (Λ) is correspondingly irreducible, reducible or equivalent.

For an infinitesimal transformation in G

$$R=1+\delta a^\sigma X_\sigma \tag{3.6}$$

where δa^σ are the infinitesimal parameters and X_σ the corresponding infinitesimal operators. Keeping terms to first order in the δa^σ,

$$[X_\sigma,T(\Lambda\lambda)]=\sum_{\lambda'}<\Lambda\lambda'|X_\sigma|\Lambda\lambda>T(\Lambda\lambda') \tag{3.7}$$

and from Eq.(3.5)

$$X_\sigma|\Lambda\lambda>=\sum_{\lambda'}<\Lambda\lambda'|X_\sigma|\Lambda\lambda>|\Lambda\lambda'> \tag{3.8}$$

■ 3.5 Tensor operators for SO_3

For the group SO_3 the infinitesimal operators are $J_z, J_\pm$ and in an angular momentum basis that diagonalises $\mathbf{J}^2$ and J_z

$$J_z|JM>=M|JM> \tag{3.9a}$$

$$J_\pm|JM>=\sqrt{J(J+1)-M(M\pm1)}|JM\pm1> \tag{3.9b}$$

which is the SO_3 equivalent of Eq.(3.5).

If $\mathbf{T}(k)$ is an irreducible tensor operator in SO_3 transforming as the irreducible representation $\mathcal{D}(k)$ of SO_3 it follows from Eq.(3.7) that the $(2k+1)$ components $T(kq)$ where $q=-k,-k+1,\ldots,k-1,k$ must satisfy the commutation relations

$$[J_z,T(kq)]=qT(kq) \tag{3.10a}$$

$$[J_\pm,T(kq)]=\sqrt{k(k+1)-q(q\pm1)}T(k,q\pm1) \tag{3.10b}$$

which we will take as the defining relations for irreducible tensor operators for SO_3. The tensor operator $\mathbf{T}(k)$ will be said to be of *rank* k.

■ 3.6 Coupling coefficients

If $|\Lambda_1\lambda_1>$ and $|\Lambda_2\lambda_2>$ are two basis vectors of (Λ_1) and (Λ_2), respectively, then the reduction of the Kronecker product is accomplished by the *coupling coefficients*

$$<\Lambda_1\lambda_1\Lambda_2\lambda_2|\Lambda_1\Lambda_2;\alpha\Lambda_{12}\lambda_{12}>$$

where

$$|\alpha\Lambda_{12}\lambda_{12}>=\sum_{\lambda_1,\lambda_2}<\Lambda_1\lambda_1\Lambda_2\lambda_2|\Lambda_1\Lambda_2;\alpha\Lambda_{12}\lambda_{12}>|\Lambda_1\lambda_1>|\Lambda_2\lambda_2> \tag{3.11}$$

with α being a *multiplicity* symbol to distinguish repeated irreducible representations. In the case of SO_3 the coupling coefficients are just the usual Clebsch-Gordan coefficients.

The inverse transformation can be written as

$$|\Lambda_1\lambda_1>|\Lambda_2\lambda_2>=\sum_{\alpha,\Lambda_{12},\lambda_{12}}<\alpha\Lambda_{12}\lambda_{12}|\lambda_1\lambda_2>^*|\Lambda_1\Lambda_2;\alpha\Lambda_{12}\lambda_{12}> \tag{3.12}$$

Since the transformations are unitary, we have the orthogonality relations

$$\sum_{\lambda_1,\lambda_2}<\alpha\Lambda_{12}\lambda_{12}|\lambda_1\lambda_2>^*<\lambda_1\lambda_2|\alpha'\Lambda'_{12}\lambda'_{12}>=\delta_{\alpha\alpha'}\delta_{\Lambda_{12}\Lambda'_{12}}\delta_{\lambda_{12}\lambda'_{12}} \tag{3.13a}$$

$$\sum_{\alpha,\Lambda_1,\Lambda_2}<\lambda_1\lambda_2|\alpha\Lambda_{12}\lambda_{12}>^*<\alpha\Lambda_{12}\lambda_{12}|\lambda'_1\lambda'_2>=\delta_{\lambda_1\lambda'_1}\delta_{\lambda_2\lambda'_2} \tag{3.13b}$$

■ 3.7 The Wigner-Eckart theorem in general

It is the Wigner-Eckart theorem that makes group theoretical calculations quantitative. Consider a tensor operator $T(\Lambda\lambda)$ acting on a basis state $|\Lambda_2\lambda_2>$. Then

$$T(\Lambda\lambda)|\Lambda_2\lambda_2>=\sum_{\alpha,\Lambda_1,\lambda_1}<\alpha\Lambda_1\lambda_1|\Lambda\lambda\Lambda_2\lambda_2>^*|T(\Lambda)\Lambda_2;\alpha\Lambda_1\lambda_1> \tag{3.14}$$

The matrix elements of $T(\Lambda\lambda)$ are given by

$$<\Lambda_1\lambda_1|T(\Lambda\lambda)|\Lambda_2\lambda_2>=\sum_{\alpha}<\alpha\Lambda_1\lambda_1|\Lambda\lambda\Lambda_2\lambda_2>^*<\Lambda_1\lambda_1|T(\Lambda)|\Lambda_2;\alpha\Lambda_1\lambda_1> \tag{3.15}$$

Consider the transformation

$$|\alpha\Lambda_1\lambda_1>=\sum_{\beta}<\beta\Lambda_1\lambda_1|\alpha\Lambda_1\lambda_1>|\beta\Lambda_1\lambda_1> \tag{3.16}$$

Suppose that X_μ is an arbitrary infinitesimal operator of the group G and that

$$|\alpha\Lambda_1\lambda_1+\mu>=\sum_{\beta}<\beta\Lambda_1\lambda_1+\mu|\alpha\Lambda_1\lambda_1+\mu>|\beta\Lambda_1\lambda_1+\mu> \tag{3.17}$$

For $\mu\neq 0$

$$\begin{aligned}|\alpha\Lambda_1\lambda_1+\mu> &= \frac{X_\mu|\alpha\Lambda_1\lambda_1>}{<\Lambda_1\lambda_1+\mu|X_\mu|\Lambda_1\lambda_1>}\\ &=\sum_{\beta}<\beta\Lambda_1\lambda_1|\beta\Lambda_1\lambda_1>|\beta\Lambda_1\lambda_1+\mu>\end{aligned} \tag{3.18}$$

Comparison with Eq.(3.17) gives

$$<\beta\Lambda_1\lambda_1+\mu|\alpha\Lambda_1\lambda_1+\mu>=<\beta\Lambda_1\lambda_1|\beta\Lambda_1\lambda_1> \tag{3.19}$$

for all $\mu\neq 0$, and hence the coefficients $<\beta\Lambda_1\lambda_1|\beta\Lambda_1\lambda_1>$ must be independent of the component λ_1.

Making use of Eq.(3.15) gives the Wigner-Eckart theorem as

$$< \Lambda_1\lambda_1|T(\Lambda\lambda)|\Lambda_2\lambda_2 >= \sum_{\alpha} < \alpha\Lambda_1\lambda_1|\lambda\lambda_2 >^* < \alpha\Lambda_1\|T(\Lambda)\|\Lambda_2 > \tag{3.20}$$

where we have written $< \alpha\Lambda_1\|T(\Lambda)\|\Lambda_2 >$ in the place of $< \Lambda_1\lambda_1|T(\Lambda)|\Lambda_2;\alpha\Lambda_1\lambda_1 >$, since the latter is independent of λ_1. The double-barred matrix elements are independent of the weights of λ_i of the representations (Λ_i) and are referred to as *reduced matrix elements*. The entire dependence of the matrix element on the weights of the bra and ket representations together with the component of the tensor operator $\mathbf{T}(\Lambda)$ is encased in the coupling coefficients $< \alpha\Lambda_1\lambda_1|\lambda\lambda_2 >^*$. Inverting Eq.(3.20) gives

$$< \alpha\Lambda_1\|T(\Lambda)\|\Lambda_2 >= \sum_{\lambda_1,\lambda_2} < \lambda\lambda_2|\alpha\Lambda_1\lambda_1|T(\Lambda\lambda)|\Lambda_2\lambda_2 > \tag{3.21}$$

Ultimately the calculation of matrix elements comes down to the evaluation of coupling coefficients and reduced matrix elements. The Wigner-Eckart theorem may be generalised to apply successively to every group-subgroup along a chain of nested groups.

■ 3.8 Selection rules

The Wigner-Eckart theorem leads directly to *selection rules* which follow from the requirements for the vanishing of the coupling coefficients. The coupling coefficient in Eq.(3.20) will vanish unless the weights of the bra, ket and tensor operator component satisfy the relation

$$\lambda + \lambda_2 = \lambda_1 \tag{3.22}$$

The coupling coefficient will vanish unless the triple Kronecker product

$$\Lambda_1^* \times \Lambda \times \Lambda_2 \supset 0 \tag{3.23}$$

where here 0 is the identity representation of G. We will write $c(\Lambda_1, \Lambda, \Lambda_2)$ for the number of times the identity representation occurs in the triple Kronecker product. This number gives the number of terms that occur in Eq. (3.20).

■ 3.9 The Wigner-Eckart theorem for SO_3

The group SO_3 is *multiplicity free* and the Wigner-Eckart theorem in this case simplifies to just

$$< \alpha_1 j_1 m_1|T_q^{(k)}|\alpha_2 j_2 m_2 >= C^{j_1 k j_2}_{m_1 q m_2} < \alpha_1 j_1\|T^{(k)}\|\alpha_2 j_2 > \tag{3.24}$$

where $C^{j_1 k j_2}_{m_1 q m_2}$ is the usual Clebsch-Gordan coefficient. In terms of the $3jm-$symbol we have

$$< \alpha_1 j_1 m_1|T_q^{(k)}|\alpha_2 j_2 m_2 >= (-1)^{j_1 - m_1} \begin{pmatrix} j_1 & k & j_2 \\ -m_1 & q & m_2 \end{pmatrix} < \alpha_1 j_1\|T^{(k)}\|\alpha_2 j_2 > \tag{3.25}$$

The matrix elements of $T_q^{(k)}$ vanish unless

$$m_1 = q + m_2 \tag{3.26}$$

while the reduced matrix element will vanish unless

$$j_1 + j_2 \geq k \geq |j_1 - j_2| \tag{3.27}$$

■ 3.10 The Clebsch-Gordan coefficients

The Clebsch-Gordan coefficient $< j_1 m_1 j_2 m_2|j_1 j_2 jm >$ represents the elements of a unitary transformation that couples the uncoupled states $|j_1 m_1 > |j_2 m_2 >$ to produce the coupled states $|j_1 j_2 jm >$. i.e.,

$$|j_1 j_2 jm >= \sum_{m_1,m_2} < j_1 m_1 j_2 m_2|j_1 j_2 jm > |j_1 m_1 > |j_2 m_2 > \tag{3.28}$$

Such transformations arise, for example in relating basis states in the $|SM_S LM_L >$ scheme to the coupled basis states $|SLJM >$ where $M = M_S + M_L$. Thus,

$$|SLJM >= \sum_{M_S,M_L} < M_S M_L|SLJM > |SM_S LM_L > \tag{3.29}$$

Note that we shall often abbreviate the Clebsch-Gordan coefficient $< j_1 m_1 j_2 m_2 | j_1 j_2 j m >$ to just $< m_1 m_2 | j_1 j_2 j m >$. The Clebsch-Gordan coefficients may be expressed precisely as

$$\begin{aligned} &< m_1 m_2 | j_1 j_2 j m >= \delta_{m_1+m_2,m} \\ &\times \sqrt{\frac{(2j+1)(j_1+j_2-j)!\,(j_1-m_1)!\,(j_2-m_2)!\,(j+m)!\,(j-m)!}{(j_1+j_2+j+1)!\,(j+j_1-j_2)!\,(j-j_1+j_2)!\,(j_1+m_1)!\,(j_2+m_2)!}} \\ &\times \sum_z (-1)^{j_1-m_1-z} \frac{(j_1+m_1+z)!\,(j+j_2-m_1-z)!}{z!\,(j-m-z)!\,(j_1-m_1-z)!\,(j_2-j+m_1+z)!} \end{aligned} \tag{3.30}$$

While Clebsch-Gordan coefficients possesses considerable symmetry a more symmetrical object was defined by Wigner and is now commonly known as the $3jm-$symbol.

■ 3.11 The $3jm-$symbol

The $3jm-$symbol is related to the Clebsch-Gordan coefficient by

$$\begin{pmatrix} j_1 & j_2 & j_3 \\ m_1 & m_2 & m_3 \end{pmatrix} = (-1)^{j_1-j_2-m_3} \frac{< m_1 m_2 | j_1 j_2 j_3 - m_3 >}{\sqrt{(2j_3+1)}} \tag{3.31}$$

The $3jm-$symbol is invariant with respect to an *even* permutation of its columns while for *odd* permutations of its columns is multiplied by a phase factor equal to the sum of the arguments in its top row. i.e.,

$$\begin{pmatrix} j_1 & j_2 & j_3 \\ m_1 & m_2 & m_3 \end{pmatrix} = (-1)^{j_1+j_2+j_3} \begin{pmatrix} j_2 & j_1 & j_3 \\ m_2 & m_1 & m_3 \end{pmatrix} \tag{3.32}$$

Furthermore, changing the sign of all three lower arguments results also in multiplication by a phase factor equal to the sum of the arguments in its top row. i.e.,

$$\begin{pmatrix} j_1 & j_2 & j_3 \\ m_1 & m_2 & m_3 \end{pmatrix} = (-1)^{j_1+j_2+j_3} \begin{pmatrix} j_1 & j_2 & j_3 \\ -m_1 & -m_2 & -m_3 \end{pmatrix} \tag{3.33}$$

A $3jm-$symbol having all its m quantum numbers zero will be null unless $j_1 + j_2 + j_3$ is *even*. Likewise any $3jm-$symbol having two identical columns will vanish unless $j_1 + j_2 + j_3$ is *even*.

The unitarity property of the Clebsch-Gordan coefficients lead directly to the orthonormality conditions for the $3jm-$symbols

$$\sum_{j_3,m_3} (2j_3+1) \begin{pmatrix} j_1 & j_2 & j_3 \\ m_1 & m_2 & m_3 \end{pmatrix} \begin{pmatrix} j_1 & j_2 & j_3 \\ m_1' & m_2' & m_3 \end{pmatrix} = \delta_{m_1,m_1'} \delta_{m_2,m_2'} \tag{3.34a}$$

$$\sum_{m_1,m_2} \begin{pmatrix} j_1 & j_2 & j_3 \\ m_1 & m_2 & m_3 \end{pmatrix} \begin{pmatrix} j_1 & j_2 & j_3' \\ m_1 & m_2 & m_3' \end{pmatrix} = \frac{\delta_{j_3,j_3'} \delta_{m_3,m_3'}}{\sqrt{(2j_3+1)}} \tag{3.34b}$$

■ 3.12 Computing $3jm-$symbols

The $3jm-$symbols may be variously expressed starting with the result given for the Clesch-Gordan formula given in Eq. (3.30). Extensive tables exist such as those of Rotenbrg, Bivins, Metropolis and Wooten, "*The* $3-j$ *and* $6-j$ *Symbols*" Technology Press, Mass. (1959). The difficulty with implementing formulas based upon Eq.(3.30) is the summation term which often leads to large intermediate numbers that overflow. Roothan(private communication 1990) has noted that the $3jm-$symbol formula can be usefully written in the form

$$\begin{aligned} &\begin{pmatrix} a & b & c \\ \alpha & \beta & \gamma \end{pmatrix} = \sqrt{\Delta(\tfrac{b+c-\alpha}{2}, \tfrac{c+a-\beta}{2}, \tfrac{a+b+\alpha+\beta}{2}) \Delta(\tfrac{b+c+\alpha}{2}, \tfrac{c+a+\beta}{2}, \tfrac{a+b-\alpha-\beta}{2})} \\ &\times \sum_z (-1)^{a+b+\alpha-\beta+z} \begin{pmatrix} a+b-c \\ z \end{pmatrix} \begin{pmatrix} c+a-b \\ a-\alpha-z \end{pmatrix} \begin{pmatrix} b+c-a \\ b+\beta-z \end{pmatrix} \end{aligned} \tag{3.35}$$

where

$$\Delta(abc)^{-1} = \begin{pmatrix} a+b+c \\ b+c-a \end{pmatrix} \begin{pmatrix} 2a \\ c+a-b \end{pmatrix} (a+b+c+1) \tag{3.36}$$

The binomial coefficients in Eq. (3.35) are first computed as integers in a Pascal's triangle and then read from the table as required and thus the awkward summation may be calculated as a sum of reals which may be rounded to produce an exact integer. The Δ terms are rapidly calculated using prime number arithmetic to produce integers and the resulting symbol outputted as a squared number expressed in prime number notation with a phase factor. With 32-bit words almost the entire tables of Rotenberg *etal* may be rapidly reproduced. With a 64-bit word such as on SUN machines the entire table and much more can be generated without overflow. Packages such as MapleV the entire calculation can be carried out using the exact arithmetic routines.

■ 3.13 Reduced matrix elements of angular momentum operators

The angular momentum **J** is a rank 1 tensor operator $\mathbf{J}^{(1)}$ with the $z-$ component J_z corresponding to the tensor operator component $J_0^{(1)}$. Application of the Wigner-Eckart theorem as in Eq.(3.25) gives

$$< \alpha jm|J_0^{(1)}|\alpha' j'm' >= (-1)^{j-m} \begin{pmatrix} j & 1 & j' \\ -m & 0 & m' \end{pmatrix} < \alpha j\|J^{(1)}\|\alpha' j' > \tag{3.37}$$

However, from the elementary quantum theory of angular momentum we have

$$< \alpha jm|J_z|\alpha' j'm' >= \delta_{\alpha,\alpha'}\delta_{j,j'}\delta_{m,m'}m \tag{3.38}$$

The matrix element is independent of all other quantum numbers α and diagonal in the angular momentum j. Comparison of Eqs. (3.37) and (3.38) then leads to

$$\begin{aligned} < jm|J_0^{(1)}|jm > &= m \\ &= (-1)^{j-m} \begin{pmatrix} j & 1 & j \\ -m & 0 & m \end{pmatrix} < j\|J^{(1)}\|j > \end{aligned} \tag{7.11}$$

The $3jm-$symbol may be explicitly evaluated to give

$$(-1)^{j-m} \begin{pmatrix} j & 1 & j \\ -m & 0 & m \end{pmatrix} = \frac{m}{\sqrt{j(j+1)(2j+1)}}$$

from which we immediately deduce the important reduced matrix element

$$< j\|J^{(1)}\|j >= \sqrt{j(j+1)(2j+1)} \tag{3.39}$$

In deriving Eq.(3.39) we have made no assumptions as to the nature of the angular momentum and our result holds equally well for spin or orbital angular momentum operators.

■ 3.14 The $6j-$symbol

The $3jm-$symbol arose in the problem of coupling two angular momentum states to produce a coupled state. In the case of coupling three angular momenta, say j_1, j_2, j_3, to produce a total angular momentum state $|jm >$ different orders of coupling the three angular momenta can be considered. Both $|(j_1j_2)j_{12}, j_3; jm >$ and $|j_1, (j_2j_3)j_{23}; jm >$ represent distinct coupling procedures. The two coupling schemes are linked by a unitary transformation such that

$$|j_1, (j_2j_3)j_{23}; jm >= \sum_{j_{12}} < (j_1j_2)j_{12}, j_3; jm|j_1, (j_2j_3)j_{23}; jm > |(j_1j_2)j_{12}, j_3; jm > \tag{3.40}$$

Acting on both sides with j_+ shows that the transformation coefficients are independent of m.

The $6j-$symbol is defined by the relation

$$\begin{aligned} &< (j_1j_2)j_{12}, j_3; jm|j_1, (j_2j_3)j_{23}; jm >= \\ &(-1)^{j_1+j_2+j_3+j} \sqrt{(2j_{12}+1)(2j_{23}+1)} \begin{Bmatrix} j_1 & j_2 & j_{12} \\ j_3 & j & j_{23} \end{Bmatrix} \end{aligned} \tag{3.41}$$

The $6j-$symbol may be evaluated by first expressing it as a sum over a triple product of $3jm-$symbols and then using the fact that the $6j-$symbol is independent of m to produce a sum involving a single variable to finally yield

$$\begin{Bmatrix} a & b & c \\ d & e & f \end{Bmatrix} =$$

$$\sqrt{\Delta(abc)\Delta(aef)\Delta(dbf)\Delta(dec)}$$
$$\times \sum_z (-1)^z (z+1)!$$
$$\times [(z-a-b-c)!(z-a-e-f)!(z-d-b-f)!(z-d-e-c)!$$
$$\times (a+b+d+e-z)!(b+c+e+f-z)!(a+c+d+f-z)!]^{-1} \tag{3.42}$$

The $6j-$symbol vanishes unless the four triangular conditions portrayed below are satisfied.

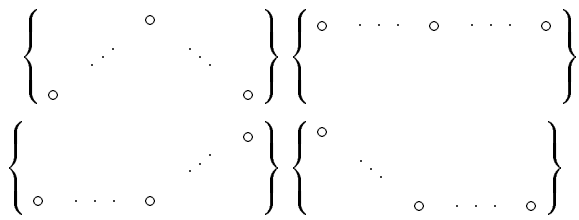

(3.43)

where for example $a+b \geq c \geq |a-b|$.

The $6j-$symbol is invariant with respect to any interchange of columns and also with respect to the interchange of the upper and lower arguments of any two columns.The $6j-$symbols satisfy the orthogonality condition

$$\sum_{j_{12}} (2j_{12}+1)(2j_{23}+1) \begin{Bmatrix} j_3 & j & j_{12} \\ j_1 & j_2 & j_{23} \end{Bmatrix} \begin{Bmatrix} j_3 & j & j_{12} \\ j_1 & j_2 & j'_{23} \end{Bmatrix}$$
$$= \delta_{j_{23}, j'_{23}} \tag{3.44}$$

Roothan(private communication 1990) has given the computationally convenient form for calculating $6j-$symbols

$$\begin{Bmatrix} a & b & c \\ d & e & f \end{Bmatrix}$$
$$= \sqrt{\Delta(abc)\Delta(dbf)\Delta(dec)\Delta(aef)}$$
$$\times \sum_z (-1)^z \begin{pmatrix} z+1 \\ z-a-b-c \end{pmatrix} \begin{pmatrix} b+c-a \\ z-a-e-f \end{pmatrix} \begin{pmatrix} c+a-b \\ z-d-b-f \end{pmatrix} \begin{pmatrix} a+b-a \\ z-d-e-c \end{pmatrix} \tag{3.45}$$

■ 3.15 The $9j-$symbol

The $6j-$symbol arose in discussing the coupling of three angular momentum. Clearly more complex $nj-$symbols will arise for couplings involving more than three angular momentum. The $9j-$symbol may be defined as

$$< (j_1 j_2) j_{12}, (j_3 j_4) j_{34}; j | (j_1 j_3) j_{13}, (j_2 j_4) j_{24}; j >$$
$$= \sqrt{(2j_{12}+1)(2j_{34}+1)(2j_{13}+1)(2j_{24}+1)} \begin{Bmatrix} j_1 & j_2 & j_{12} \\ j_3 & j_4 & j_{34} \\ j_{13} & j_{24} & j \end{Bmatrix} \tag{3.46}$$

The $9j-$symbol may be expressed in terms of $6j-$symbols as

$$\begin{Bmatrix} a & b & c \\ d & e & f \\ g & h & i \end{Bmatrix}$$
$$= \sum_z (-1)^{2z} [z] \begin{Bmatrix} a & d & g \\ h & i & z \end{Bmatrix} \begin{Bmatrix} b & e & h \\ d & z & f \end{Bmatrix} \begin{Bmatrix} c & f & i \\ z & a & b \end{Bmatrix} \tag{3.47}$$

The $9j-$symbol is left invariant with respect to any *even* permutation of its rows or columns or a transposition of rows and columns. Under an *odd* permutation of rows or columns the symbol is invariant

but for a phase factor equal to the sum of its arguments. If one argument of the $9j-$symbol is zero the symbol collapses to a single $6j-$symbol *viz.*

$$\left\{ \begin{array}{ccc} a & b & c \\ d & e & f \\ g & h & 0 \end{array} \right\} = \delta_{c,f}\delta_{g,h}\frac{(-1)^{b+d+f+g}}{\sqrt{(2c+1)(2g+1)}} \left\{ \begin{array}{ccc} a & b & c \\ e & d & g \end{array} \right\} \tag{3.48}$$

■ 3.16 Coupled tensor operators

We have noted the close connection between the transformation properties of tensor operators and angular momentum states. Consider two tensor operators $\mathbf{T}^{(k_1}$ and $\mathbf{U}^{(k_2}$. We can define a coupled tensor operator $\mathbf{X}^{(k_1k_2;K)}$ via

$$\mathbf{X}_Q^{k_1k_2;K} = \sum_{q_1,q_2} T_{q_1}^{(k_1)} U_{q_2}^{(k_2)} < k_1q_1k_2q_2|k_1k_2;KQ > \tag{3.49}$$

Explicit evaluation of the Clebsch-Gordan coefficient for the case of $K = 0$ leads to

$$[\mathbf{T}^{(k)}\mathbf{U}^{(k)}]_0^0 = \frac{(-1)^k}{\sqrt{(2k+1)}}\sum_q (-1)^{-q} T_q^{(k)} U_{-q}^{(k)} \tag{3.50}$$

The scalar product of two tensor operators is defined as

$$(\mathbf{T}^{(k)} \cdot \mathbf{U}^{(k)}) = \sum_q (-1)^q T_q^{(k)} U_{-q}^{(k)} \tag{3.51}$$

It follows from Eqs.(3.49) and (3.51) that

$$[\mathbf{T}^{(k)}\mathbf{U}^{(k)}]_0^0 = \frac{(-1)^k}{\sqrt{(2k+1)}}(\mathbf{T}^{(k)} \cdot \mathbf{U}^{(k)}) \tag{3.52}$$

■ 3.17 Matrix elements of tensor operators

Henceforth we shall often write simply $\mathbf{X}^{(K)}$ rather than $\mathbf{X}^{(k_1k_2;K)}$ for a coupled tensor operator. It follows immediatedly from the Wigner-Eckart theorem that

$$\begin{aligned} &< \alpha j_1 j_2 JM|X_Q^{(K)}|\alpha' j_1' j_2' J'M' > \\ &= (-1)^{J-M} \left(\begin{array}{ccc} J & K & J' \\ -M & Q & M \end{array} \right) < \alpha j_1 j_2 J\|X^{(K)}\|\alpha' j_1' j_2' J' > \end{aligned} \tag{3.53}$$

Our problem is now to evaluate the reduced matrix element in Eq.(3.53). Basically this is done by an uncoupling of the bra and ket states and of the tensor operator followed by appropriate recouplings and summations. For the details I refer you to the books of Judd and of Edmonds.

If $\mathbf{T}^{(k)}$ and $\mathbf{U}^{(k)}$ act separately on parts 1 and 2 of a system such as in spin and orbit spaces or on different particles, or sets of particles, then we obtain the result

$$\begin{aligned} < \alpha j_1 j_2 J\|X^{(K)}\|\alpha' j_1' j_2' J' > = &\sum_{\alpha"} < \alpha j_1\|T^{(k_1)}\|\alpha" j_1' >< \alpha" j_2\|U^{(k_2)}\|\alpha' j_2' > \\ &\times \sqrt{(2J+1)(2K+1)(2J'+1)} \left\{ \begin{array}{ccc} j_1 & j_1' & k_1 \\ j_2 & j_2' & k_2 \\ J & J' & K \end{array} \right\} \end{aligned} \tag{3.54}$$

We can specialise the above result for $K = 0$ to obtain the scalar product as

$$\begin{aligned} &< \alpha j_1 j_2 JM\|(\mathbf{T}^{(k)} \cdot \mathbf{U}^{(k)})\|\alpha' j_1' j_2' J'M' > \\ &= \delta_{J,J'}\delta_{M,M'}(-1)^{j_1'+j_2+J} \left\{ \begin{array}{ccc} j_1' & j_2' & J \\ j_2 & j_1 & k \end{array} \right\} \\ &\times \sum_{\alpha"} < \alpha j_1\|T^{(k)}\|\alpha" j_1' >< \alpha" j_2\|U^{(k)}\|\alpha' j_2' > \end{aligned} \tag{3.55}$$

The action of an operator $\mathbf{T}^{(k)}$ acting on part 1 of a system can be found by putting $k_2 = 0$ in Eq.(3.54) to yield

$$< \alpha j_1 j_2 J \| T^{(k)} \| \alpha' j_1' j_2' J' > = \delta_{j_2, j_2'} (-1)^{j_1 + j_2 + J' + k} \sqrt{(2J+1)(2J'+1)} \left\{ \begin{array}{ccc} J & k & J' \\ j_1' & j_2 & j_1 \end{array} \right\}$$
$$\times < \alpha j_1 \| T^{(k)} \| \alpha' j_1' > \tag{3.56}$$

while the action on part 2 is found by putting $k_1 = 0$ in Eq.(3.54) to yield

$$< \alpha j_1 j_2 J \| U^{(k)} \| \alpha' j_1' j_2' J' > = \delta_{j_1, j_1'} (-1)^{j_1 + j_2' + J + k} \sqrt{(2J+1)(2J'+1)} \left\{ \begin{array}{ccc} J & k & J' \\ j_2' & j_1 & j_2 \end{array} \right\}$$
$$\times < \alpha j_2 \| U^{(k)} \| \alpha' j_2' > \tag{3.57}$$

A weaker result applicable to both cases where the operators act either on different parts of a system or indeed the same system may be derived to give

$$< \alpha J \| X^{(K)} \| \alpha' J' > = (-1)^{J + K + J'} \sqrt{(2K+1)} \sum_{\alpha", J"} \left\{ \begin{array}{ccc} k_2 & K & k_1 \\ J & J" & J' \end{array} \right\}$$
$$\times < \alpha J \| T^{(k_1)} \| \alpha" J" >< \alpha" J" \| U^{(k_2)} \| \alpha' J' > \tag{3.58}$$

The results given by Eqs. (3.53) to (3.58) form the basis for all subsequent applications of the theory of tensor operators.

■ 3.18 Spherical harmonics as tensor operators

The spherical harmonics $Y_{kq}(\theta, \phi)$ play a key role in many atomic and crystal field calculations. The spherical harmonics transform under the action of the generators of SO_3 just like the angular momentum states $|kq >$. Rather than using the spherical harmonics themselves it is usual to use tensor operators $\mathbf{C}^{(k)}$ whose $2k+1$ components $C_q^{(k)}$ are related to the spherical harmonics as

$$C_q^{(k)} = \sqrt{\frac{4\pi}{2k+1}} Y_{kq}(\theta, \phi) = (-1)^q \sqrt{\frac{(k-q)!}{(k+q)!}} P_k^q(\cos\theta) \exp iq\phi \tag{3.59}$$

where the $P_k^q(\cos\theta)$ are the usual Legendré polynomials.

The reduced matrix elements of $\mathbf{C}^{(k)}$ may be calculated by choosing to evaluate the matrix element of the component $C_0^{(k)}$ in an $\ell s-$basis between states with $m_\ell = 0$ as done, for example, by Judd to give

$$< \ell \| C^{(k)} \| \ell' > = (-1)^\ell \sqrt{(2\ell+1)(2\ell'+1)} \begin{pmatrix} \ell & k & \ell' \\ 0 & 0 & 0 \end{pmatrix} \tag{3.60}$$

The $3jm-$symbol vanishes unless $\ell + \ell' + k$ is $even$. The corresponding result for a $jj-$basis can be found by use of Eq. (7.30) followed by Eq. (7.33) to give

$$< s\ell j \| C^{(k)} \| s\ell' j' > = (-1)^{j - \frac{1}{2}} \sqrt{(2j+1)(2j'+1)} \begin{pmatrix} j & k & j' \\ -\frac{1}{2} & 0 & \frac{1}{2} \end{pmatrix} \tag{3.61}$$

where necessarily $\ell + \ell' + k$ is $even$.

■ 3.19 The njsymbol MAPLE file

It is useful to be able to calculate the values of the various $3nj-$symbols. This we accomplish in MAPLE by writing a batch of procedures which I have placed in a file "njsymbol" which includes necessary HELP files. These may be used as a basis for calculating quantities that require $3nj-$symbols. The relevant code is given verbatim below:

```
with(linalg):
#############################################################################
#test checks that the triangular condition on the three integers or   #
#half-integers a, b, c is satisfied.                                  #
#############################################################################
```

```
test:=proc(a,b,c)
      local result,result1,result2;
      if (evalb(a+b>=c) and evalb(c>=abs(a-b)))
      then result:=true else result:=false;
      fi;
      end:
#########################################################################
#threej evaluates 3jm-symbols.                                          #
#########################################################################
threej:=proc(j1,j2,j3,m1,m2,m3)
        local xmin,xmax,x,fact,sumx,result;
        if test(j1,j2,j3) and (m1+m2+m3 =0) then
        phase:=(-1)^(j1-j2-m3);
        fact:=sqrt(((j1+j2-j3)!*(j1-m1)!*(j2-m2)!*(j3+m3)!*(j3-m3)!)/
        ((j1+j2+j3+1)!*(j3+j1-j2)!*(j3+j2-j1)!*(j1+m1)!*(j2+m2)!));
        xmin:=max(0,j3-j2-m1);
        xmax:=min(j3+m3,j1-m1,j3+j2-m1);
        sumx:=0;
        for x from xmin to xmax do
sumx:=sumx + ((-1)^(j1-m1-x))*((j1+m1+x)!*(j3+j2-m1-x)!)/
      (x!*(j3+m3-x)!*(j1-m1-x)!*(j2-j3+m1+x)!);
                                od;
result:=simplify(phase*fact*sumx) else result:=0;
fi;
end:
#########################################################################
#ck evaluates the reduced matrix element <a//C^(k)//b>                  #
#########################################################################
ck:=proc(a,b,k)
    local result;
    result:=simplify((-1)^a*sqrt((2*a+1)*(2*b+1))*threej(a,k,b,0,0,0));
    end:
#########################################################################
#triad evaluates the triangular portion of the formulae for 6j-symbols  #
#########################################################################
triad:=proc(a,b,c)
       local triang;
       triang:=sqrt((((a+b-c)!*(a-b+c)!*(b+c-a)!)/(a+b+c+1)!));
       end:
#########################################################################
#sixj evaluates a 6j-symbol.                                            #
#########################################################################
sixj:=proc(a,b,c,d,e,f)
```

```
      local trif,sumj,zmin,zmax,z,result;
      if (test(a,b,c) and test(d,b,f) and test(d,e,c) and test(a,e,f))
      then
      trif:=simplify(triad(a,b,c)*triad(a,e,f)*triad(d,b,f)*triad(d,e,c));
      zmin:=max(a+b+c,a+e+f,d+b+f,d+e+c);
      zmax:=min(a+b+d+e,b+c+e+f,c+a+f+d);
      sumj:=0;
for z from zmin to zmax do
sumj:=sumj + (((-1)^z*(z+1)!)
/((z-a-b-c)!*(z-a-e-f)!*(z-d-b-f)!*(z-d-e-c)!*(a+b+d+e-z)!*(b+c+e+f-z)!
*(c+a+f+d-z)!));
od;
result:=simplify(trif*sumj) else result:=0;
fi;
end:
#############################################################################
#ninej evaluates a 9j-symbol                                                #
#############################################################################
ninej:=proc(a,b,c,d,e,f,h,i,j)
       local x,xmin,xmax,result;
if (test(a,d,h) and test(i,j,h) and test(b,e,i) and test(d,e,f) and
test(c,f,j) and test(c,a,b))
then
       xmax:=min(a+j,i+d,b+f);
       xmin:=max(abs(a-j),abs(i-d),abs(b-f));
       result:=0;
for x from xmin to xmax do
result:=result + ((-1)^(2*x))*(2*x + 1)*sixj(a,d,h,i,j,x)*sixj(b,e,i,d,x,f)
*sixj(c,f,j,x,a,b);
od;
result:=simplify(result)
else result:=0;
fi;
end:
#############################################################################
`help/text/njsymbol`:=TEXT(`HELP for njsymbol`,
`This package contains  procedures for calculating 3jm-, 6j- and 9j-symbols`,
`in rational form.The result appears as a fraction times square root factors.`,
`The square root factors can be combined into a single square root using the`,
`the MAPLE command combine("). The procedures can be used for inclusion in `,
`other MAPLE programmes requiring the use of njsymbols.`,
`The three procedures are as follows:-`,
``,
```

```
'threej(j1,j2,j3,m1,m2,m3):-',
'',
' This procedure evaluates the value of a 3jm-symbol involving the three',
' angular momenta j1, j2, j3 and their projections m1, m2, m3. The arguments',
' are entered as integers or half-integers as appropriate. The triangular',
' rules are automatically checked and if not satisfied the symbol is',
' evaluated to 0.',
'',
'sixj(a,b,c,d,e,f):-',
'',
' This procedure evaluates the value of a 6j-symbol involving the six',
' angular momenta a, b, c, d, e, f. The arguments are entered as integers or',
' half-integers as appropriate.The triangular rules are automatically checked',
' and if not satisfied the symbol is evaluated to 0.',
'',
'ninej(a,b,c,d,e,f,h,i):-',
'',
' This procedure evaluates the value of a 9j-symbol involving the nine',
' angular momenta a, b, c, d, e, f, g, h, i. The arguments are entered as',
' integers or half-integers as appropriate. The triangular rules are',
' automatically checked and if not satisfied the symbol is evaluated to 0.',
'',
'EXAMPLES:-',
'',
'1. threej(3/2,3/2,3,1/2,1/2,-1);',
'',
'2. sixj(3/2,3/2,3,1/2,7/2,2);',
'',
'3. ninej(3/2,3/2,3,1/2,7/2,3,2,2,2);'):
########################################################################
```

■ 3.20 Concluding Remarks

We are now at a stage to be able to consider the calculation of the influence of the crystal field of S_4 symmetry on the Ho^{3+} which we take up in the next lecture.

The Application of Symmetry Concepts
to
Physical Problems II (contd)
Analysis of Hyperfine structure in Crystals

B. G. Wybourne

It does not follow that beauty is experienced only in the context of great ideas and by great minds. This is no more true than that the jobs of creativity are restricted to a fortunate few. They are accessible to each one of us provided we are attuned to the perception of strangeness in the proportion and the conformity of the parts to one another and to the whole.

— S. Chandrasekhar, *Physics Today,* July , 1979, p30

■ Lecture 4

■ 4.1 Introduction

In this lecture I want to discuss the effect of the crystal field environment of the Ho^{3+} ion in $LiYF_4$ crystals. We will first consider give the eigenvectors that result from the free ion calculation for the low lying members of the ^5I multiplet and then consider the point syymetry group S_4 (not to be confused with the symmetric group!) and the qualitative predictions of the effect on the ground multiplet and then introduce the quantitative calculation of the crystal field effects.

■ 4.2 The free ion eigenvectors

The free ion eigenvectors for all members of the ground multiplet of Ho^{3+} may be obtained using the MAPLE commands given below:-

```
read`esof4`;
A:=mateval(energymatrix(8,20747,6608,28.79,608,0,0,0,-2163));
evalf(Eigenvals(A,V8));
j8:=array(sparse,1..7);
for i from 1 to 7 do j8[i]:=V8[i,1] od;
A:=mateval(energymatrix(7,20747,6608,28.79,608,0,0,0,-2163));
evalf(Eigenvals(A,V7));
j7:=array(sparse,1..7);
for i from 1 to 7 do j7[i]:=V7[i,1] od;
A:=mateval(energymatrix(6,20747,6608,28.79,608,0,0,0,-2163));
evalf(Eigenvals(A,V6));
```

```
j6:=array(sparse,1..13);
for i from 1 to 13 do j6[i]:=V6[i,1] od;
A:=mateval(energymatrix(5,20747,6608,28.79,608,0,0,0,-2163));
evalf(Eigenvals(A,V5));
j5:=array(sparse,1..14);
for i from 1 to 14 do j5[i]:=V5[i,1];od;
A:=mateval(energymatrix(4,20747,6608,28.79,608,0,0,0,-2163));
evalf(Eigenvals(A,V4));
j4:=array(sparse,1..19);
for i from 1 to 19 do j4[i]:=V4[i,1]; od;
print(j8);
print(j7);
print(j6);
print(j5);
print(j4);
```

The concluding print statements yield the eigenvectors as:-

```
ı print(j8);
[ -.9665441654, -.1188757869, .2221011067, .03257435612, -.01103118111,
  -.03326906193, .006512896685 ]
ı print(j7);
[ .9853358400, .03046183244, -.03222569090, .07338324177, -.1461563716,
 -.005621307008, -.01919580035 ]
ı print(j6);
[ .03111632461, -.01500275490, .08435166391, -.1351660676, .08192995026,
 -.9772280457, -.04595511259, .04540558570, .00949562729, .01921220624,
  .00793919455, -.03324327705, .07702916177 ]
ı print(j5);
[ .07174607879, .002987768121, -.03081364786, -.08131102394, .04553081666,
 -.02002957949, .1377250118, -.1944477670, .1067334993, -.03002479292,
 -.0113928741, -.9548891015, -.04740056952, .03933096028 ]
ı print(j4);
[ .003910968075, .01497113905, .006091052124, -.005552323510, .01595987535,
 -.005157397553, .003031891189, -.008909474397, -.05163280146,
  .02712445094, .01144861646, -.01592152155, -.04752158162, -.02954926223,
 -.003176349314, .1620348430, -.2247133842, .1185679116, -.9495184108 ]
```

Note that the components of the eigenvectors are listed in the same sequence as the zero-order states listed in Table 2.1. We shall be making use of the above eigenvectors later in the course.

■ 4.3 The Point Symmetry Group S_4

Ho^{3+} substitutes for the Y^{3+} in $LiYF_4$ at sites of tetragonal symmetry described by the point group S_4, not to be confused with the symmetric group on four objects! Since the ionic radii of Ho^{3+} and Y^{3+} are almost the same there is little, if any, lattice distortion. Extensive information on the group S_4 is given in:-

4.1 G.F.Koster, J.O.Dimmock, R.G.Wheeler and H.Statz, *Properties of the Thirty-Two Point Groups*, M.I.T. Press (1963).

The group S_4 is a cyclic group isomorphic to C_4, consisting of the identity, E, the rotation-reflection $S_4 = IC_4^{-1}$, a two-fold rotation C_2 and the inverse operator $S_4^{-1} = IC_4$. All rotations are taken about the $z-$axis. The character table is given below:-

	E	$\bar{E}$	S_4^{-1}	$\bar{S}_4^{-1}$	C_2	$\bar{C}_2$	S_4	$\bar{S}_4$
Γ_1	1	1	1	1	1	1	1	1
Γ_2	1	1	-1	-1	1	1	-1	-1
Γ_3	1	1	i	i	-1	-1	$-i$	$-i$
Γ_4	1	1	$-i$	$-i$	-1	-1	i	i
Γ_5	1	-1	ω	$-\omega$	i	$-i$	$-\omega^3$	ω
Γ_6	1	-1	$-\omega^3$	ω^3	$-i$	i	ω	$-\omega^3$
Γ_7	1	-1	$-\omega$	ω	i	$-i$	ω^3	ω
Γ_8	1	-1	ω^3	$-\omega^3$	$-i$	i	$-\omega$	ω^3

Table 4.1 The Character Table for the S_4 Point Group

with $\omega = \exp(\frac{\pi i}{4})$. Note that Γ_1 and Γ_2 are real one-dimensional representations whereas the remaining representations form complex pairs (Γ_3, Γ_4), (Γ_5, Γ_6), (Γ_7, Γ_8) and hence in the absence of magnetic fields are associated with doubly degenerate states. The last four representations are associated with the double group of S_4 and hence with half-integer angular momentum.

■ 4.4 Kronecker Products in S_4

The Kronecker products for S_4 may be easily established from the character table to yield the results given in Table 4.2 below:-

	Γ_1	Γ_2	Γ_3	Γ_4	Γ_5	Γ_6	Γ_7	Γ_8
Γ_1	Γ_1	Γ_2	Γ_3	Γ_4	Γ_5	Γ_6	Γ_7	Γ_8
Γ_2	Γ_2	Γ_1	Γ_4	Γ_3	Γ_7	Γ_8	Γ_5	Γ_6
Γ_3	Γ_3	Γ_4	Γ_2	Γ_1	Γ_8	Γ_5	Γ_6	Γ_7
Γ_4	Γ_4	Γ_3	Γ_1	Γ_2	Γ_6	Γ_7	Γ_8	Γ_5
Γ_5	Γ_5	Γ_7	Γ_8	Γ_6	Γ_3	Γ_1	Γ_4	Γ_2
Γ_6	Γ_6	Γ_8	Γ_5	Γ_7	Γ_1	Γ_4	Γ_2	Γ_3
Γ_7	Γ_7	Γ_5	Γ_6	Γ_8	Γ_4	Γ_2	Γ_3	Γ_1
Γ_8	Γ_8	Γ_6	Γ_7	Γ_5	Γ_2	Γ_3	Γ_1	Γ_4

Table 4.2 Kronecker Products for the Point Group S_4

■ 4.5 The $O_3 \Rightarrow S_4$ Branching rules

The degeneracies of the states of a given J in a crystal field of S_4 symmetry is determined by the $O_3 \Rightarrow S_4$ branching rules where O_3 is the *full* orthogonal group since the point group S_4 includes reflections and hence improper rotations. The irreducible representations of O_3 are labelled with a + or − superscript to distinguish those irreducible representations that are *even* under inversion (+) from those that are *odd* (-). Thus the results are given in Table 4.3 for integer and half-integer values of J. The decompositions of the D_j^- irreducible representations of O_3 may be obtained from those of D_j^+ by multiplication by Γ_2. Note that since the spin irreducible representations of S_4 are all two-dimensional the for half-integer angular momentum the levels in a crystal with point group symmetry S_4 must necessarily remain two-fold degenerate. An external magnetic field is required to lift this residual Kramer's degeneracy.

In the case of Ho^{3+} in $LiYF_4$ the electronic angular momentum J is an integer and the Stark electric field degeneracies follow from the appropriate $O_3 \Rightarrow S_4$ branching rules. Adding the half-integer angular momentum of the Ho nucleus results in states of total angular momentum $\mathbf{F}$ which is half-integer and hence the degeneracies are always two-fold. The hyperfine interaction will also change selection rules, as we shall see later.

D_J^+	S_4	D_J^-	S_4
D_0^+	Γ_1	D_0^-	Γ_2
D_1^+	$\Gamma_1 + \Gamma_3 + \Gamma_4$	D_1^-	$\Gamma_2 + \Gamma_3 + \Gamma_4$
D_2^+	$\Gamma_1 + 2\Gamma_2 + \Gamma_3 + \Gamma_4$	D_2^-	$2\Gamma_1 + \Gamma_2 + \Gamma_3 + \Gamma_4$
D_3^+	$\Gamma_1 + 2\Gamma_2 + 2\Gamma_3 + 2\Gamma_4$	D_3^-	$2\Gamma_1 + \Gamma_2 + 2\Gamma_3 + 2\Gamma_4$
D_4^+	$3\Gamma_1 + 2\Gamma_2 + 2\Gamma_3 + 2\Gamma_4$	D_4^-	$2\Gamma_1 + 3\Gamma_2 + 2\Gamma_3 + 2\Gamma_4$
D_5^+	$3\Gamma_1 + 2\Gamma_2 + 3\Gamma_3 + 3\Gamma_4$	D_5^-	$2\Gamma_1 + 3\Gamma_2 + 3\Gamma_3 + 3\Gamma_4$
D_6^+	$3\Gamma_1 + 4\Gamma_2 + 3\Gamma_3 + 3\Gamma_4$	D_6^-	$4\Gamma_1 + 3\Gamma_2 + 3\Gamma_3 + 3\Gamma_4$
D_7^+	$3\Gamma_1 + 4\Gamma_2 + 4\Gamma_3 + 4\Gamma_4$	D_7^-	$4\Gamma_1 + 3\Gamma_2 + 4\Gamma_3 + 4\Gamma_4$
D_8^+	$5\Gamma_1 + 4\Gamma_2 + 4\Gamma_3 + 4\Gamma_4$	D_8^-	$4\Gamma_1 + 5\Gamma_2 + 4\Gamma_3 + 4\Gamma_4$
$D_{1/2}^+$	$\Gamma_5 + \Gamma_6$	$D_{1/2}^-$	$\Gamma_7 + \Gamma_8$
$D_{3/2}^+$	$\Gamma_5 + \Gamma_6 + \Gamma_7 + \Gamma_8$	$D_{3/2}^-$	$\Gamma_5 + \Gamma_6 + \Gamma_7 + \Gamma_8$
$D_{5/2}^+$	$\Gamma_5 + \Gamma_6 + 2\Gamma_7 + 2\Gamma_8$	$D_{5/2}^-$	$2\Gamma_5 + 2\Gamma_6 + \Gamma_7 + \Gamma_8$
$D_{7/2}^+$	$2\Gamma_5 + 2\Gamma_6 + 2\Gamma_7 + 2\Gamma_8$	$D_{7/2}^-$	$2\Gamma_5 + 2\Gamma_6 + 2\Gamma_7 + 2\Gamma_8$
$D_{9/2}^+$	$3\Gamma_5 + 3\Gamma_6 + 2\Gamma_7 + 2\Gamma_8$	$D_{9/2}^-$	$2\Gamma_5 + 2\Gamma_6 + 3\Gamma_7 + 3\Gamma_8$
$D_{11/2}^+$	$3\Gamma_5 + 3\Gamma_6 + 3\Gamma_7 + 3\Gamma_8$	$D_{11/2}^-$	$3\Gamma_5 + 3\Gamma_6 + 3\Gamma_7 + 3\Gamma_8$
$D_{13/2}^+$	$3\Gamma_5 + 3\Gamma_6 + 4\Gamma_7 + 4\Gamma_8$	$D_{13/2}^-$	$4\Gamma_5 + 4\Gamma_6 + 3\Gamma_7 + 3\Gamma_8$
$D_{15/2}^+$	$4\Gamma_5 + 4\Gamma_6 + 4\Gamma_7 + 4\Gamma_8$	$D_{15/2}^-$	$4\Gamma_5 + 4\Gamma_6 + 4\Gamma_7 + 4\Gamma_8$
$D_{17/2}^+$	$5\Gamma_5 + 5\Gamma_6 + 4\Gamma_7 + 4\Gamma_8$	$D_{17/2}^-$	$4\Gamma_5 + 4\Gamma_6 + 5\Gamma_7 + 5\Gamma_8$
$D_{19/2}^+$	$5\Gamma_5 + 5\Gamma_6 + 5\Gamma_7 + 5\Gamma_8$	$D_{19/2}^-$	$5\Gamma_5 + 5\Gamma_6 + 5\Gamma_7 + 5\Gamma_8$
$D_{21/2}^+$	$5\Gamma_5 + 5\Gamma_6 + 6\Gamma_7 + 6\Gamma_8$	$D_{21/2}^-$	$6\Gamma_5 + 6\Gamma_6 + 5\Gamma_7 + 5\Gamma_8$
$D_{23/2}^+$	$6\Gamma_5 + 6\Gamma_6 + 6\Gamma_7 + 6\Gamma_8$	$D_{23/2}^-$	$6\Gamma_5 + 6\Gamma_6 + 6\Gamma_7 + 6\Gamma_8$

Table 4.3 Branching Rules for $O_3 \Rightarrow S_4$

■ 4.6 The D_{2d} Symmetry

The point group D_{2d} contains S_4 as a subgroup and hence exists as an *approximate* symmetry for describing Ho^{3+} in $LiYF_4$ crystals. D_{2d} is isomorphic to the group D_4 and consists of the operations of D_2 and in addition has the operations S_4 and S_4^{-1} about one of the two-fold axes of rotation about the $z-$axis, as well as two reflections σ_d through perpendicular planes containing the axis of S_4 and which bisect the angles between the two rotations of D_2 about the axes x and y, $C_{2'}$. The character table, Kronecker products, and $O_3 \Rightarrow D_{2d}$ decompositions are given in Koster *etal.* We shall refer to these later.

■ 4.7 The Crystal Field Expansion

We now must look at the effect of perturbing the "free ion" Ho^{3+} by a crystal field with point symmetry

S_4. As usual the crystal field potential is expanded as an infinite series of spherical tensors $C_q^{(k)}$ with associated coefficients B_q^k to give

$$V(r,\theta,\phi) = \sum_{k,q} B_q^k(r) C_q^{(k)}(\theta,\phi) \tag{4.1}$$

In future we will omit the spherical coordinates (r,θ,ϕ). The Hermiticity of the potential forces the axial expansion coefficients B_0^k to be real whereas the non-axial coefficients ($q \not\emptyset$) may be complex. The infinite series may be truncated by introducing various degrees of approximation. Between states of the *same* parity the triangular selection rules on the reduced matrix elements of $\mathbf{C}^{(k)}$ restrict the tensor ranks k to *even* integers and between states of *opposite* parity to *odd* integers. The values of k may be further restricted if we assume that the states of interest are limited to a single $N-$electron configuration ℓ^N. In that case not only must k be an even integer, it is bounded by

$$2\ell \geq k \geq 0 \tag{4.2}$$

Thus for f^N configurations we are restricted to the values

$$k = 0, 2, 4, 6 \tag{4.3}$$

Since the matrix elements of $C_0^{(0)}$ are constant over all the states of a configuration the term with $k = 0$ is usually omitted from consideration.

The possible values of q are restricted by two requirements. The first being simply that $k \geq |q|$ and the second that the potential be invariant with respect to all the symmetry operations of the relevant point group. Thus the S_4 symmetry forces the potential to be invariant with respect to four-fold rotations about a $z-$axis and hence restricting q to the values

$$q = 0, \pm 4 \tag{4.4}$$

The invariance with respect to the symmetry operations of the point group amounts to the requirement that the potential transform as the identity irreducible representation Γ_1 of the point group G. The number of independent expansion coefficients B_q^k for a given value of k is just the number of times Γ_1 occurs in the decomposition $O_3 \Rightarrow G$ of the O_3 irreducible representation D_k^+ which from Table 4.3 we find is 1 for $k = 2$ and 3 for both $k = 4$ and $k = 6$. This may be compared with the higher symmetry group D_2d where Γ_1 occurs once for $k = 2$ and twice for each of $k = 4$ and $k = 6$. Thus in D_{2d} the crystal field expansion for the states of f^N configurations will be:-

$$D_{2d} : V = B_0^2 C_0^{(2)} + B_0^4 C_0^{(4)} + B_4^4 (C_{-4}^{(4)} + C_4^{(4)}) + B_0^6 C_0^{(6)} + B_4^6 (C_{-4}^{(6)} + C_4^{(6)}) \tag{4.5}$$

The potential is Hermitian with the expansion coefficients B_q^k all *real*.

The lower symmetry of the point group S_4 manifests itself in the need for an extra expansion coefficient for each of the non-axial terms. This can be realised by taking the non-axial terms as *complex* rather than real. Thus for S_4 the crystal field potential becomes:-

$$S_4 : V = B_0^2 C_0^{(2)} + B_0^4 C_0^{(4)} + B_{\pm 4}^4 C_{\pm 4}^{(4)} + B_0^6 C_0^{(6)} + B_{\pm 4}^6 C_{\pm 4}^{(6)} \tag{4.6}$$

where

$$B_{\pm q}^k = B_q^k \pm i A_q^k \tag{4.7}$$

with B_q^k and A_q^k are both real. Thus the S_4 crystal field is associated with seven independent crystal field parameters whereas D_{2d} has five independent parameters. Note we now say *parameters* as along with most work we will treat the expansion coefficients as parameters to be determined from the experimental data rather than from some *ab initio* calculation. Before fitting the parameters to data we must calculate the angular matrix elements of the $C_q^{(k)}$ tensor operator components. This we will normally do in the customary angular momentum basis.

■ 4.8 Calculation of the Matrix elements of $C_q^{(k)}$

It follows from the Wigner-Eckart theorem that the M and q dependence of the matrix elements of $C_q^{(k)}$ is entirely cased in a single $3j-$symbol viz.

$$\langle \beta JM|C_q^{(k)}|\beta' J'M'\rangle = (-1)^{J-M}\begin{pmatrix} J & k & J' \\ -M & q & M' \end{pmatrix}\langle \beta J||C^{(k)}||\beta' J'\rangle \tag{4.8}$$

The selection rules for the $3j-$symbol to be non-vanishing force the triad (J, k, J') to satisfy the triangular condition

$$J + J' \geq k \geq |J - J'| \tag{4.9a}$$

and that

$$M - M' = q \tag{4.9b}$$

The reduced matrix elements in Eq. (4.8) may be evaluated in, an $|\alpha SLJ\rangle$ basis obtained from the earlier "free ion" calculation using the tensor operator algebra to give

$$\langle \alpha SLJ||C^{(k)}||\alpha' SL'J'\rangle = (-1)^{S+L'+J+k}\sqrt{(2J+1)(2J+1)}\begin{Bmatrix} J & k & J' \\ L' & S & L \end{Bmatrix}\langle \alpha SL||C^{(k)}||\alpha' SL'\rangle \tag{4.10}$$

Notice that the matrix elements are *diagonal* in the spin quantum number S[1]. However, there may be off-diagonal elements in L and J. The latter leads to so-called $J-$*mixing*. For most of our study we shall neglect $J-$mixing and assume that the significant matrix elements of interest are diagonal in J. Since our "free ion" eigenvectors involve non-trivial admixtures of states of different L we shall at times need to consider matrix elements off-diagonal in L and more often, in the auxilliary quantum numbers designated by α. The doubly reduced matrix elements in Eq. (4.10) may be directly taken from the tables of Nielson and Koster. They give the matrix elements for the unit tensor operators $U^{(k)}$ and multiplication by the reduced matrix elements $\langle f||C^{(k)}||f\rangle$ gives us the desired matrix elements. Nielson and Koster list the matrix elements for f^4 and to obtain them for f^{10} we must multiply by -1.

■ 4.9 Intermediate Coupling Reduced Matrix Elements

The "free ion" calculation yields an eigenvector expansion for the state $|\beta J\rangle$ (We suppress M quantum numbers here) of

$$|\beta J\rangle = \sum_{\alpha SL} a_{\alpha SLJ}|\alpha SLJ\rangle \tag{4.11}$$

Remembering that the matrix elements of the crystal field are diagonal in spin S we obtain the reduced matrix elements of the unit tensor operator, $U^{(k)}$, corrected for intermediate coupling as

$$\langle \beta J||U^{(k)}||\beta' J'\rangle = \sum_{\alpha SL}\sum_{\alpha' SL'} a_{\alpha SLJ}a^*_{\alpha' SL'J'}\langle \alpha SLJ||U^{(k)}||\alpha' SL'J'\rangle \tag{4.12}$$

Let us carry out the calculation for $k = 2$ for the "free ion" groundstate of Ho^{3+} in detail. From Table 3.1 we have the eigenvector expansion

$$|\beta J = 8\rangle = 0.9665|^5I_8\rangle + 0.1189|(21)^3K_8\rangle - 0.2221|(30)^3K_8\rangle \tag{4.13}$$

From page 74 of the tables of Nielson and Koster and multiplying by -1 to obtain results for f^{10} we have the required doubly reduced matrix elements of $U^{(2)}$ as

$$\begin{aligned} \langle {}^5I\|U^{(2)}\|{}^5I\rangle &= +\sqrt{\frac{13}{66}} \\ \langle (21)^3K\|U^{(2)}\|(21)^3K\rangle &= -\frac{1}{14}\sqrt{\frac{221}{2}} \\ \langle (21)^3K\|U^{(2)}\|(30)^3K\rangle &= -\frac{9}{7}\sqrt{\frac{2}{13}} \\ \langle (30)^3K\|U^{(2)}\|(30)^3K\rangle &= -5\sqrt{\frac{2}{221}} \end{aligned} \tag{4.14}$$

[1] NB. This is only strictly true if we ignore relativistic effects. See: B. G. Wybourne, *Use of Relativistic Wave Functions in Crystal Field Theory*, J. Chem. Phys., **43**, 4506-7 (1965).

The next step is to multiply these matrix elements to produce the singly reduced matrix elements from Eq. (4.10). This may be readily calculated using our MAPLE package "njsymbol" described in lecture three and the following extra MAPLE code:-

```
#############################################################################
#redmatrix is a single reduced matrix element produced from the doubly     #
#reduced matrix element rm.                                                #
#############################################################################
read`esof4`;
read`njsymbol`;
redmatrix:=proc(S,L1,J1,L2,J2,k,rm)
           local result;
  result:=combine(simplify((-1)^(S + L2 + J1 + k)*sqrt((2*J1 + 1)*(2*J2 + 1))/
*sixj(J1,k,J2,L2,S,L1)*ck(3,3,k)*rm));
  end:
#############################################################################
```

We finally tabulate our singly reduced matrix elements as a 3×3 matrix to give

$$A = \begin{array}{c} \\ {}^5I_8 \\ (21)^3K_8 \\ (30)^3K_8 \end{array} \begin{array}{c} \begin{array}{ccc} {}^5I_8 & (21)^3K_8 & (30)^3K_8 \end{array} \\ \begin{pmatrix} -\frac{\sqrt{9690}}{150} & 0 & 0 \\ 0 & \frac{13\sqrt{9690}}{1200} & \frac{3\sqrt{570}}{150} \\ 0 & \frac{3\sqrt{570}}{150} & \frac{7\sqrt{9690}}{1020} \end{pmatrix} \end{array}$$

We can input Eq.(4.13) into MAPLE as a column vector,V, and carry out the multiplication AV followed by the dotproduct of the resultant with V to finally yield the single number

$$\langle \beta J = 8 \| C^{(2)} \| \beta J = 8 \rangle = -0.6024 \tag{4.15a}$$

which may be compared with the $LS-$coupling value of

$$\langle {}^5I_8 \| C^{(2)} \| {}^5I_8 \rangle = -0.6563 \tag{4.15b}$$

■ **Exercises**

1. Complete the above calculation for $k = 4, 6$.
2. Repeat the calculation for the other levels of the ${}^5I$ multiplet.

In the next lecture we will use the results of the above exercises to calculate the crystal field splittings in the ground multiplet of Ho^{3+} in $LiYF_4$ crystals. We append the necessary doubly reduced matrix elements required in the exercises.

■ **4.10 Additional Reduced Matrix Elements**

The following doubly reduced matrix elements have been extracted from the tables of Nielson and Koster. Remembering that Professors often make mistakes you should check the entries.

MatrixElement	$k = 2$	$k = 4$	$k = 6$
$\langle {}^5I \Vert U^{(k)} \Vert {}^5I \rangle$	$+\sqrt{\frac{13}{66}}$	$\frac{-\sqrt{442}}{33}$	$+\frac{5}{11}\sqrt{\frac{323}{21}}$
$\langle (21)^3K \Vert U^{(k)} \Vert (20)^3K \rangle$	$-\frac{1}{14}\sqrt{\frac{221}{2}}$	$-\frac{1}{462}\sqrt{\frac{1615}{26}}$	$-\frac{4}{143}\sqrt{\frac{3230}{7}}$
$\langle (21)^3K \Vert U^{(k)} \Vert (30)^3K \rangle$	$-\frac{9}{7}\sqrt{\frac{2}{13}}$	$-\frac{115}{231}\sqrt{\frac{95}{26}}$	$-\frac{1}{143}\sqrt{1330}$
$\langle (30)^3K \Vert U^{(k)} \Vert (30)^3K \rangle$	$-5\sqrt{\frac{2}{221}}$	$-\frac{2}{33}\sqrt{\frac{3230}{13}}$	$+\frac{9}{143}\sqrt{\frac{190}{119}}$
$\langle (21)^3H \Vert U^{(k)} \Vert (21)^3H \rangle$	$-\frac{1}{5}\sqrt{\frac{143}{14}}$	$-\frac{11}{6}\sqrt{\frac{1}{91}}$	$-\frac{11}{13}\sqrt{\frac{17}{35}}$
$\langle (21)^3H \Vert U^{(k)} \Vert (30)^3H \rangle$	$-\frac{31}{15}\sqrt{\frac{11}{39}}$	$-\frac{19}{6}\sqrt{\frac{1}{68}}$	$-\frac{1}{39}\sqrt{\frac{170}{3}}$
$\langle (21)^3H \Vert U^{(k)} \Vert (11)^3H \rangle$	$-\frac{4}{45}\sqrt{11}$	$-\frac{5}{9}\sqrt{2}$	$+\frac{4}{9}\sqrt{\frac{34}{65}}$
$\langle (30)^3H \Vert U^{(k)} \Vert (30)^3H \rangle$	$-\frac{89}{30}\sqrt{\frac{11}{182}}$	$-\frac{53}{9}\sqrt{\frac{1}{91}}$	$+\frac{29}{68}\sqrt{\frac{17}{35}}$
$\langle (30)^3H \Vert U^{(k)} \Vert (11)^3H \rangle$	$-\frac{29}{15}\sqrt{\frac{11}{42}}$	$+2\sqrt{\frac{1}{21}}$	$-\frac{1}{3}\sqrt{\frac{119}{195}}$
$\langle (11)^3H \Vert U^{(k)} \Vert (11)^3H \rangle$	$-\frac{1}{5}\sqrt{\frac{143}{14}}$	$+\frac{2}{5}\sqrt{\frac{13}{7}}$	$+\sqrt{\frac{17}{35}}$

■ 4.11 The MAPLE commands for the intermediate coupling calculation

The following is a list of MAPLE commands to calculate the intermediate coupling calculations:-

```
#Calculation of intermediate coupling matrix elements for J = 8
read`redmat`;
#Intermediate coupling eigenvector V
 V:=array(1..3);
 V[1]:=0.9665;
 V[2]:=0.1189;
 V[3]:=-0.2221;
#Initialise A matrix
 S:=array(sparse,1..3,1..3);
 A:=array(symmetric,1..3,1..3);
 copyinto(S,A,1,1);
#Evaluate matrix elements of A in the LS-basis for k = 2
 A[1,1]:=redmatrix(2,6,8,6,8,2,sqrt(13/66));
 A[2,2]:=redmatrix(1,7,8,7,8,2,-sqrt(221/2)/14);
 A[2,3]:=redmatrix(1,7,8,7,8,2,-9*sqrt(2/13)/7);
 A[3,3]:=redmatrix(1,7,8,7,8,2,-5*sqrt(2/221));
 B:=mateval(A);
 print(B);
 multiply(B,V);
 dotprod(",V);
#Evaluate matrix elements of A in the LS-basis for k = 4
 A[1,1]:=redmatrix(2,6,8,6,8,4,-sqrt(442)/33);
 A[2,2]:=redmatrix(1,7,8,7,8,4,-sqrt(1615/26)/462);
 A[2,3]:=redmatrix(1,7,8,7,8,4,-115*sqrt(95/26)/231);
 A[3,3]:=redmatrix(1,7,8,7,8,4,-2*sqrt(3230/13)/33);
 B:=mateval(A);
 print(B);
 multiply(B,V);
 dotprod(",V);
#Evaluate matrix elements of A in the LS-basis for k = 6
 A[1,1]:=redmatrix(2,6,8,6,8,6,5*sqrt(323/21)/11);
 A[2,2]:=redmatrix(1,7,8,7,8,6,-4*sqrt(3230/7)/143);
 A[2,3]:=redmatrix(1,7,8,7,8,6,-sqrt(1330)/143);
 A[3,3]:=redmatrix(1,7,8,7,8,6,9*sqrt(190/119)/143);
 B:=mateval(A);
 print(B);
 multiply(B,V);
 dotprod(",V);
#End of J = 8 calculation
#Calculation of intermediate coupling matrix elements for J = 7
read`redmat`;
```

```
#Intermediate coupling eigenvector V
 V:=array(1..2);
 V[1]:=0.9853;
 V[2]:=-0.1462;
#Initialise A matrix
 S:=array(sparse,1..2,1..2);
 A:=array(symmetric,1..2,1..2);
 copyinto(S,A,1,1);
#Evaluate matrix elements of A in the LS-basis for k = 2
 A[1,1]:=redmatrix(2,6,7,6,7,2,sqrt(13/66));
 A[2,2]:=redmatrix(1,7,7,7,7,2,-5*sqrt(2/221));
 B:=mateval(A);
 print(B);
 multiply(B,V);
 dotprod(",V);
#Evaluate matrix elements of A in the LS-basis for k = 4
 A[1,1]:=redmatrix(2,6,7,6,7,4,-sqrt(442)/33);
 A[2,2]:=redmatrix(1,7,7,7,7,4,-115*sqrt(95/26)/231);
 B:=mateval(A);
 print(B);
 multiply(B,V);
 dotprod(",V);
#Evaluate matrix elements of A in the LS-basis for k = 6
 A[1,1]:=redmatrix(2,6,7,6,7,6,5*sqrt(323/21)/11);
 A[2,2]:=redmatrix(1,7,7,7,7,6,-sqrt(1330)/143);
 B:=mateval(A);
 print(B);
 multiply(B,V);
 dotprod(",V);
#End of J = 7 calculation
#Calculation of intermediate coupling matrix elements for J = 6
read`redmat`;
#Intermediate coupling eigenvector V
 V:=array(1..2);
 V[1]:=0.9772;
 V[2]:=0.1352;
#Initialise A matrix
 S:=array(sparse,1..2,1..2);
 A:=array(symmetric,1..2,1..2);
 copyinto(S,A,1,1);
#Evaluate matrix elements of A in the LS-basis for k = 2
 A[1,1]:=redmatrix(2,6,6,6,6,2,sqrt(13/66));
 A[2,2]:=redmatrix(1,7,6,7,6,2,-89*sqrt(11/182)/30);
```

```
 B:=mateval(A);
 print(B);
 multiply(B,V);
 dotprod(",V);
#Evaluate matrix elements of A in the LS-basis for k = 4
 A[1,1]:=redmatrix(2,6,6,6,6,4,-sqrt(442)/33);
 A[2,2]:=redmatrix(1,5,6,5,6,4,-53*sqrt(1/91)/9);
 B:=mateval(A);
 print(B);
 multiply(B,V);
 dotprod(",V);
#Evaluate matrix elements of A in the LS-basis for k = 6
 A[1,1]:=redmatrix(2,6,6,6,6,6,5*sqrt(323/21)/11);
 A[2,2]:=redmatrix(1,5,6,5,6,6,-sqrt(170/3)/39);
 B:=mateval(A);
 print(B);
 multiply(B,V);
 dotprod(",V);
#End of J = 6 intermediate coupling calculation.
#Calculation of intermediate coupling matrix elements for J = 5
read`redmat`;
#Intermediate coupling eigenvector V
 V:=array(1..4);
 V[1]:=0.9549;
 V[2]:=-0.1377;
 V[3]:=0.1944;
 V[4]:=-0.1067;
#Initialise A matrix
 S:=array(sparse,1..4,1..4);
 A:=array(symmetric,1..4,1..4);
 copyinto(S,A,1,1);
#Evaluate matrix elements of A in the LS-basis for k = 2
 A[1,1]:=redmatrix(2,6,5,6,5,2,sqrt(13/66));
 A[2,2]:=redmatrix(1,5,5,5,5,2,-sqrt(143/14)/5);
 A[2,3]:=redmatrix(1,5,5,5,5,2,-31*sqrt(11/39)/15);
 A[2,4]:=redmatrix(1,5,5,5,5,2,-4*sqrt(11)/45);
 A[3,3]:=redmatrix(1,5,5,5,5,2,-89*sqrt(11/182)/30);
 A[3,4]:=redmatrix(1,5,5,5,5,2,-29*sqrt(11/42)/15);
 A[4,4]:=redmatrix(1,5,5,5,5,2,-sqrt(143/14)/5);
 B:=mateval(A);
 print(B);
 multiply(B,V);
 dotprod(",V);
```

```
#Evaluate matrix elements of A in the LS-basis for k = 4
 A[1,1]:=redmatrix(2,6,5,6,5,4,-sqrt(442)/33);
 A[2,2]:=redmatrix(1,5,5,5,5,4,-11*sqrt(1/91)/6);
 A[2,3]:=redmatrix(1,5,5,5,5,4,-19*sqrt(1/68)/6);
 A[2,4]:=redmatrix(1,5,5,5,5,4,-5*sqrt(2)/9);
 A[3,3]:=redmatrix(1,5,5,5,5,4,-53*sqrt(1/91)/9);
 A[3,4]:=redmatrix(1,5,5,5,5,4,2*sqrt(1/21));
 A[4,4]:=redmatrix(1,5,5,5,5,4,2*sqrt(13/7)/5);
 B:=mateval(A);
 print(B);
 multiply(B,V);
 dotprod(",V);
#Evaluate matrix elements of A in the LS-basis for k = 6
 A[1,1]:=redmatrix(2,6,5,6,5,6,5*sqrt(323/21)/11);
 A[2,2]:=redmatrix(1,5,5,5,5,6,-11*sqrt(17/35)/13);
 A[2,3]:=redmatrix(1,5,5,5,5,6,-sqrt(170/3)/39);
 A[2,4]:=redmatrix(1,5,5,5,5,6,4*sqrt(34/65)/9);
 A[3,3]:=redmatrix(1,5,5,5,5,6,29*sqrt(17/35)/68);
 A[3,4]:=redmatrix(1,5,5,5,5,6,-sqrt(119/195)/3);
 A[4,4]:=redmatrix(1,5,5,5,5,6,sqrt(17/35));
 B:=mateval(A);
 print(B);
 multiply(B,V);
 dotprod(",V);
#End of J = 5 intermediate coupling calculation
#Calculation of intermediate coupling matrix elements for J = 4
read`redmat`;
#Intermediate coupling eigenvector V
 V:=array(1..4);
 V[1]:=0.9495;
 V[2]:=-0.1620;
 V[3]:=0.2247;
 V[4]:=-0.1186;
#Initialise A matrix
 S:=array(sparse,1..4,1..4);
 A:=array(symmetric,1..4,1..4);
 copyinto(S,A,1,1);
#Evaluate matrix elements of A in the LS-basis for k = 2
 A[1,1]:=redmatrix(2,6,4,6,4,2,sqrt(13/66));
 A[2,2]:=redmatrix(1,5,4,5,4,2,-sqrt(143/14)/5);
 A[2,3]:=redmatrix(1,5,4,5,4,2,-31*sqrt(11/39)/15);
 A[2,4]:=redmatrix(1,5,4,5,4,2,-4*sqrt(11)/45);
 A[3,3]:=redmatrix(1,5,4,5,4,2,-89*sqrt(11/182)/30);
```

```
 A[3,4]:=redmatrix(1,5,4,5,4,2,-29*sqrt(11/42)/15);
 A[4,4]:=redmatrix(1,5,4,5,4,2,-sqrt(143/14)/5);
 B:=mateval(A);
 print(B);
 multiply(B,V);
 dotprod(",V);
#Evaluate matrix elements of A in the LS-basis for k = 4
 A[1,1]:=redmatrix(2,6,4,6,4,4,-sqrt(442)/33);
 A[2,2]:=redmatrix(1,5,4,5,4,4,-11*sqrt(1/91)/6);
 A[2,3]:=redmatrix(1,5,4,5,4,4,-19*sqrt(1/68)/6);
 A[2,4]:=redmatrix(1,5,4,5,4,4,-5*sqrt(2)/9);
 A[3,3]:=redmatrix(1,5,4,5,4,4,-53*sqrt(1/91)/9);
 A[3,4]:=redmatrix(1,5,4,5,4,4,2*sqrt(1/21));
 A[4,4]:=redmatrix(1,5,4,5,4,4,2*sqrt(13/7)/5);
 B:=mateval(A);
 print(B);
 multiply(B,V);
 dotprod(",V);
#Evaluate matrix elements of A in the LS-basis for k = 6
 A[1,1]:=redmatrix(2,6,4,6,4,6,5*sqrt(323/21)/11);
 A[2,2]:=redmatrix(1,5,4,5,4,6,-11*sqrt(17/35)/13);
 A[2,3]:=redmatrix(1,5,4,5,4,6,-sqrt(170/3)/39);
 A[2,4]:=redmatrix(1,5,4,5,4,6,4*sqrt(34/65)/9);
 A[3,3]:=redmatrix(1,5,4,5,4,6,29*sqrt(17/35)/68);
 A[3,4]:=redmatrix(1,5,4,5,4,6,-sqrt(119/195)/3);
 A[4,4]:=redmatrix(1,5,4,5,4,6,sqrt(17/35));
B:=mateval(A);
print(B);
multiply(B,V);
dotprod(",V);
```

The above commands have been added to the diskette of MAPLE code for this lecture course.

■ 4.12 Intermediate Coupling corrected Reduced Matrix Elements

We list in the table below the intermediate coupling corrected matrix elements of the reduced matrix elements computed by the MAPLE code. The uncorrected matrix elements are in each case given immediately *below* each corrected matrix element.

$MatrixElement$	$k = 2$	$k = 4$	$k = 6$
$\langle {}^5I_8 \| C^{(k)} \| {}^5I_8 \rangle$	-0.6024	-0.6317	-1.6039
	-0.6563	-0.6797	-1.7061
$\langle {}^5I_7 \| C^{(k)} \| {}^5I_7 \rangle$	-0.5231	-0.4112	-0.2285
	-0.5524	-0.4042	-0.2399
$\langle {}^5I_6 \| C^{(k)} \| {}^5I_6 \rangle$	-0.4445	-0.2615	$+0.3000$
	-0.4775	-0.2614	$+0.3105$
$\langle {}^5I_5 \| C^{(k)} \| {}^5I_5 \rangle$	-0.4643	-0.2533	$+0.2549$
	-0.4428	-0.2437	$+0.2957$
$\langle {}^5I_4 \| C^{(k)} \| {}^5I_4 \rangle$	-0.4775	-0.4139	-0.7252
	-0.4505	-0.4103	-0.7679

The Application of Symmetry Concepts
to
Physical Problems II (contd)
Analysis of Hyperfine structure in Crystals

B. G. Wybourne

The creative principle resides in mathematics. In a certain sense, therefore, I hold it true that pure thought can grasp reality, as ancients dreamed
— A. Einstein
Continental people do not seem to be in the least interested to form a physical idea as a basis of theory. They are quite content to explain everything on a certain assumption and do not bother their heads about the real cause of a thing. I must say that the English point of view is much more physical and much to be preferred
— E. R. Rutherford

■ Lecture 5

■ 5.1 Introduction

In the previous lecture we outlined the crystal field expansion for S_4 symmetry and calculated the intermediate coupling corrections to give the reduced matrix elements $\langle \beta J \| C^{(k)} \| \beta J \rangle$ tabulated in Table 4.12. We must now use these to develop the calculation of the crystal field perturbation of the Ho^{3+} "free-ion" levels.

■ 5.2 Crystal Field Matrix Elements

We saw in the previous lecture that the crystal field potential for S_4 point symmetry acting on $f-$electrons can be written as

$$S_4 : V = B_0^2 C_0^{(2)} + B_0^4 C_0^{(4)} + B_{\pm 4}^4 C_{\pm 4}^{(4)} + B_{\pm 4}^6 C_{\pm 4}^{(6)} \tag{4.6}$$

where

$$B_{\pm q}^k = B_q^k \pm i A_q^k \tag{4.7}$$

and both B_q^k and A_q^k are real. In practice we can perform a rotation of the x and y axes about the $z-$axis to eliminate the imaginary part of either $B_{\pm 4}^4$ or $B_{\pm 4}^6$. Most workers choose $B_{\pm 4}^4$ to be real.

Recall the Wigner-Eckart theorem and write

$$\langle \beta J M | C_q^{(k)} | \beta' J' M' \rangle = (-1)^{J-M} \begin{pmatrix} J & k & J' \\ -M & q & M' \end{pmatrix} \langle \beta J \| C^{(k)} \| \beta' J' \rangle \tag{4.8}$$

For the present we shall only consider states within a given $J-$manifold, i.e. we shall ignore $J-$mixing. The reduced matrix elements can be taken from Table 4.12 to be corrected for intermediate coupling. Hermiticity conditions allow us to write

$$\langle \beta J M | V | \beta J M \rangle = \langle \beta J - M | V | \beta J - M \rangle \tag{5.1}$$

and

$$\langle \beta J M | V | \beta J M' \rangle = \langle \beta J M' | V | \beta J M \rangle^* \tag{5.2}$$

■ 5.3 Basis States and Crystal Field Splittings

A state of total angular momentum J is associated with $(2J+1)$ basis states $|JM\rangle$. In general the number of crystal field levels will be less than $(2J+1)$. Thus, for example, we have from Table 4.3 that a $J = 8$ level splits in S_4 point symmetry as

$$D_8^+ \Rightarrow 5\Gamma_1 + 4\Gamma_2 + 4(\Gamma_3 + \Gamma_4) \tag{5.3}$$

Remembering that the two irreducible representations Γ_3 and Γ_4 are complex conjugates and hence remain degenerate in an electric field, we obtain 13 sublevels. This means that in an appropriate basis that reflects the S_4 point symmetry the rank 17crystal field energy matrix will break into a rank 5 matrix involving 5 Γ_1 states, a rank 4 matrix involving 4 Γ_2 states and two rank 4 matrices associated with the Γ_3 and Γ_4 states.

The off-diagonal crystal field matrix elements will vanish unless

$$M' = M \pm 4 \tag{5.4}$$

Thus for $J = 8$ the following $|JM\rangle$ basis states are coupled by the crystal field potential:

$$\mu = 0 : |80\rangle, |8 \pm 4\rangle, |8 \mp 8\rangle \tag{5.5a}$$
$$\mu = \pm 1 : |8 \pm 1\rangle, |8 \mp 3\rangle, |8 \pm 5\rangle, |8 \mp 7\rangle \tag{5.5b}$$
$$\mu = 2 : |82\rangle, |8-2\rangle, |86\rangle |8-6\rangle \tag{5.5c}$$

where we have introduced the *crystal quantum numbers* μ. It can be readily seen that these correspond to the S_4 point symmetry group labels as

$$\mu = 0 : \Gamma_1, \mu = \pm 1 : \Gamma_{3,4}, \mu = 2 : \Gamma_2 \tag{5.6}$$

It is useful to introduce, for the $\mu = 0, 2$ states the symmetric and antisymmetric linear combinations

$$|JM\rangle_{\pm} = \frac{1}{\sqrt{2}}(|JM\rangle \pm |J - M\rangle) \tag{5.7}$$

We then have that

$$\langle JM|V|JM'\rangle_{++} = < JM|V|JM'\rangle_{--}, real \tag{5.8a}$$
$$\langle JM|V|JM'\rangle_{+-} = \langle JM'|V|JM\rangle^*_{-+}, imaginary \tag{5.8b}$$

■ 5.4 Example of the Ground Level of Ho^{3+}

It is instructive to focus attention on the ${}^5I_8$ level of Ho^{3+} in a S_4 point symmetry environment. Individual matrix elements, corrected for intermediate coupling may be computed using the following MAPLE code in the file "vs4"

```
########################################################################
#Calculates crystal field matrix elements for S4-point symmetry with#
#intermediate coupling correction within a given J-manifold.        #
########################################################################
read`njsymbol`;
read`icrm`;
ic();
vs4:=proc(J,M1,M2,k,q)
     local result;
     result:=(-1)^(J-M1)*threej(J,k,J,-M1,q,M2)*icrm[9-J,k/2];
     end:
crystal:=proc(J,M1,M2)
     local result;
     result:=simplify(B20*vs4(J,M1,M2,2,0) + B40*vs4(J,M1,M2,4,0) + B60*vs4(J,M1,M2,6,0)
 + (B44 + I*A44)*vs4(J,M1,M2,4,4) + (B44 - I*A44)*vs4(J,M1,M2,4,-4)
 + (B64 + I*A64)*vs4(J,M1,M2,6,4) + (B64 - I*A64)*vs4(J,M1,M2,6,-4));
  end:
```

where the file "icrm" contains the intermediate coupling reduced matrix elements

```
#############################################################################
#Array of intermediate coupling corrected matrix elements for the ground    #
#multiplet of Ho^3+. The first index i of the array corresponds to J = 9 - i#
#while the second index j corresponds to k = 2j.                            #
#############################################################################
ic:=proc()
icrm:=array(1..5,1..3);
icrm[1,1]:=-0.6024;
icrm[1,2]:=-0.6317;
icrm[1,3]:=-1.6039;
icrm[2,1]:=-0.5231;
icrm[2,2]:=-0.4112;
icrm[2,3]:=-0.2285;
icrm[3,1]:=-0.4445;
icrm[3,2]:=-0.2615;
icrm[3,3]:=0.3000;
icrm[4,1]:=-0.4643;
icrm[4,2]:=-0.2533;
icrm[4,3]:=0.2549;
icrm[5,1]:=-0.4775;
icrm[5,2]:=-0.4139;
icrm[5,3]:=-0.7252;
print();
end:
#############################################################################
```

The complete crystal field matrices for $\mu = 0, 1, 2$ are computed using the MAPLE files "crystal.8", "crystal.u81" and "crystal.u82" given below:

```
#############################################################################
#Calculation of crystal field matrix for the mu=0 states. Digits set at#
#5 for five figure accuracy.                                               #
#############################################################################
read`vs4`;
Digits:=5;
S:=array(sparse,1..5,1..5);
S[1,1]:=crystal(8,0,0);
S[1,2]:=evalf((crystal(8,0,4) + crystal(8,0,-4))/sqrt(2));
S[1,4]:=evalf((crystal(8,0,4) - crystal(8,0,-4))/sqrt(2));
S[2,1]:=S[1,2];
S[2,2]:=evalf((crystal(8,4,4) + crystal(8,-4,-4))/2);
S[2,3]:=evalf((crystal(8,4,8) + crystal(8,-4,-8))/2);
S[2,5]:=evalf((crystal(8,4,8) - crystal(8,-4,-8))/2);
S[3,2]:=S[2,3];
S[3,3]:=evalf((crystal(8,8,8) + crystal(8,-8,-8))/2);
S[3,4]:=evalf((crystal(8,8,4) - crystal(8,-8,-4))/2);
```

```
S[4,1]:=-S[1,4];
S[4,3]:=-S[3,4];
S[4,4]:=S[2,2];
S[4,5]:=S[3,2];
S[5,2]:=-S[2,5];
S[5,4]:=S[2,3];
S[5,5]:=S[3,3];
print(S);
#########################################################################
#Calculation of crystal field matrix for the mu=1 states. Digits set at#
#5 for five figure accuracy.                                            #
#########################################################################
read`vs4`;
Digits:=5;
C:=array(sparse,1..4,1..4);
C[1,1]:=crystal(8,1,1);
C[1,2]:=crystal(8,1,-3);
C[1,3]:=crystal(8,1,5);
C[2,1]:=evalc(conjugate(C[1,2]));
C[2,2]:=crystal(8,-3,-3);
C[2,4]:=crystal(8,-3,-7);
C[3,1]:=evalc(conjugate(C[1,3]));
C[3,3]:=crystal(8,5,5);
C[4,2]:=evalc(conjugate(C[2,4]));
C[4,4]:=crystal(8,-7,-7);
print(C);
#########################################################################
#Calculation of crystal field matrix for the mu=2 states. Digits set at#
#5 for five figure accuracy.                                            #
#########################################################################
read`vs4`;
Digits:=5;
B:=array(sparse,1..4,1..4);
B[1,1]:=evalf((crystal(8,2,2)+crystal(8,2,-2)
 +crystal(8,-2,2)+crystal(8,-2,-2))/2);
B[1,2]:=evalf((crystal(8,2,6)+crystal(8,-2,-6))/2);
B[1,3]:=evalf((crystal(8,2,2)-crystal(8,2,-2)
+crystal(8,-2,2)-crystal(8,-2,-2))/2);
B[1,4]:=evalf((crystal(8,2,6)-crystal(8,-2,-6))/2);
B[2,1]:=B[1,2];
B[2,2]:=evalf((crystal(8,6,6)+crystal(8,-6,-6))/2);
B[2,3]:=evalf((crystal(8,6,2)-crystal(8,-6,-2))/2);
B[2,4]:=0;
```

```
B[3,1]:=-B[1,3];
B[3,2]:=-B[2,3];
B[3,3]:=evalf((crystal(8,2,2)-crystal(8,2,-2)
-crystal(8,-2,2)+crystal(8,-2,-2))/2);
B[3,4]:=evalf((crystal(8,2,6)+crystal(8,-2,-6))/2);
B[4,1]:=-B[1,4];
B[4,2]:=0;
B[4,3]:=B[3,4];
B[4,4]:=B[2,2];
print(B);
```

Running the above files leads to the crystal field matrices

	$\|80\rangle$	$\|84\rangle_+$	$\|88\rangle_+$	$\|84\rangle_-$	$\|88\rangle_-$
$\langle 80\|$	$+.073435B_0^2$ $-.058492B_0^4$ $+.12642B_0^6$	$-.10224B_4^4$ $+.059290B_4^6$	0	$+.10224iA_4^4$ $-.059290iA_4^6$	0
${}_+\langle 84\|$	$-.10224B_4^4$ $+.059290B_4^6$	$+.024478B_0^2$ $+.038994B_0^4$ $-.13485B_0^6$	$-.016569B_4^4$ $-.14415B_4^6$	0	$+.016569iA_4^4$ $+.14415iA_4^6$
${}_+\langle 88\|$	0	$-.016569B_4^4$ $-.14415B_4^6$	$-.12240B_0^2$ $-.084486B_0^4$ $-.10956B_0^6$	$-.016569iA_4^4$ $-.14415iA_4^6$	0
${}_-\langle 84\|$	$-.10224iA_4^4$ $+.059290iA_4^6$	0	$+.016569iA_4^4$ $+.14415iA_4^6$	$+.024478B_0^2$ $+.038994B_0^4$ $-.13485B_0^6$	$-.016569B_4^4$ $-.14415B_4^6$
${}_-\langle 88\|$	0	$-.016569iA_4^4$ $-.14415iA_4^6$	0	$-.016569B_4^4$ $-.14415B_4^6$	$-.12240B_0^2$ $-.084486B_0^4$ $-.10956B_0^6$

Table 5.1 Crystal field matrix for the $\mu = 0$ states.

	$\|81\rangle_+$	$\|8-3\rangle_+$	$\|85\rangle_-$	$\|8-7\rangle_-$
$\langle 81\|$	$+.070377B_0^2$ $-.050370B_0^4$ $+.089551B_0^6$	$-.079194B_4^4$ $-.079194iA_4^4$ $+.11483B_4^6$ $+.11483iA_4^6$	$-.061444B_4^4$ $+.061444iA_4^4$ $-.053452B_4^6$ $+.053452iA_4^6$	0
$\langle 8-3\|$	$-.079194B_4^4$ $+.11483B_4^6$ $+.079194iA_4^4$ $-.11483iA_4^6$	$+.045897B_0^2$ $+.0048744B_0^4$ $-.097976B_0^6$	0	$-.032086B_4^4$ $-.17679B_4^6$ $-.032086iA_4^4$ $-.17679iA_4^6$
$\langle 85\|$	$-.061444B_4^4$ $-.053452B_4^6$ $-.061444iA_4^4$ $-.053452iA_4^6$	0	$-.0030598B_0^2$ $+.063366B_0^4$ $-.068476B_0^6$	0
$\langle 8-7\|$	0	$-.032086B_4^4$ $-.17679B_4^6$ $+.032086iA_4^4$ $+.17679iA_4^6$	0	$-.076496B_0^2$ $+.021122B_0^4$ $+.17803B_0^6$

Table 5.2 Crystal field matrix for the $\mu = 1$ states.

	$\|82\rangle_+$	$\|86\rangle_+$	$\|82\rangle_-$	$\|86\rangle_-$
$_+\langle 82\|$	$+.061196B_0^2$ $-.027622B_0^4$ $-.0021070B_0^6$ $-.081566B_4^4$ $+.14192B_4^6$	$-.047594B_4^4$ $-.13802B_4^6$	$+.081566iA_4^4$ $-.14192iA_4^6$	$.047594iA_4^4$ $+.13802iA_4^6$
$_+\langle 86\|$	$-.047594B_4^4$ $-.13802B_4^6$	$-.036720B_0^2$ $+.063366B_0^4$ $+.082174B_0^6$	$-.047594iA_4^4$ $-.13802iA_4^6$	0
$_-\langle 82\|$	$-.081566iA_4^4$ $+.14192iA_4^6$	$.047594iA_4^4$ $+.13802iA_4^6$	$.061196B_0^2$ $-.027622B_0^4$ $-.0021070B_0^6$ $+.081566B_4^4$ $-.14192B_4^6$	$-.047594B_4^4$ $-.13802B_4^6$
$_-\langle 86\|$	$-.047594iA_4^4$ $-.13802iA_4^6$	0	$-.047594B_4^4$ $-.13802B_4^6$	$-.036720B_0^2$ $+.063366B_0^4$ $+.082174B_0^6$

Table 5.3 Crystal field matrix for the $\mu = 2$ states.

■ 5.5 D_{2d} and S_4 Point Group Symmetry

The above matrices are Hermitian as required. It will be noted that with our choice of basis the imaginary elements occur as off-diagonal block matrices and indeed putting $A_4^4, A_4^6 = 0$ reduces the matrices to block diagonal form. Thus the rank 5 matrix for $\mu = 0$ splits into two submatrices of rank 3 and 2 and the rank 4 matrix for $\mu = 2$ splits into two identical matrices of rank 2. The matrix for $\mu = \pm 1$ remains irreducible. This can be understood by recalling that the crystal field potential for D_{2d}, Eq.(4.7), involves only real parameters and putting the imaginary parameters of the S_4 potenital to zero leads to the higher symmetry of D_{2d} symmetry. For a $J = 8$ level we have the $O_3 \Rightarrow D_{2d}$ decomposition

$$D_8^+ \Rightarrow 3\Gamma_1 + 2\Gamma_2 + 2\Gamma_3 + 2\Gamma_4 + 4\Gamma_5 \tag{5.9}$$

Furthermore, under $D_{2d} \Rightarrow S_4$ we have the compatibility table:

D_{2d}	Γ_1	Γ_2	Γ_3	Γ_4	Γ_5	Γ_6	Γ_7
S_4	Γ_1	Γ_1	Γ_2	Γ_2	$\Gamma_3 + \Gamma_4$	$\Gamma_5 + \Gamma_6$	$\Gamma_7 + \Gamma_8$

Table 5.4 $D_{2d} : S_4$ Group Compatibility table

In the case of the $\mu = 0$ matrix putting the imaginary part to zero leaves a rank 3 matrix involving 3 symmetric basis states whereas the rank 2 matrix involves 2 antisymmetric basis states. Under D_{2d} symmetry the 3 symmetric states transform as Γ_1 states while the 2 antisymmetric states transform as Γ_2 states. The effect of including the imaginary terms is to lead to a coupling of the five basis states to yield states transforming under S_4 as Γ_1. This is consistent with S_4 being a *lower symmetry* than D_{2d}.

Inspection of Eq.(5.9) and of Table 5.4 suggests that the number of crystal field levels in S_4 and D_{2d} for $J = 8$ is in each case 13. In practice the $\mu = 2$ levels are two-fold degenerate in D_{2d} whereas for S_4 the $\mu = 2$ levels are non-degenerate, the degeneracy being lifted by the imaginary term. This is seen experimentally with the $\mu = 2$ levels occurring at energies (in cm^{-1})

$$\mu = 0 : 7,\ 23,\ 289,\ 315$$

Here we have two pairs of levels and their comparatively small splittings is a measure of the strength of the imaginary term.

Our next problem is to deduce a set of crystal field parameters that is consistent with the observed crystal field levels - the subject of our next lecture.

■ Exercises

5.1 Construct the crystal field matrices for the $J = 4,\ 5,\ 6,\ 7$ levels of the ground multiplet of Ho^{3+} in $LiYF_4$.

5.2 Consider how you could determine the parameters of the crystal fields to optimise the description of the experimental levels.

The Application of Symmetry Concepts
to
Physical Problems II (contd)
Analysis of Hyperfine structure in Crystals

B. G. Wybourne

Where in the Schrødinger equation do you put the joy of being alive?
— E. P. Wigner
The most important thing accomplished by the discovery of the radiation background in 1965 was to force all of us to take seriously the idea that there **was** *an early universe*
— Steven Weinberg, *The First Three Minutes*

■ Lecture 6

■ 6.1 Introduction

In the last lecture we showed how to include the crystal field potential and to construct the relevant crystal field matrices suitably corrected for intermediate coupling. In this lecture we diagonalise the matrices and make a comparison with experimental data. We shall find that while the splitting of the ground level ($J = 8$) the higher members of the multiplet show significant deviations from experiment, especially for the $J = 5$ and $J = 4$. We illustrate how the situation can be improved by allowing the crystal field to couple the adjacent J levels, so-called $J-$mixing. Finally we view the eigenvectors of the low-lying states and consider the Zeeman matrix elements for the two lowest states. We should then be ready to consider the final perturbation coming from the nuclear hyperfine interaction.

■ 6.2 Construction of the Crystal Field Matrix Elements

The key to the calculation is our Maple file "vs4" which calculates individual matrix elements diagonal in J but with correction for intermediate coupling using the coefficients stored in the file "icrm":-

```
#########################################################################
#Calculates crystal field matrix elements for S4-point symmetry with#
#intermediate coupling correction within a given J-manifold.        #
#########################################################################
read`njsymbol`;
read`icrm`;
ic();
vs4:=proc(J,M1,M2,k,q)
     local result;
     result:=(-1)^(J-M1)*threej(J,k,J,-M1,q,M2)*icrm[9-J,k/2];
     end:
crystal:=proc(J,M1,M2)
     local result;
 result:=simplify(B20*vs4(J,M1,M2,2,0) + B40*vs4(J,M1,M2,4,0)
      + B60*vs4(J,M1,M2,6,0) + (B44 + I*A44)*vs4(J,M1,M2,4,4)
      + (B44 - I*A44)*vs4(J,M1,M2,4,-4) + (B64 + I*A64)*vs4(J,M1,M2,6,4)
      + (B64 - I*A64)*vs4(J,M1,M2,6,-4));
  end:
```

The individual crystal field matrices are then computed using the crystal field parameters defined in the Maple file "crystal.par". As an initial estimate we take those deduced in

6.1 N.Karayianus, D. E. Wortman and H. P. Jenssen, *Analysis of the optical spectrum of Ho^{3+} in $LiYF_4$*, J. Phys. Chem. Solids, **37**, 675-662 (1976).

who made a least-squares fit to the experimental data known at that time and found (in cm^{-1})

$$B_0^2 = 410,\ B_0^4 = -615,\ B_0^6 = -27.9,\ B_4^4 = 819,\ B_4^6 = 677,\ A_4^6 = \pm 32.8 \tag{6.1}$$

More complete experimental data is given in Table IX in

6.2 N. I. Agladze, M. N. Popova, M. A. Koreiba, B. Z. Malkin and V. R. Pekurovskii, *Isotope effects in the lattice structure and vibrational and optical spectra of $^6Li_x{}^7Li_{1-x}YF_4 : Ho$ crystals*, JETP **77**, 1021-1033 (1993).

The relevant crystal field matrices are contained in the Maple files crystal.J where J is the integer value of the angular momentum of the level. We print below the file "crystal.8"

```
Digits:=5:
read`vs4`:
read`crystal.par`:
#############################################################################
#Crystal field matrix for J = 8 with $\mu = 0$.                             #
#############################################################################
crystal.par();
crystal80:=proc()
S80:=array(sparse,1..5,1..5);
S80[1,1]:=Eadd8+crystal(8,0,0);
S80[1,2]:=evalf((crystal(8,0,4) + crystal(8,0,-4))/sqrt(2));
S80[1,4]:=evalf((crystal(8,0,4) - crystal(8,0,-4))/sqrt(2));
S80[2,1]:=S80[1,2];
S80[2,2]:=evalf(Eadd8+(crystal(8,4,4) + crystal(8,-4,-4))/2);
S80[2,3]:=evalf((crystal(8,4,8) + crystal(8,-4,-8))/2);
S80[2,5]:=evalf((crystal(8,4,8) - crystal(8,-4,-8))/2);
S80[3,2]:=S80[2,3];
S80[3,3]:=evalf(Eadd8+(crystal(8,8,8) + crystal(8,-8,-8))/2);
S80[3,4]:=evalf((crystal(8,8,4) - crystal(8,-8,-4))/2);
S80[4,1]:=-S80[1,4];
S80[4,3]:=-S80[3,4];
S80[4,4]:=S80[2,2];
S80[4,5]:=S80[3,2];
S80[5,2]:=-S80[2,5];
S80[5,4]:=S80[2,3];
S80[5,5]:=S80[3,3];
print();
end:
crystal80();
print(`Eigenvalues for J=8 with mu=0`);
evalf(Eigenvals(S80,V80));
print(`Eigenvectors for J = 8 with mu=0`);
print(V80);
#############################################################################
```

```
#Crystal field matrix for J = 8 with $\mu = 1$.                                #
################################################################################
crystal81:=proc()
S81:=array(sparse,1..4,1..4);
S81[1,1]:=Eadd8+crystal(8,1,1);
S81[1,2]:=crystal(8,1,-3);
S81[1,3]:=crystal(8,1,5);
S81[2,1]:=evalc(conjugate(S81[1,2]));
S81[2,2]:=Eadd8+crystal(8,-3,-3);
S81[2,4]:=crystal(8,-3,-7);
S81[3,1]:=evalc(conjugate(S81[1,3]));
S81[3,3]:=Eadd8+crystal(8,5,5);
S81[4,2]:=evalc(conjugate(S81[2,4]));
S81[4,4]:=Eadd8+crystal(8,-7,-7);
end:
crystal81();
print(`Eigenvalues for J=8 with mu=1`);
evalf(Eigenvals(S81,V81));
print(`Eigenvectors for J = 8 with mu=1`);
print(V81);
################################################################################
#Crystal field matrix for J = 8 with $\mu = 2$.                                #
################################################################################
crystal82:=proc()
S82:=array(sparse,1..4,1..4);
S82[1,1]:=evalf(Eadd8+(crystal(8,2,2)+crystal(8,2,-2)+crystal(8,-2,2)
 +crystal(8,-2,-2))/2);
S82[1,2]:=evalf((crystal(8,2,6)+crystal(8,-2,-6))/2);
S82[1,3]:=evalf((crystal(8,2,2)-crystal(8,2,-2)+crystal(8,-2,2)
 -crystal(8,-2,-2))/2);
S82[1,4]:=evalf((crystal(8,2,6)-crystal(8,-2,-6))/2);
S82[2,1]:=S82[1,2];
S82[2,2]:=evalf(Eadd8+(crystal(8,6,6)+crystal(8,-6,-6))/2);
S82[2,3]:=evalf((crystal(8,6,2)-crystal(8,-6,-2))/2);
S82[2,4]:=0;
S82[3,1]:=-S82[1,3];
S82[3,2]:=-S82[2,3];
S82[3,3]:=evalf(Eadd8+(crystal(8,2,2)-crystal(8,2,-2)-crystal(8,-2,2)
 +crystal(8,-2,-2))/2);
S82[3,4]:=evalf((crystal(8,2,6)+crystal(8,-2,-6))/2);
S82[4,1]:=-S82[1,4];
S82[4,2]:=0;
S82[4,3]:=S82[3,4];
```

```
S82[4,4]:=S82[2,2];
print();
end:
crystal82();
print(‘Eigenvalues for J=8 with mu=2‘);
evalf(Eigenvals(S82,V82));
print(‘Eigenvectors for J = 8 with mu=2‘);
print(V82);
#########################################################################
```

■ 6.3 Calculation of Crystal Field Sublevels

Running the Maple files "crystal.J" using the parameters given in Eq. (6.1) and setting the EaddJ parameters so as to make the lowest crystal field level zero we obtain the results given in Table 6.1.

Inspection of Table 6.1 shows that the agreement between the experimental and calculated values is very good for the $J = 8$ and gets progressively worse as we move to higher levels. The levels for $J = 5$ and $J = 4$ are particularly distorted. Several sublevels for $J = 5$ are calculated as too high whereas for $J = 4$ the corresponding sublevels are too low. This suggests that the $J = 4$ and $J = 5$ states need to interact in such a way as to repel sublevels. This would be the case if there was $J-$mixing by the crystal field potential.

J	μ	$Expt$	$Calc$
8	1	0	0
$(0cm^{-1})$	2	7	7
	2	23	26
	0	48	46
	0	56	52
	1	72	76
	0	217	219
	1	270	272
	0	276	275
	2	283	281
	0	290	290
	1	303	304
	2	315	321
7	2	0	0
$(5152cm^{-1}$	1	3.4	6
	0	10.5	18
	2	11.0	11
	1	32.4	32
	0	53.8	47
	1	75.5	82
	2	80.3	89
	2	138.7	141
	1	140.6	145
	0	140.8	147
6	2	0	0
$(8671cm^{-1})$	0	2.4	9
	1	9.4	11
	1	15.0	15
	2	16.8	22
	0	26.5	21
	2	31.1	35
	0	98.1	100
	1	112.8	111
	2	125.7	121
5	1	0	0
$(11242cm^{-1})$	0	5.6	1
	1	8.4	16
	2	12.4	1
	0	14.0	7
	0	59.4	92
	1	88.4	103
	2	94.4	149
4	0	0	0
$(13188cm^{-1})$	1	81.5	76
	2	133.0	136
	0	152.6	127
	2	162.7	150
	1	219	208
	0	351.5	342

■ 6.4 $J-$Mixing by the Crystal Field Potential

As a partial example of the effects of $J-$mixing let us consider the matrix elements that couple the $J = 4$ states to those of $J = 5$. Here we must choose Eadd4 and Eadd5 to include the free ion energies which we will however take as the experimental mean energies given in Table 6.1. We must also compute the matrix elements of the crystal field potential between the $J = 4$ and $J = 5$ states for each value of μ. This may be done in Maple by generalising the file "vs4" to the file "vs4g" given below

```
#########################################################################
#Calculates crystal field matrix elements for S4-point symmetry with#
#intermediate coupling correction between two J-manifolds.          #
#########################################################################
read`njsymbol`;
vs4g:=proc(J1,k,J2,M1,q,M2)
     local result;
     result:=(-1)^(J1-M1)*threej(J1,k,J2,-M1,q,M2)*icjmix[k/2];
     end:
crystalg:=proc(J1,J2,M1,M2)
     local result;
     result:=simplify(B20*vs4g(J1,2,J2,M1,0,M2) + B40*vs4g(J1,4,J2,M1,0,M2)
 + B60*vs4g(J1,6,J2,M1,0,M2) + (B44 + I*A44)*vs4g(J1,4,J2,M1,4,M2)
 + (B44 - I*A44)*vs4g(J1,4,J2,M1,-4,M2) + (B64 + I*A64)*vs4g(J1,6,J2,M1,4,M2)
 + (B64 - I*A64)*vs4g(J1,6,J2,M1,-4,M2));
  end:
#########################################################################
```

and then use our Maple files "j45.mu" where mu is the integer μ of the crystal quantum number. The case of "j45.0" is given below

```
#########################################################################
#Crystal field matrix for mu = 0 states of J =4 and 5 combined.        #
#########################################################################
read`vs4`;
read`icjm`;
read`vs4g`;
read`crystal.par`;
Digits:=5;
#########################################################################
#Crystal field matrix for J=4 with $\mu = 0$.                          #
#########################################################################
crystal40:=proc()
crystal.par();
S40:=array(sparse,1..3,1..3);
S40[1,1]:=Eadd4+crystal(4,0,0);
S40[1,2]:=evalf((crystal(4,0,4) + crystal(4,0,-4))/sqrt(2));
S40[1,3]:=evalf((crystal(4,0,4) - crystal(4,0,-4))/sqrt(2));
S40[2,1]:=evalc(conjugate(S40[1,2]));
S40[2,2]:=Eadd4+evalf((crystal(4,4,4) + crystal(4,-4,-4))/2);
```

```
S40[2,3]:=evalf((crystal(4,4,4) - crystal(4,-4,-4))/2);
S40[3,1]:=evalc(conjugate(S40[1,3]));
S40[3,2]:=evalc(conjugate(S40[2,3]));
S40[3,3]:=S40[2,2];
end:
#########################################################################
#Crystal field matrix for J=5 with $\mu = 0$.                           #
#########################################################################
crystal50:=proc()
crystal.par();
S50:=array(sparse,1..3,1..3);
S50[1,1]:=Eadd5+crystal(5,0,0);
S50[1,2]:=evalf((crystal(5,0,4) + crystal(5,0,-4))/sqrt(2));
S50[1,3]:=evalf((crystal(5,0,4) - crystal(5,0,-4))/sqrt(2));
S50[2,1]:=evalc(conjugate(S50[1,2]));
S50[2,2]:=evalf(Eadd5+(crystal(5,4,4) + crystal(5,-4,-4))/2);
S50[2,3]:=evalf((crystal(5,4,4) - crystal(5,-4,-4))/2);
S50[3,1]:=evalc(conjugate(S50[1,3]));
S50[3,2]:=evalc(conjugate(S50[2,3]));
S50[3,3]:=S50[2,2];
end:
#########################################################################
#Matrix elements coupling J=4 to J=5  for mu=0.                         #
#########################################################################
crystal45:=proc()
crystal.par();
icj();
jmix:=array[1..3];
jmix:=jmix45();
S45:=array(sparse,1..6,1..6);
S45[1,4]:=crystalg(4,5,0,0);
S45[1,5]:=evalf((crystalg(4,5,0,4)+crystalg(4,5,0,-4))/sqrt(2));
S45[1,6]:=evalf((crystalg(4,5,0,4)-crystalg(4,5,0,-4))/sqrt(2));
S45[2,4]:=evalf((crystalg(4,5,4,0)+crystalg(4,5,-4,0))/sqrt(2));
S45[2,5]:=evalf((crystalg(4,5,4,4)+crystalg(4,5,-4,-4))/2);
S45[2,6]:=evalf((crystalg(4,5,4,4)-crystalg(4,5,-4,-4))/2);
S45[3,4]:=evalf((crystalg(4,5,4,0)-crystalg(4,5,-4,0))/sqrt(2));
S45[3,5]:=evalf((crystalg(4,5,4,4)-crystalg(4,5,-4,-4))/2);
S45[3,6]:=evalf((crystalg(4,5,4,4)+crystalg(4,5,-4,-4))/2);
S45[4,1]:=evalc(conjugate(S45[1,4]));
S45[5,1]:=evalc(conjugate(S45[1,5]));
S45[6,1]:=evalc(conjugate(S45[1,6]));
S45[4,2]:=evalc(conjugate(S45[2,4]));
```

```
S45[5,2]:=evalc(conjugate(S45[2,5]));
S45[6,2]:=evalc(conjugate(S45[2,6]));
S45[4,3]:=evalc(conjugate(S45[3,4]));
S45[5,3]:=evalc(conjugate(S45[3,5]));
S45[6,3]:=evalc(conjugate(S45[3,6]));
end:
Ecalc:=proc()
A0:=array(sparse,1..6,1..6);
crystal40();
crystal45();
crystal50();
copyinto(S45,A0,1,1);
copyinto(S40,A0,1,1);
copyinto(S50,A0,4,4);
print(`Crystal Field Energy Matrix for mu = 0 for J = 4 and 5 combined`);
print(A0);
end:
Ecalc();
print(`Eigenvalues for mu = 0 for J = 4 and 5 combined`);
evalf(Eigenvals(A0,V0));
print(`Eigenvectors for mu = 0 for J = 4 and 5 combined`);
print(V0);
```

Running the above file leads to the following crystal field energy matrix for the $\mu = 0$ states with $J = 4$ and 5. The introduction of $J-$mixing has produced the additional matrix elements coupling the two rank 3 matrices for the states with $J = 4$ and 5. In particular note the rather large coupling between the $|44\rangle_-$ and $|50\rangle$ states.

$$\begin{array}{c} \\ \langle 40| \\ {}_+\langle 44| \\ {}_-\langle 44| \\ \langle 50| \\ {}_+\langle 54| \\ {}_-\langle 54| \end{array} \begin{array}{c} \begin{array}{cccccc} |40\rangle & |44\rangle_+ & |44\rangle_- & |50\rangle & |54\rangle_+ & |54\rangle_- \end{array} \\ \begin{pmatrix} 13402. & -166.13 & 5.6261i & 0 & -1.2351i & -48.192 \\ -166.13 & 13317. & 0 & 8.6457i & 0 & -24.530 \\ -5.6261i & 0 & 13317. & 202.99 & -24.530 & 0 \\ 0 & -8.6457i & 202.99 & 11331. & -17.549 & -.83070i \\ 1.2351i & 0 & -24.530 & -17.549 & 11249. & 0 \\ -48.192 & -24.530 & 0 & .83070i & 0 & 11249. \end{pmatrix} \end{array}$$

Diagonalisation of the complex Hermitian energy matrix yields the six eigenvalues as

$$[13530., 13187., 13337., 11312., 11246., 11242.]$$

and the eigenvectors

$$\begin{array}{cc} Eigenvalue & \begin{array}{cccccc} 13530 & 13187 & 13337 & 11312 & 11246 & 11242 \end{array} \\ |40\rangle & \begin{pmatrix} .79449 & .60677 & .0031973 & -.00019 & .02341 & .00077 \\ -.60689 & .79386 & .03535 & .00397 & .01388 & .00156 \\ -.01907i & .03024i & -.99419i & -.10132i & -.00176i & -.00843i \\ .00062i & -.00037i & -.10147i & .97399i & .00528i & .20293i \\ .00063i & 0 & .01240i & -.20254i & -.05059i & .97763i \\ -.01018 & -.02523 & -.00114 & -.01559 & .99835 & .05524 \end{pmatrix} \\ |44\rangle_+ & \\ |44\rangle- & \\ |50\rangle & \\ |54\rangle_+ & \\ |54\rangle_- & \end{array}$$

Notice that the eigenvectors indicate that there is significant $J-$mixing for the eigenvalues 13337, 11312

and 11246. Furthermore, whereas without $J-$mixing the relative separations of the $J=4$ states were 0, 127, 342 with $J-$mixing they have become 0, 150, 343 comparing more favourably with the relative experimental separations of 0, 152.65, 351.5 - a substantial improvement. Likewise for the $J=4$ states without $J-$mixing the relative separations were 0, 6, 92, with $J-$mixing they became 0, 4, 66 comparing favourably with the experimental values of 0, 8.4, 53.8. Some additional improvement could be expected by extending the $J-$mixing calculation to include the $J=6$ states and by fine tuning the parameters.

■ 6.5 Quenching of Angular Momentum

In carrying out the above calculations we made use of symmetric and antisymmetric combinations of angular momentum $|JM\rangle$ states. This resulted in combining states $|JM\rangle$ and $|J-M\rangle$ in equal parts and hence to form states whose angular momentum was "quenched". Inspection of the eigenvectors shows that indeed many of the states do occur with quenched angular momentum which has ramifications for their magnetic behaviour and, as we shall see later, consequences for the magnetic nuclear hyperfine structure.

■ 6.6 The Groundstate of $LiYF_4 : Ho^{3+}$

We may summarise our information on the groundstate of $LiYF_4 : Ho^{3+}$ in terms of the following eigenvalues and eigenvectors calculated using the Maple file "crystal.8"

Eigenvalues and eigenvectors for $J=8$ with $\mu=0$

$$\begin{array}{lc} Eigenvalue & \begin{array}{ccccc} 45.9 & 218.6 & 290.1 & 51.6 & 274.6 \end{array} \\ |80\rangle & \left(\begin{array}{ccccc} .17575 & .87070 & -.45932 & 0 & 0 \end{array} \right. \\ |84\rangle_+ & \left(\begin{array}{ccccc} .73385 & .19446 & .64932 & -.032543 & .030424 \end{array} \right. \\ |88\rangle_+ & \left(\begin{array}{ccccc} .65532 & -.45164 & -.60543 & -.00140 & -.00151 \end{array} \right. \\ |84\rangle_- & \left(\begin{array}{ccccc} -.03273i & -.00868i & -.02897i & -.72989i & .68215i \end{array} \right. \\ |88\rangle_- & \left(\begin{array}{ccccc} -.001356i & .00093i & .00125i & -.68280i & -.73056i \end{array} \right) \end{array}$$

Eigenvalues and eigenvectors for $J=8$ with $\mu=1$

$$\begin{array}{lc} Eigenvalue & \begin{array}{cccc} 271.5 & 303.4 & 76.5 & 0 \end{array} \\ |81\rangle & \left(\begin{array}{cccc} .81810+.00046i & .26792-.00011i & .50101+.07371i & -.05078-.00008i \end{array} \right. \\ |8-3\rangle & \left(\begin{array}{cccc} -.20867+.06104i & .72162-.21129i & .015696-.00222i & .59736-.17382i \end{array} \right. \\ |85\rangle & \left(\begin{array}{cccc} -.49134-.01021i & -.13187-.00262i & .84838+.14242i & -.034439-.00076i \end{array} \right. \\ |8-7\rangle & \left(\begin{array}{cccc} .19423-.065253i & -.55716+.18742i & .057251-.010321i & .74017-.24759i \end{array} \right) \end{array}$$

Eigenvalues and eigenvectors for $J=8$ with $\mu=2$

$$\begin{array}{lc} Eigenvalue & \begin{array}{cccc} 320.7 & 280.7 & 26.3 & 7.0 \end{array} \\ |82\rangle_+ & \left(\begin{array}{cccc} .84454 & -.062284 & .52961 & -.048188 \end{array} \right. \\ |86\rangle_+ & \left(\begin{array}{cccc} -.52791 & .06899 & .84164 & -.08921 \end{array} \right. \\ |82\rangle_- & \left(\begin{array}{cccc} .06672i & .78857i & .04192i & .61000i \end{array} \right. \\ |86\rangle_- & \left(\begin{array}{cccc} -.05992i & -.60792i & .09559i & .78589i \end{array} \right) \end{array}$$

Notice that angular momentum is completely quenched for the $\mu=0,\ 2$ states but not for the $\mu=\pm 1$ states.

■ 6.7 The Diagonal Zeeman Matrix Elements for Atoms

Consider a magnetic field B_z directed along the $z-$axis and a set of states $|\alpha SLJM>$ associated with a spectroscopic term ^{2S+1}L. The presence of the magnetic field adds to the Hamiltonian a term

$$H_{mag} = -B_z\mu_z = B_z\mu_0[L_z + g_sS_z] \tag{6.2}$$

where $g_s \cong 2.0023$. In terms of tensor operators
we need to evaluate the matrix elements of the operator $L_0^{(1)} + g_sS_0^{(1)}$. Consider first the diagonal matrix elements

$$< \alpha SLJM|L_0^{(1)} + g_sS_0^{(1)}|\alpha SLJM >$$

Application of the Wigner-Eckart theorem, Eq.(3.25), gives

$$\begin{aligned} &< \alpha SLJM|L_0^{(1)} + g_s S_0^{(1)}|\alpha SLJM > \\ &= (-1)^{J-M} \begin{pmatrix} J & 1 & J \\ -M & 0 & M \end{pmatrix} < \alpha SLJ\|L^{(1)} + g_s S^{(1)}\|\alpha SLJ > \\ &= \frac{M}{\sqrt{J(J+1)(2J+1)}} < \alpha SLJ\|L^{(1)} + g_s S^{(1)}\|\alpha SLJ > \end{aligned} \tag{6.3}$$

Use of Eq.(3.56) gives

$$\begin{aligned} &< \alpha SLJ\|g_s S^{(1)}\|\alpha SLJ > \\ &= g_s(-1)^{S+L+J+1}(2J+1) \begin{Bmatrix} J & 1 & J \\ S & L & S \end{Bmatrix} < \alpha S\|S^{(1)}\|\alpha S > \end{aligned} \tag{6.4a}$$

Use of Eq.(3.57) gives

$$\begin{aligned} &< \alpha SLJ\|L^{(1)}\|\alpha SLJ > \\ &= (-1)^{S+L+J+1}(2J+1) \begin{Bmatrix} J & 1 & J \\ L & S & L \end{Bmatrix} < \alpha L\|L^{(1)}\|\alpha L > \end{aligned} \tag{6.4b}$$

The reduced matrix elements follow from Eq.(3.40) and the $6j-$symbols may be evaluated explicitly using Eq.(3.42). Combining terms we finally obtain

$$< \alpha SLJM|H_{mag}|\alpha SLJM >= B_z \mu_0 M g(SLJ) \tag{6.5}$$

where

$$g(SLJ) = 1 + (g_s - 1)\frac{J(J+1) - L(L+1) + S(S+1)}{2J(J+1)} \tag{6.6}$$

is the so-called Landé $g-$factor. Eq.(6.5) shows that for a weak magnetic field with states of different J well separated the magnetic field will produce splittings linearly dependent on the M quantum number. This is the so-called weak field Zeeman effect.

For a $J = \frac{1}{2}$ level we obtain the pattern

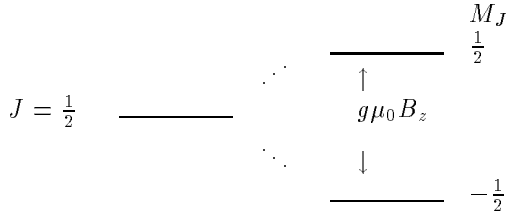

Note that we have not only determined the number of sublevels (two) but also the *magnitude* of splitting. For a $J = 1$ level we obtain the pattern

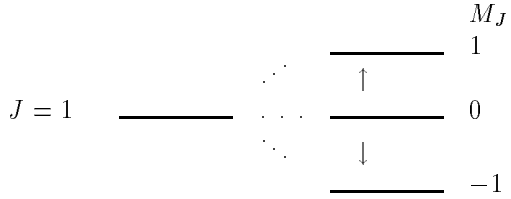

In this case we obtain three sublevels. In general we obtain $(2J + 1)$ sublevels. For a system having an *odd* number of electrons we obtain an *even* number of sublevels while for an *even* number of electrons we obtain an *odd* number of sublevels.

■ 6.8 Off-diagonal Zeeman Matrix Elements for Atoms

For a magnetic field in the $z-$direction the $M-$quantum number remains a good quantum number. This is because we have preserved SO_2 symmetry. However, H_{mag} does not preserve SO_3 symmetry - we

have chosen a particular direction in 3−space. The total angular momentum J is no longer a good quantum number. There exist matrix elements of H_{mag} coupling states with $\Delta J = \pm 1$. We first note that $J_z = L_z + S_z$ and hence $L_z + g_s S_z = J_z + (g_s - 1)S_z$. But the matrix elements of J_z are diagonal in J and hence to calculate the off-diagonal matrix elements we need only calculate the off-diagonal matrix element of S_z as follows:

$$\begin{aligned} &< \alpha SLJM|S_0^{(1)}|\alpha SLJ+1M > \\ &= (-1)^{J-M} \begin{pmatrix} J & 1 & J+1 \\ -M & 0 & M \end{pmatrix} < \alpha SLJ\|S^{(1)}\|\alpha SLJ+1 > \end{aligned} \tag{6.7}$$

Explicit evaluation of the $3j-$symbol gives

$$\begin{aligned} &(-1)^{J-M} \begin{pmatrix} J & 1 & J+1 \\ -M & 0 & M \end{pmatrix} \\ &= -2\sqrt{\frac{(J+M+1)(J-M+1)}{(2J+1)(2J+2)}} \end{aligned} \tag{6.8}$$

Evaluation of the reduced matrix element in Eq.(6.8) using Eq.(3.40) gives

$$\begin{aligned} &< \alpha SLJ\|S^{(1)}\|\alpha SLJ+1 > \\ &= (-1)^{S+L+J}\sqrt{(2J+1)(2J+3)} \begin{Bmatrix} J & 1 & J+1 \\ S & L & S \end{Bmatrix} < S\|S^{(1)}\|S > \\ &= -\sqrt{\frac{(S+L+J+2)(S+J+1-L)(J+1+L-S)(S-J+L)}{4(J+1)}} \end{aligned} \tag{6.9}$$

Combining Eqs. (6.8) and (6.9) in Eq.(6.7) finally yields

$$\begin{aligned} &< \alpha SLJM|H_{mag}|\alpha SLJ+1M > \\ &= B_z\mu_0(g_s-1)\sqrt{(J+1)^2 - M^2)} \\ &\times \sqrt{\frac{(S+L+J+2)(S+J+1-L)(J+1+L-S)(S-J+L)}{4(J+1)^2(2J+1)(2J+3)}} \end{aligned} \tag{6.10}$$

■ 6.9 Zeeman Effect in Crystals

In a crystal it is useful to consider states constructed in a $|JM\rangle$ basis. For the moment we will restrict our attention to the case of the magnetic field B_z being parallel to the $z-$axis of the crystal. A state $|\alpha J\mu\rangle$ with crystal quantum number μ may be expanded as a linear combination of $|\alpha JM\rangle$ states as

$$|\alpha J\mu\rangle = \sum_M a^{\mu}_{\alpha JM}|\alpha JM\rangle \tag{6.11}$$

The expansion coefficients $a^{\mu}_{\alpha JM}$ are just the eigenvector components obtained from the crystal field matrix diagonalization.

In D_{2d} point group symmetry the angular momentum operator $L_z + 2S_z$ transforms as the Γ_2 representation and since $\Gamma_1 \times \Gamma_2 = \Gamma_2$ we can conclude that for D_{2d} symmetry there can be no diagonal Zeeman matrix elements for Γ_1 states of D_{2d}. The situation is different for S_4 point group symmetry as then $L_z + 2S_z$ transforms under S_4 as Γ_1 leading us to conclude that non-zero diagonal Zeeman matrix elements are possible for all values of μ. However, we must also consider time reversal!

Note that for the symmetric and antisymmetric linear combinations $|JM\rangle_{\pm}$ we have

$${}_{\pm}\langle JM|L_z + 2S_z|JM\rangle_{\pm} = 0, \quad {}_{\pm}\langle JM|L_z + 2S_z|JM\rangle_{\mp} = Mg \tag{6.12}$$

The expectation value of $L_z + 2S_z$ for the two lowest levels for $J = 8$ may be readily calculated using the Maple file "gcrystal" for the lowest $\mu = 1$ and $\mu = 1$ levels as given below

```
#########################################################################
#Calculation of the Zeeman matrix element for the lowest $\mu = 1$ level#
#of $J = 8$ for $LiYF_4:Ho^{3+}.                                        #
#########################################################################
with(linalg):
g811:= proc()
     local A,V811,gm,result;
V811:=array(1..4);
gm:=array(sparse,1..4,1..4);
V811[1]:=-0.5078 - 0.00008*I;
V811[2]:=0.59736 - 0.17382*I;
V811[3]:=-0.034439 - 0.00076*I;
V811[4]:=0.74017 - 0.24759*I;
gm[1,1]:=1;
gm[2,2]:=-3;
gm[3,3]:=5;
gm[4,4]:=-7;
A:=multiply(gm,V811);
print(A);
result:=dotprod(A,V811)*g;
print(‘Zeeman diagonal matrix element for the lowest J = 8 level with mu = 1‘);
print(result);
end:
g811();
#########################################################################
#Calculation of the Zeeman matrix element for the lowest $\mu = 2$ level#
#of $J = 8$ for $LiYF_4:Ho^{3+}.                                        #
#########################################################################
g822:= proc()
     local A,V822,gm,result;
V822:=array(1..4);
gm:=array(sparse,1..4,1..4);
V822[1]:=-0.048188;
V822[2]:=-0.08921;
V822[3]:=0.61000*I;
V822[4]:= 0.78589*I;
gm[1,3]:=2;
gm[2,4]:=6;
gm[3,1]:=2;
gm[4,2]:=6;
multiply(gm,V822);
result:=dotprod(",V822)*g;
```

```
print('Zeeman diagonal matrix element for the lowest J = 8 level with mu = 2');
print(result);
end:
g822();
```

Recall that in lecture 3.1 we found the "free ion" Ho^{3+} ground state had a Landé $g-$factor, corrected for intermediate coupling, of

$$g = 1.2416$$

Running the file "gcrystal" leads to the matrix element for the lowest $\mu = \pm 1$ level, the ground state of

$$\mp 6.408$$

and for the first excited state, with $\mu = 2$, of

$$0$$

in units of the Bohr magneton μ_0. Time-reversal invariance gaurantees that the matrix elements

$$\langle \Gamma_1 | J_z | \Gamma_1 \rangle = \langle \Gamma_2 | J_z | \Gamma_2 \rangle = 0$$

Note that in S_4 only those levels with $\mu = \pm 1$ will exhibit a Zeeman splitting. This gives an experimental method of distinguishing $\mu = \pm 1$ levels from levels with $\mu = 0,\ 2$.

■ 6.10 Electric dipole and Magnetic dipole selection rules

Electric dipole transitions involve the matrix elements of z for polarization parallel to the $z-$axis ($\pi-$polarization) and for polarization perpendicular to the $z-$axis ($\sigma-$polarization) matrix elements of $x \pm iy$. For S_4 z transforms as the Γ_2 representation and $x \pm iy$ as $\Gamma_3,\ \Gamma_4$ leading to the electric dipole selection rules

$$\begin{array}{cc} E.d & \begin{array}{cccc} \Gamma_1 & \Gamma_2 & \Gamma_3 & \Gamma_4 \end{array} \\ \begin{array}{c} \Gamma_1 \\ \Gamma_2 \\ \Gamma_3 \\ \Gamma_4 \end{array} & \begin{pmatrix} - & \pi & \sigma & \sigma \\ \pi & - & \sigma & \sigma \\ \sigma & \sigma & - & \pi \\ \sigma & \sigma & \pi & - \end{pmatrix} \end{array} \tag{6.13}$$

For magnetic dipole transitions we need the matrix elements of J_z for $\sigma-$polarization and $J_x \pm iJ_y$ for $\pi-$polarization. For S_4 J_z transforms as Γ_1 and $J_x \pm iJ_y$ as $\Gamma_3,\ Gamma_4$ leading to the magnetic dipole selection rules

$$\begin{array}{cc} M.d & \begin{array}{cccc} \Gamma_1 & \Gamma_2 & \Gamma_3 & \Gamma_4 \end{array} \\ \begin{array}{c} \Gamma_1 \\ \Gamma_2 \\ \Gamma_3 \\ \Gamma_4 \end{array} & \begin{pmatrix} \sigma & - & \pi & \pi \\ - & \sigma & \pi & \pi \\ \pi & \pi & \sigma & - \\ \pi & \pi & - & \sigma \end{pmatrix} \end{array} \tag{6.14}$$

The experimental study of the polarization of transitions gives a further tool for determining the symmetry of the observed levels. Note that the electric dipole transitions are *forced* electric dipole transitions as they nominally occur between states of the same parity. The crystal field potential expansion possesses *odd rank* terms that can mix states of opposite parity. Furthermore, the crystal field can mix states of different J and L lifting the $\Delta J,\ \Delta L = 0,\ \pm 1$ of the free ion while spin-orbit interaction can lead to a breakdown of the spin selection rule $\Delta S = 0$. Magnetic dipole transitions are allowed between states of the same parity. In the free ion in pure $LS-$coupling we have the magnetic dipole selection rules

$$\Delta S,\ \Delta L = 0, \quad \Delta J = 0,\ \pm 1 \tag{6.15}$$

Again these selection rules can be broken by spin-orbit interaction and crystal field selection rules. Nevertheless, the selection rules of Eq. (6.13) and (6.14) are, in the absence of other interactions, rigorous. An interaction which can break those selection rules is the nuclear hyperfine interaction that can weakly mix close-by crystal field levels. Nuclear hyperfine interaction will be the subject of our next lecture.

■ Exercise

6.1 Extend Eq. (6.13) and (6.14) to include states transforming as Γ_i where $i = 5, \ldots, 8$.

6.2 Extend the calculation of the intermediate coupling corrections for the reduced matrix elements

$$\langle \beta J \| C^{(k)} \| \beta J' \rangle \quad k = 2,\ 4,\ 6$$

for $J = 4,\ 5$ and J'.

6.3 Complete the $J-$mixing calculation for the complete set of states with $\mu = 0$ and $J = 4,\ 5,\ 6$.

The Application of Symmetry Concepts
to
Physical Problems II (contd)
Analysis of Hyperfine structure in Crystals

B. G. Wybourne

I have carried out researches which will halt many savants in theirs
— Évariste Galois —1830
I hope we still have some bright twelve-year olds who are interested in science. We must be careful not to discourage our twelve-year-olds by making them waste the best years of their lives on preparing for examinations
— Freeman J. Dyson, *Infinite in all Directions* Penguin 1989

■ Lecture 7

■ 7.1 Introduction

We now come, at last to our central subject - analysis of hyperfine structure in crystal fields. ^{165}Ho is distinguished from the other rare earths by possessing a large nuclear magnetic dipole and electric quadrupole moment. Having a nuclear spin $I = \frac{7}{2}$ which couples to the electron angular momentum leads in the atom to the appearance in its atomic spectrum hyperfine patterns of up to 8 closely place lines. The treatment in crystalline environments is somewhat different as the electric field splittings are very much greater than the hyperfine splittings. This means that while basis states for the free atom are well described by the quantum numbers $IJFM$ such a scheme is wholly inappropriate in a crystal. The appropriate basis then involves the quantum numbers JJ_zII_z. The existance of spin-orbit coupling must also be considered. In this lecture we first indicate how to calculate the matrix elements of the hyperfine interaction in a JJ_zII_z basis and correct them for the effects of intermediate coupling. Much of todays lecture originates from

7.1 B. G. Wybourne, *Nuclear Moments and Intermediate Coupling*, J. Chem. Phys. **37**, 1807–1811 (1962).

Details of the relevant tensor operator formalism can be found in the notes of Lecture 3 and in

7.2 B. R. Judd, *Tensor Operator Techniques in Atomic Spectroscopy*, New York: McGraw-Hill (1962).

7.3 L.Armstrong, Jr. *Theory of the Hyperfine Structure of Free Atoms* New York: Wiley-Interscience (1971).

■ 7.2 Matrix elements of the Magnetic Dipole Hyperfine Interaction

Let us define

$$a_\ell = 2\mu_B^2(m_e/M_p)g_I\langle r^{-3}\rangle \tag{7.1}$$

where μ_B is the Bohr magneton, g_I the nuclear g factor and $\langle r^{-3}\rangle$ the average inverse-cube radius of the electron orbital ℓ. Further, let

$$\begin{aligned}\mathbf{H}_m(i)^{(1)} &= a_\ell[\mathbf{l}_i^{(1)} - \sqrt{10}(\mathbf{s}^{(1)}\mathbf{x}\mathbf{C}^{(2)})_i^{(1)}] \\ &= a_\ell[\mathbf{l}_i - \sqrt{10}\mathbf{X}_i^{(1)}]\end{aligned} \tag{7.2}$$

with

$$\mathbf{H}_m^{(1)} = \sum_{i=1}^{n} H_m(i)^{(1)} \tag{7.3}$$

where the sum is over a group of equivalent electrons in the configuration ℓ^n.

The interaction of a nuclear magnetic moment with the orbital and spin moments of n electrons can be

written in the above tensor operator notation as

$$\mathcal{H}_m = a_\ell(\mathbf{H}^{(1)} \cdot \mathbf{I}^{(1)}) \tag{7.4}$$

In the $JIFM$ scheme the matrix elements of the nuclear magnetic hyperfine operator $\mathcal{H}_m$, diagonal in J, may be evaluated as

$$\langle \alpha JIFM | a_\ell(\mathbf{H}^{(1)} \cdot \mathbf{I}^{(1)}) | \alpha' JIFM \rangle \tag{7.5}$$

$$= a_\ell (-1)^{J+I+F} \begin{Bmatrix} J & I & F \\ I & J & 1 \end{Bmatrix} \langle \alpha J \| H^{(1)} \| \alpha' J \rangle \langle I \| I^{(1)} \| I \rangle \tag{7.6}$$

$$= a_\ell \frac{K}{2\sqrt{J(J+1)(2J+1)}} \langle \alpha J \| H^{(1)} \| \alpha' J \rangle \tag{7.7}$$

where

$$K = F(F+1) - J(J+1) - I(I+1) \tag{7.8}$$

■ **Exercises**

7.1 Use the work done in Lecture 3 to derive Eqs (7.5) to (7.7).

7.2 Obtain the corresponding results for the matrix elements that are non-diagonal in J.

Our principal problem now is to evaluate the matrix element in Eq. (7.7). Let us enlarge our state description to $|\alpha SLJ\rangle$ and allow for matrix elements non-diagonal in αSL. Then noting that

$$\sum_{i=1}^{n} \ell_i^{(1)} = L^{(1)} \tag{7.9}$$

we can show, as done earlier for the Zeeman effect, that

$$\mathcal{L} = \frac{\langle \alpha SLJ \| L^{(1)} \| \alpha' S' L' J \rangle}{\sqrt{J(J+1)(2J+1)}} = \delta_{\alpha,\alpha'} \delta_{S,S'} \delta_{L,L'} (2 - g) \tag{7.10}$$

where g is the usual Landé $g-$factor for the electronic state. The correction for intermediate coupling follows exactly as in Lecture 6. We simply replace g by its intermediate coupling value.

The second part of the matrix elements of $H^{(1)}$ requires the evaluation of the operator

$$\mathcal{S} = -\frac{\sqrt{10}\langle \alpha SLJ \| \sum_i^n (s^{(1)} C^{(2)})^{(1)} \| \alpha' S' L' J \rangle}{\sqrt{J(J+1)(2J+1)}} \tag{7.11}$$

This may be evaluated using the results of Lecture 3 to give

$$\mathcal{S} = (-1)^{\ell+1}(2\ell+1) \begin{pmatrix} \ell & \ell & 2 \\ 0 & 0 & 0 \end{pmatrix} \sqrt{\frac{30(2J+1)}{J(J+1)}} \begin{Bmatrix} S & S' & 1 \\ L & L' & 2 \\ J & J & 1 \end{Bmatrix} \langle \alpha SL \| V^{(12)} \| \alpha' S' L' \rangle \tag{7.12}$$

where the last matrix element involves the double tensor $V^{(12)}$ that acts in the spin and orbital spaces and whose one-electron reduced matrix elements satisfy

$$\langle \ell \| v^{(12)} \| \ell \rangle = \sqrt{\frac{3}{2}} \tag{7.13}$$

We shall consider these matrix elements later.

The magnetic hyperfine-structure constant A, as normally defined, is given by

$$A = a_\ell [\mathcal{L} + \mathcal{S}] \tag{7.14}$$

■ **Exercises**

7.3 Fill out the derivations of Eqs. (7.10) and (7.12).

7.4 Generalise Eqs. (7.10) and (7.12) to give the matrix elements that are non-diagonal in J.

■ 7.3 Nuclear magnetic hyperfine matrix elements in the JJ_zII_z scheme

In the JJ_zII_z scheme the diagonal elements are given by

$$(\alpha SLJJ_zII_z|\mathcal{H}_m|\alpha' S'L'JJ_zII_z) = J_zI_zA \tag{7.15}$$

whereas the off-diagonal matrix elements are given by

$$(\alpha SLJJ_zII_z|\mathcal{H}_m|\alpha' S'L'JJ_z \pm 1II_z \mp 1) = \frac{1}{2}A[(J \mp J_z)(J \pm J_z + 1)(I \pm I_z)(I \mp I_z + 1)]^{\frac{1}{2}} \tag{7.16}$$

■ **Exercise**

7.5 Sketch derivations of Eqs. (7.15) and (7.16).

■ 7.4 Nuclear electric quadrupole hyperfine interactions

The ^{165}Ho nucleus is highly deformed and possesses an electric quadrupole moment Q. The matrix elements in the $JIFM$ scheme are given by

$$\begin{aligned}
&(\alpha SLJIFM|\sum_{i=1}^{n}(\mathbf{C}_i^{(2)} \cdot \mathbf{Q}^{(2)})|\alpha' S'L'JIFM) \\
&= e^2Q\langle r^{-3}\rangle \left(\frac{\frac{3}{4}K(K+1) - I(I+1)J(J+1)}{2I(2I-1)J(2J-1)}\right)\sqrt{\frac{8J(2J-1)}{(2J+3)(2J+1)(2J+1)}} \\
&(-1)^{\ell+1}(2\ell+1)\begin{pmatrix}\ell & \ell & 2\\ 0 & 0 & 0\end{pmatrix}(\alpha SLJ\|U^{(2)}\|\alpha' S'L'J)\delta_{SS'} \qquad (7.17)\\
&= b_\ell X_J\left(\frac{\frac{3}{4}K(K+1) - I(I+1)J(J+1)}{2I(2I-1)J(2J-1)}\right) \qquad (7.18)
\end{aligned}$$

where

$$b_\ell = e^2Q\langle r^{-3}\rangle \tag{7.19}$$

The electric quadrupole hyperfine constant B, as normally defined, is given by

$$B = b_\ell X_J \tag{7.20}$$

The matrix elements of the unit tensor $U^{(2)}$ may be evaluated by first noting that

$$\langle \alpha SLJ\|U^{(2)}\|\alpha' SL'J\rangle = (-1)^{S+L'+J}(2J+1)\begin{Bmatrix} J & J & 2\\ L & L' & S\end{Bmatrix}\langle \alpha SL\|U^{(2)}\|\alpha' SL'\rangle \tag{7.21}$$

The doubly reduced matrix elements are listed by Nielson and Koster.

Note that the matrix elements of the electric-quadrupole interaction are, unlike for the magnetic-dipole interaction, diagonal in spin. Furthermore, the matrix elements of the electric-quadrupole interaction for the f^{10} configuration are *opposite* in sign to those for f^4 while the matrix elements of the magnetic-dipole interaction have the same sign for both configurations.

In the JJ_zII_z scheme the matrix elements of the electric- quadrupole interaction are given by

$$\begin{aligned}
&(\alpha SLJJ_zII_z|\sum_{i=1}^{n}(\mathbf{C}_i^{(2)} \cdot \mathbf{Q}^{(2)})|\alpha' SL'JJ_z \pm q, II_z \mp q) \\
&= (-1)^{J-J_z}\begin{pmatrix} J & 2 & J\\ -J_z & q & J_z \pm q\end{pmatrix}(-1)^{I-I_z}\begin{pmatrix} I & 2 & I\\ -I_z & q & I_z \mp q\end{pmatrix} \\
&\frac{b_\ell X_J}{4}\sqrt{\frac{(2I+1)(I+1)(2I+3)(2J+1)(J+1)(2J+3)}{I(2I-1)J(2J-1)}}
\end{aligned} \tag{7.22}$$

where q is limited to the values 0, ± 1, ± 2. In all cases the matrix elements in the JJ_zII_z scheme are diagonal in $M = J_z + I_z$.

■ 7.5 The matrix elements of $V^{(12)}$

Various tables of the matrix elements of $V^{(12)}$ exist in the literature and of varying reliability. Most of the matrix elements of $V^{(12)}$ may be obtained from the matrix elements of $U^{(2)}$ tabulated by Nielson and Koster by making use of the identity

$$\frac{\langle \ell^{n_a}\alpha v_1 S_1 L\|V^{(12)}\|\ell^{n_a}\alpha v_1 S_1' L'\rangle}{\langle \ell^{n_b}\alpha v_2 S_2 L\|U^{(2)}\|\ell^{n_b}\alpha v_2' S_2 L'\rangle}$$

$$= (-1)^{v_1+v_2\delta(v_2,v_2')+1+(n_b-n_a+v_2-v_1)/2}\sqrt{\frac{2S_2+1}{4}}\frac{\begin{pmatrix}\frac{1}{2}(2\ell+1-v_1) & 0 & \frac{1}{2}(2\ell+1-v_1)\\ \frac{1}{2}(2\ell+1-n_a) & 0 & -\frac{1}{2}(2\ell+1-n_a)\end{pmatrix}}{\begin{pmatrix}\frac{1}{2}(2\ell+1-v_2) & 1 & \frac{1}{2}(2\ell+1-v_2')\\ \frac{1}{2}(2\ell+1-n_b) & 0 & -\frac{1}{2}(2\ell+1-n_b)\end{pmatrix}} \quad (7.23)$$

with $n_a \not= n_b$. Thus we find that

$$\langle f^4 4[111]U^5 L\|V^{(12)}\|f^4 4[111]U^5 L'\rangle = -\frac{\sqrt{30}}{4}\langle f^3 3[111]U^4 L\|U^{(2)}\|f^3 3[111]U'^4 L'\rangle \quad (7.24)$$

$$\langle f^4 4[111]U^5 L\|V^{(12)}\|f^4 4[211]U'^3 L'\rangle = -\frac{1}{2}\sqrt{10}\langle f^5 3[111]U^4 L\|U^{(2)}\|f^5 5[211]U'^4 L'\rangle \quad (7.25)$$

and

$$\langle f^4 4[211]U^3 L\|V^{(12)}\|f^4 4[211]U'^3 L'\rangle = \frac{\sqrt{6}}{2}\langle f^5 5[211]U^4 L\|U^{(2)}\|f^5 5[211]U'^4 L'\rangle \quad (7.26)$$

leading directly to the results given as a matrix below

$$\begin{array}{l} V^{(12)} \\ \langle {}^5I| \\ \langle (21)^3H| \\ \langle (30)^3H| \\ \langle (21)^3K| \\ \langle (30)^3K| \end{array}\begin{array}{c} \begin{array}{ccccc} |{}^5I\rangle & |(21)^3H\rangle & |(30)^3H\rangle & |(21)^3K\rangle & |(30)^3K\rangle \end{array} \\ \begin{pmatrix} -\frac{\sqrt{715}}{44} & \frac{19\sqrt{42}}{162} & -\frac{11}{12} & -\frac{\sqrt{105}}{42} & \frac{\sqrt{1785}}{21} \\ \frac{19\sqrt{42}}{162} & \frac{5\sqrt{3003}}{702} & \frac{\sqrt{286}}{1170} & \frac{-4\sqrt{130}}{195} & \frac{-10\sqrt{221}}{273} \\ -\frac{11}{12} & \frac{\sqrt{286}}{1170} & \frac{-17\sqrt{3003}}{2340} & \frac{-10\sqrt{1365}}{273} & \frac{\sqrt{23205}}{546} \\ \frac{-\sqrt{105}}{42} & \frac{-4\sqrt{130}}{195} & \frac{-10\sqrt{1365}}{273} & \frac{2\sqrt{663}}{273} & \frac{46\sqrt{39}}{273} \\ \frac{\sqrt{1785}}{21} & \frac{-10\sqrt{221}}{273} & \frac{\sqrt{23205}}{546} & \frac{46\sqrt{39}}{273} & \frac{113\sqrt{663}}{4641} \end{pmatrix} \end{array} \quad (7.27)$$

■ 7.6 Matrix elements of the spin part of the magnetic-hyperfine operator

With the matrix elements of the double tensor $V^{(12)}$ established in Eq. (7.27) it is a simple matter to complete the calculation of the matrix elements of the spin part of the magnetic hyperfine interaction given in Eq. (7.11) using the Maple code of the file "mhfs" given below

```
#############################################################################
#Programme to calculate the spin part of the magnetic hyperfine structure.#
#Uses Eq.(7.12) and V is the reduced matrix element of the double tensor. #
#############################################################################
read`njsymbol`;
S:=proc(S1,L1,S2,L2,J,V)
   local result;
   result:=7*threej(3,3,2,0,0,0)*sqrt((30*(2*J + 1))/(J*(J + 1)))
   *ninej(S1,S2,1,L1,L2,2,J,J,1)*V;
   end:
#############################################################################
```

Running the above code for $J = 7$ and $J = 8$ gives the relevant results given in Eqs. (7.28) and (7.29).

$$\begin{array}{l} 420\mathcal{S} \\ \langle {}^5I_7| \\ \langle (30)^3K_7| \end{array}\begin{array}{c} \begin{array}{cc} |{}^5I_7\rangle & |(30)^3K_7\rangle \end{array} \\ \begin{pmatrix} 1 & \frac{19\sqrt{119}}{14} \\ \frac{19\sqrt{119}}{14} & \frac{113}{42} \end{pmatrix} \end{array} \quad (7.28)$$

$$\begin{array}{lccc} 60\mathcal{S} & |^5I_8\rangle & |(21)^3K_8 & |(30)^3K_8\rangle \\ \langle^5I_8| & 1 & -\frac{\sqrt{3}}{40} & \frac{\sqrt{51}}{2} \\ \langle(21)^3K_8| & -\frac{\sqrt{3}}{40} & -\frac{1}{3} & -\frac{23\sqrt{17}}{51} \\ \langle(30)^3K_8| & \frac{\sqrt{51}}{2} & -\frac{23\sqrt{17}}{51} & -\frac{113}{102} \end{array} \tag{7.29}$$

■ 7.7 Intermediate Coupling Corrections for the spin part

Using the eigenvectors for $J = 8$ and $J = 7$ states given in Table 3.1 leads to the intermediate coupling results for the lowest two members of the ^5I multiplet

$$\mathcal{S}(^5I_8) = \frac{1}{60}[-0.5700], \quad \mathcal{S}(^5I_7) = \frac{1}{420}[-3.2369] \tag{7.30}$$

where the first part of the result is given as a fraction and the second part is the intermediate coupling correction factor. The latter factor would be unity for pure $LS-$coupling. Notice that the intermediate coupling corrections for the spin part of the interaction can be quite large even for relatively small departures from $LS-$coupling. However, in general the spin part is very much smaller than the orbital part.

■ 7.8 Intermediate Coupling Corrections for the orbital part

Again, using the eigenvectors for the $J = 8$ and $J = 7$ states given in Table 3.1 leads to theintermediate coupling results for the two lowest members of the ^5I multiplet as

$$\mathcal{L}(^5I_8) = \frac{3}{4}[1.0082], \quad \mathcal{L}(^5I_7) = \frac{23}{28}[0.9964] \tag{7.31}$$

The corrections for small departures from $LS-$coupling make for quite small corrections compared with those for the spin part of the magnetic hyperfine interaction.

■ 7.9 Total Intermediate Coupling Corrections for Magnetic-Dipole HFS

The total intermediate coupling correction for the magnetic-dipole hyperfine structure comes from combining Eqs. (7.10) and (7.12) to to form total magnetic hyperfine interaction matrices and then transforming them to diagonal form with the appropriate intermediate coupling eigenvectors to yield

$$[\mathcal{L}+\mathcal{S}](^5I_8) = \frac{23}{30}[0.9735], \quad [\mathcal{L}+\mathcal{S}](^5I_7) = \frac{173}{210}[0.9591] \tag{7.32}$$

Here we see again that the total effect is quite small and comes primarily from the factor $(2 - g)$.

■ 7.10 Intermediate Coupling Corrections for Electric-Quadrupole HFS

The intermediate coupling correction for the electric-quadrupole hyperfine interaction is exactly the same for the crystal field potential term with $k = 2$ and hence the factors are the same as found in column 2 of Table 4.12.

■ 7.11 Concluding Remarks

We now have all the results necessary to discuss the hyperfine structure in the two lowest levels of the ^5I multiplet. In the next lecture we shall discuss first some of the qualitative aspects of hyperfine structure in crystal field and then commence the calculations specific to $LiYF_4 : Ho^{3+}$ crystals.

The Application of Symmetry Concepts
to
Physical Problems II (contd)
Analysis of Hyperfine structure in Crystals

B. G. Wybourne

The universe is infinite in all directions, not only above us in the large but also below us in the small. If we start from the human scale of existence and explore the content of the universe further and further, we finally arrive, both in the large and in the small, at misty distances where first our senses and then even our concepts fail us.
—Emil Wiechert, Königsberg, 1896

■ Lecture 8

■ 8.1 Introduction

Today I propose to first make some qualitative remarks about hyperfine structure in crystals and then to commence some detailed calculations towards obtaining an understanding of the hyperfine structure in the two lowest levels of the ground multiplet of Ho^{3+} in the crystal field produced at the substitutional site in single crystals of $LiYF_4$.

■ 8.2 The Experimental Data

Most of the experimental data we shall be drawing upon comes from the references given in Lecture 1. Some of the relevant data is collected together in Table 8.1 below

J	E_e	E_c	E_{hfs_e}	E_{hfs_c}	$\langle J_z\rangle_e$	$\langle J_z\rangle_c$	$\langle g_z\rangle_e$	$\langle g_z\rangle_c$
8	0	0	−0.147		−5.2	−5.09	13.0	12.6
7	3.4	6.0	0.082		2.75	2.47	6.49	5.8
	32.4	32	−0.131		−4.39	−4.87	10.36	11.5
	75.5	82	−0.08		−2.74	−2.81	6.48	6.6
	140.6	145				1.22		2.9

Table 8.1 Comparison of Experimental and Calculated Levels for Γ_{34}

The experimental quantities are subscripted by an e and calculated quantities by a c. E_{hfs} is the mean spacing of the hyperfine levels in units of cm^{-1}. $\langle g_z\rangle$ is the magnetic splitting factor for the level.

■ 8.3 General features of Magnetic-Dipole HFS in Crystals

The inclusion of the crystal field produces Stark splittings that may be labelled by the ordinary irreducible representations of the point group S_4. The irreducible representations Γ_1, Γ_2 are one-dimensional and distinct whereas the Γ_3, Γ_4 are complex conjugates and in the absence of external magnetic fields occur as degenerate pairs, often designated as Γ_{34} levels. The various states in the crystal fields can be conveniently described in a $|JJ_z\rangle$ basis with the states involving various linear combinations of these basis states. The matrix elements

$$\langle\Gamma_1|J_z|\Gamma_1\rangle,\ \langle\Gamma_2|J_z|\Gamma_2\rangle,\ \langle\Gamma_1|J_z|\Gamma_2\rangle = 0 \tag{8.1}$$

The diagonal matrix elements of the magnetic-dipole hyperfine interaction involve (cf. Eq. (7.15)) are proportional to those of the operator J_zI_z and hence must vanish within and between states involving the Γ_1 and Γ_2 states and thus these states cannot exhibit first-order magnetic hyperfine structure. There is no such restriction for the Γ_{34} states and thus only those states can directly exhibit magnetic hyperfine structure. The first order magnetic hyperfine structure for the Γ_{34} states will consist of $2I + 1 = 8$ equispaced levels each two-fold degenerate which is consistent with the fact that the spin irreducible representations of the double group S_4 are all two-dimensional. A typical Γ_{34} level schematically as

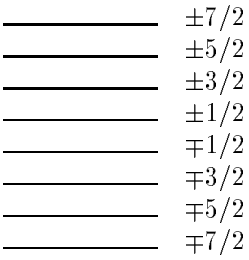

Schematic magnetic hyperfine splitting for a Γ_{34}

The off-diagonal matrix elements of the magnetic-dipole hyperfine interaction, Eq. (7.16), couple states differing in J_z by one unit and hence can couple the Γ_1 and Γ_2 states to the Γ_{34} states in second-order. This can lead to the appearance of second-order hyperfine levels in the Γ_1 and Γ_2 states. In that case their levels will not exhibit equispacing. This property helps in distinguishing Γ_{34} states from the Γ_1, Γ_2 states.

In the absence of hyperfine interaction the crystal field levels exhibit the precise symmetries of the ordinary irreducible representations of S_4. However, since in Holmium the nuclear spin $I = \frac{7}{2}$ is half-integer the hyperfine levels must be classified with respect to the spin irreducible representations of S_4. This means that the crystal field quantum numbers μ can be mixed by the hyperfine interaction and cease to be good quantum numbers breaking down the usual selection rules.

■ 8.4 Electric-Quadrupole HFS in Crystals

The electric-quadrupole hyperfine interaction in crystals is weaker than that of the magnetic-dipole interaction but still needs to be considered. The matrix elements were given in Eq. (7.22). The diagonal elements arise for $q = 0$ and may be specialised to

$$\langle \alpha SLJJ_z II_z | \sum_{i=1}^{n} (\mathbf{C}_i^{(2)} \cdot \mathbf{Q}^{(2)}) | \alpha' SL'JJ_z II_z \rangle = b_\ell X_J \frac{[3J_z^2 - J(J+1)][3I_z^2 - I(I+1)]}{4IJ(2J-1)(2I-1)} \tag{8.2}$$

Thus the electric-quadrupole hyperfine interaction, in first-order, differs markedly from that of the magnetic-dipole hyperfine interaction producing sublevels that are quadratic, rather than linear, in J_z. This produces a complication making it difficult to distinguish non-linear second-order magnetic hyperfine structure from first-order electric-quadrupole hyperfine structure.

■ 8.5 Eigenvectors for $J = 7$ States

The eigenvectors for the $J = 8$ level of the ground multiplet were given in Lecture 6 §6.6. For our calculations we will also need the eigenvalues and eigenvectors for the states associated with the $J = 7$ level of the ground multiplet. These can be found by running the Maple file "crystal.7" to give

Eigenvalues and eigenvectors for $J = 7$ with $\mu = 0$

$$\begin{array}{lccc} \textit{Eigenvalue} & 147 & 18 & 47 \\ |70\rangle & .8806 & -.47396 & 0 \\ |74\rangle_+ & -.47396 & -.88056 & -.00192 \\ |74\rangle_- & .00091I & .001687I & -1.0000I \end{array}$$

Eigenvalues and eigenvectors for $J = 7$ with $\mu = 1$

$$\begin{array}{lcccc} \textit{Eigenvalue} & 145 & 82 & 6 & 32 \\ |71\rangle & .83546 & .34796 & .42302 & .04504 \\ |7-3\rangle & -.44200 - .00703I & .63594 + 0.01013I & .28974 + .00500I & .56219 + .00889I \\ |75\rangle & -.29616 - .00340I & -.26367 - .00303I & .84100 + .01079I & -.36807 - .00418I \\ |7-7\rangle & .13779 - .00173I & -.63623 + .00798I & .17245 - .00193I & .73915 - .00936I \end{array}$$

Eigenvalues and eigenvectors for $J = 7$ with $\mu = 2$

$$\begin{array}{lcccc} \textit{Eigenvalue} & 81 & 0 & 141 & 11 \\ |72\rangle_+ & -.84982 & -.52688 & .01064 & -.00362 \\ |76\rangle_+ & .52687 & -.84972 & .00329 & .00972 \\ |72\rangle_- & .00958I & .00593I & .94639I & -.32263I \\ |76\rangle_- & .00540I & -.00873I & -.32261I & -.94649I \end{array}$$

■ 8.6 Calculation of $\langle J_z \rangle$ for $J = 8$ and $J = 7$

The expectation values of J_z may be calculated in precisely the same manner as used to calculate the Zeeman matrix element on page 70 of Lecture 6. Continuing in that way we obtain the entries given in the seventh column of Table 8.1.

The detailed calculation is shown in the following Maple session for $J = 7$:

```
L:=array(sparse,1..4,1..4);
                    L := array(sparse, 1 .. 4, 1 .. 4, [])
L[1,1]:=1;
                                  L[1, 1] := 1
L[2,2]:=-3;
                                 L[2, 2] := -3
L[3,3]:=5;
                                  L[3, 3] := 5
L[4,4]:=-7;
                                 L[4, 4] := -7
v1:=array(1..4);
                           v1 := array(1 .. 4, [])
for i from 1 to 4 do v1[i]:=V71[1,i] od;
                                                  -5
                       v1[1] := .83546 - .25724*10  I
                                                  -5
                       v1[2] := .34796 + .51083*10  I
                        v1[3] := .42302 + .00057401I
                                                   -5
                       v1[4] := .045039 - .19382*10   I
dotprod(multiply(L,v1),v1);
                                              -7
                            1.2153 + .21206*10   I
v2:=array(1..4);
                           v2 := array(1 .. 4, [])
for i from 1 to 4 do v2[i]:=V71[2,i] od;
                       v2[1] :=  - .44200 - .0070321 I
                       v2[2] := .63594 + .010129 I
                       v2[3] := .28974 + .0050042 I
                       v2[4] := .56219 + .0088915 I
```

```
dotprod(multiply(L,v2),v2);
                                                    -6
                              - 2.8112 - .75042*10    I
v3:=array(1..4);
                              v3 := array(1 .. 4, [])
for i from 1 to 4 do v3[i]:=V71[3,i] od;
                         v3[1] :=  - .29616 - .0034002 I
                         v3[2] :=  - .26367 - .0030331 I
                         v3[3] := .84100 + .010799 I
                         v3[4] :=  - .36807 - .0041872 I
dotprod(multiply(L,v3),v3);
                                                   -6
                               2.4676 + .18910*10    I
v4:=array(1..4);
                              v4 := array(1 .. 4, [])
for i from 1 to 4 do v4[i]:=V71[4,i] od;
                           v4[1] := .13779 - .0017311 I
                           v4[2] :=  - .63623 + .0079844 I
                           v4[3] := .17245 - .0019314 I
                           v4[4] := .73915 - .0093621 I
dotprod(multiply(L,v4),v4);
                                                    -6
                              - 4.8719 - .45345*10    I
```

The matrix L is diagonal with elements J_z and the column vector vk is the eigenvector associated with the $k-$th eigenvalue. The eigenvector arrays $V71$ were generated by first running the Maple file "crystal.7". The imaginary part of the resultant in each case is rounded to zero to give the final values of $\langle J_z \rangle$.

■ 8.7 Calculation of the Magnetic Splitting Factors $\langle g_z \rangle$

The magnetic splitting factors $\langle g_z \rangle$ may be readily calculated by noting that

$$\langle g_z \rangle = 2|\langle J_z \rangle| g_{IC} \tag{8.3}$$

where g_{IC} is the intermediate coupling corrected "free ion" Landé $g-$factor, in our case

$$g_8 = 1.242, \qquad g_7 = 1.177 \tag{8.4}$$

Use of these values in Eq. (8.3) together with the calculated values of $\langle J_z \rangle$ give the entries in column 9 of Table 8.1.

■ 8.8 The Magnetic Hyperfine Structure Constant A

The magnetic hyperfine structure constant was defined in Eq. (7.14) as

$$A = a_\ell [\mathcal{L} + \mathcal{S}] \tag{7.14}$$

It follows from Eq. (7.15) that in a crystal the average spacing between successive hyperfine levels, E_{hfs} will be

$$E_{hfs} = \langle J_z \rangle A \tag{8.5}$$

This means that if the hyperfine structure is purely magnetic-dipole in character and if there is no hyperfine interaction with other Stark levels the hyperfine pattern should consist of eight equally spaced sublevels. Departures from this equality indicates either second-order magnetic dipole effects and/or electric-quadrupole interactions. As noted earlier, the Γ_{34} Stark levels can show first-order magnetic-dipole splittings whereas the Γ_1, Γ_2 Stark levels can only show second-order magnetic-dipole hyperfine

structure which in general will be smaller than that shown for Γ_{34} levels and cannot be expected to exhibit equally spaced sublevels. This gives a practical way for distinguishing Γ_{34} levels from Γ_1, Γ_2 levels.

■ 8.9 Selection Rules and Hyperfine Structure

We discussed the selection rules for electric dipole and magnetic dipole transitions involving the Stark levels that transformed as the ordinary irreducible representations of the point group S_4. However, the situation is changed by the presence of the hyperfine interaction. The nuclear spin of Ho is half-integer while the electronic angular momentum is integer leading to a net angular momentum in the free ion that is necessarily half-integer. As a result the Stark levels in the presence of the hyperfine interaction will involve states belonging to the double group of S_4. The additional irreducible representations $\Gamma_i \;\; i = 5, \ldots, 8$ are one-dimensional but occur as complex pairs. For electric-dipole transitions the $\sigma-$polarization transitions involve the matrix elements of z whichs transforms as the Γ_2 irreducible representation while for $\pi-$polarization transitions $x \pm iy$ transform as the Γ_3, Γ_4 irreducible representations of S_4 leading to the electric-dipole selection rules for the relevant irreducible representations as

$$\begin{array}{cc} E.d & \begin{array}{cccc} \Gamma_5 & \Gamma_6 & \Gamma_7 & \Gamma_8 \end{array} \\ \begin{array}{c} \Gamma_5 \\ \Gamma_6 \\ \Gamma_7 \\ \Gamma_8 \end{array} & \left(\begin{array}{cccc} - & \sigma & \pi & \sigma \\ \sigma & - & \sigma & \pi \\ \pi & \sigma & - & \sigma \\ \sigma & \pi & \sigma & - \end{array} \right) \end{array}$$

Likewise, for magnetic-dipole transitions we have

$$\begin{array}{cc} M.d & \begin{array}{cccc} \Gamma_5 & \Gamma_6 & \Gamma_7 & \Gamma_8 \end{array} \\ \begin{array}{c} \Gamma_5 \\ \Gamma_6 \\ \Gamma_7 \\ \Gamma_8 \end{array} & \left(\begin{array}{cccc} \sigma & \pi & - & \pi \\ \pi & \sigma & \pi & - \\ - & \pi & \sigma & \pi \\ \pi & - & \pi & \sigma \end{array} \right) \end{array}$$

Taking into account the degeneracy of the pairs Γ_{56}, Γ_{78} we see that some of the transitions will occur in pure $\pi-$ or $\sigma-$ polarization with the rest as $\sigma\pi-$polarization as shown below

$$\begin{array}{cc} E.d & \begin{array}{cc} \Gamma_{56} & \Gamma_{78} \end{array} \\ \begin{array}{c} \Gamma_{56} \\ \Gamma_{78} \end{array} & \left(\begin{array}{cc} \sigma & \sigma\pi \\ \sigma\pi & \sigma \end{array} \right) \end{array}$$

and

$$\begin{array}{cc} M.d & \begin{array}{cc} \Gamma_{56} & \Gamma_{78} \end{array} \\ \begin{array}{c} \Gamma_{56} \\ \Gamma_{78} \end{array} & \left(\begin{array}{cc} \sigma\pi & \pi \\ \pi & \sigma\pi \end{array} \right) \end{array}$$

which gives a way of sometimes distinguishing the different symmetries by polarization measurements. Within the ground ${}^5I$ multiplet we expect the transitions within and between the sublevels for $J = 7, 8$ to exhibit both magnetic dipole and forced electric dipole transitions whereas for transitions from sublevels of $J = 8$ to levels with $\Delta J \geq 2$ should exhibit only electric dipole transitions.

■ 8.10 First-Order Magnetic Hyperfine Structure

As noted earlier non-zero first-order magnetic hyperfine structure is only possible for Γ_{34} levels in S_4 point symmetry. The first part of the calculation is to diagonalize the crystal field matrices to produce eigenvalues and eigenvectors of the form (in the absence of $J-$mixing)

$$|J\Gamma_\rho I_z\rangle = \sum_{J_z} a_{J\Gamma_\rho J_z} |JJ_z I_z\rangle \tag{8.6}$$

where the $a_{J\Gamma_\rho J_z}$ are the *complex* eigenvector components which are independent of the nuclear spin projection I_z and the nuclear spin I is assumed to be fixed. The first-order magnetic hyperfine matrix

elements are then

$$\begin{aligned}\langle J\Gamma_\rho I_z|\mathcal{H}_{mag}|J\Gamma_\rho I_z\rangle &= \sum_{J_z} a^*_{J\Gamma_\rho J_z} a_{J\Gamma_\rho J_z} \langle JJ_zII_z|\mathcal{H}_{mag}|JJ_zII_z\rangle \\ &= \delta_{\Gamma_\rho,\Gamma_{34}} A\langle J_z\rangle I_z \end{aligned} \tag{8.6}$$

where $\langle J_z\rangle$ is the expectation value of J_z.

■ 8.11 Second-Order Magnetic Hyperfine Structure

The magnetic hyperfine structure constant A for the ground state is $\sim 2.79\times 10^{-2} cm^{-1}$ which is a typical value for Ho and thus the splittings are $\sim 0.15 cm^{-1}$. When Stark levels are very close in the crystal field calculation we can anticipate that second-order magnetic hyperfine interactions will couple the Γ_{34} states to those of Γ_1, Γ_2. This can lead to the latter levels showing hyperfine structure and to the hyperfine structure patterns of the Γ_{34} levels becoming distorted. Inspection of Table 6.1 would suggest that the three top crystal field levels for for $^5I_7$ would be prime candidates for exhibiting such a perturbation. Likewise for the third and fourth crystal field levels. To calculate these effects we need to compute matrix elements that are non-diagonal in J_z and I_z such that $J_z + I_z = J'_z + I'_z$ to give

$$\langle J\Gamma_\rho I_z|\mathcal{H}_{mag}|J\Gamma_{\rho'} I_z \mp 1\rangle = \sum_{J_z} a^*_{\Gamma_\rho J_z I_z} a_{\Gamma_{\rho'} J_z \pm 1 I_z \mp 1} \langle JJ_zII_z|\mathcal{H}_{mag}|JJ_z \pm 1 II_z \mp 1\rangle \tag{8.7}$$

with the matrix element in the JJ_zII_z basis being computed using Eq. (7.16). This calculation will be the subject of the next lecture.

The Application of Symmetry Concepts to Physical Problems II (contd) Analysis of Hyperfine structure in Crystals

B. G. Wybourne

It is hard for me to believe, as some have tried to maintain, that such superb theories could have arisen merely by some random natural selection of ideas leaving only the good ones as survivors. The good ones are simply much too good to be survivors of ideas that have arisen in that random way. There must, instead, be some deep underlying reason for the accord between mathematics and physics
—R. G. Penrose, *The Emperor's New Mind 1990*

■ Lecture 9

■ 9.1 Introduction

This is the last lecture in this course and I would like to conclude with a detailed example of the magnetic hyperfine interaction mixing two adjacent crystal field levels to show how the first-order equal spacing hfs pattern becomes distorted by second-order effects and how crystal field levels that show no first-order hfs can acquire hfs patterns. This exercise will also give us insight into intensity and selection rule changes. Finally I shall remark on directions for future studies of hyperfine structure in crystal field environments.

■ 9.2 The Particular Example, Two levels of $^5I_7$

As a very specific example I shall consider the two highest crystal field levels of the $^5I_7$ member of the groundstate multiplet. The top level is a non-degenerate Γ_1 level (or equivalently, a $\mu = 0$ level) at $5293.1cm^{-1}$ and the next to top level is a two-fold degenerate Γ_{34} level (or equivalently, a $\mu = \pm 1$ level) at $5292.9cm^{-1}$. Thus these two levels are separated by $0.2cm^{-1}$ and can be expected to perturb one another. The question is "By how much?".

■ 9.3 The First-order Calculation

The first step in our calculation is to establish the first-order hfs splitting for the Γ_{34} level. To do that we need an estimate of the hfs constant A for the $^5I_7$ term. This is essentially deducible from the experimental data given in Table 8.1. The crystal field level at $5184.66cm^{-1}$ ($140.6cm^{-1}$ in Table 8.1) has a mean hyperfine spacing of $-0.131cm^{-1}$ and a measured expectation value of $\langle J_z \rangle = -4.39cm^{-1}$ leading via Eq. 8.5 to

$$A_{expt}(^5I_7) = 0.0275cm^{-1} \tag{9.1}$$

There does not seem to be data available for the Γ_{34} level of interest, but having computed, in Table 8.1, $\langle J_z \rangle$ for the level we can deduce that the mean first order spacing is

$$E_{hfs_c} = 1.22A = 0.0335cm^{-1} \tag{9.2}$$

which is at the borderline of the Moscow groups resolution and explains why they do not report a value for this level. Nevertheless, we expect at this order to have an unresolved hfs pattern of eight lines and hence of a width of $0.23cm^{-1}$ which can be expected to be larger than the linewidth of the Γ_1 level which has no first-order hfs. The result of our first order calculation maybe portrayed in Fig. 9.1.

Notice that there are a total of 16 states associated with the Γ_{34} level and 8 with the Γ_1 level as expected for a nuclear spin of $I = 7/2$, the doubling in the Γ_{34} coming from the fact that Γ_{34} is two-fold degenerate before coupling with the nuclear angular momentum. To proceed further we must consider the crystal field eigenvectors for the two relevant Stark levels.

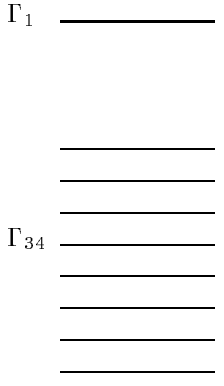

Fig. 9.1. Schematic of the first-order hfs splittings

■ 9.4 Crystal Field Eigenvectors

The second-order magnetic hyperfine calculation proceeds via Eq. (8.7). The eigenvectors are given on p78. However to a good approximation we may discard the imaginary coefficients for the two relevant eigenvectors and write

$$|\mu = 0\rangle = 0.8806|70\rangle - 0.4740|74\rangle_+ \tag{9.3a}$$

$$|\mu = 1\rangle = 0.8355|71\rangle - 0.4420|7-3\rangle - 0.2962|75\rangle + 0.1378|7-7\rangle \tag{9.3b}$$

Inspection of Eq. (8.6) shows that there are no non-zero off-diagonal matrix elements involving the $|7-7\rangle$ state.

■ 9.5 The Off-Diagonal Matrix Elements

Noting Eq. (8.6) and making explicit use of the eigenvectors given above we have

$$\begin{aligned}&\langle \mu = 0 I_z|\mathcal{H}_m|\mu = 1 I_z - 1\rangle \\ &= 0.8806 \times 0.8355\langle 70 I_z|\mathcal{H}_m|71 I_z - 1\rangle \\ &+ (0.4740 \times 0.4420\langle 7-4 I_z|\mathcal{H}_m|7-3 I_z - 1\rangle + 0.2962 \times 0.4740\langle 74 I_z|\mathcal{H}_m|75 I_z - 1\rangle/\sqrt{2}\end{aligned} \tag{9.4a}$$

and

$$\begin{aligned}&\langle \mu = 1 I_z|\mathcal{H}_m|\mu = 0 I_z + 1\rangle \\ &= 0.8806 \times 0.8355\langle 71 I_z|\mathcal{H}_m|70 I_z + 1\rangle \\ &+ (0.4740 \times 0.4420\langle 7-3 I_z|\mathcal{H}_m|7-4 I_z + 1\rangle + 0.2962 \times 0.4740\langle 75 I_z|\mathcal{H}_m|74 I_z + 1\rangle)/\sqrt{2}\end{aligned} \tag{9.4b}$$

The above is readily evaluated using the Maple file "hfs.cry" given below

```
#############################################################################
#This programme is for calculating the crystal field transformed magnetic #
#hyperfine matrix elements for the specific case given in lecture 9.      #
#hfsup calculates the matrix element <mu=1 I_z/H/mu=0 I_z + 1> while hfsdo#
#calculates the matrix element <mu=0 I_z/H/mu=1 I_z - 1>.                 #
#############################################################################
#############################################################################
#Programme to calculate the off-diagonal magnetic hyperfine matrix elements#
#as in Eq. (7.17) of the lecture notes. Ou for increasing J_z and Od for   #
#decreasing J_z.                                                           #
#############################################################################
Ou:=proc(J,Jz,I,Iz)
   local result;
   result:=combine(simplify(sqrt((J-Jz)*(J+Jz+1)*(I+Iz)*(I-Iz+1))
```

```
   /(2*sqrt(2))))*A;
end:
Od:=proc(J,Jz,I,Iz)
   local result;
   result:=combine(simplify(sqrt((J+Jz)*(J-Jz+1)*(I-Iz)*(I+Iz+1))
   /(2*sqrt(2))))*A;
end:
Digits:=5:
hfsup:=proc(Iz)
       local result;
result:=evalf(0.8806*0.8355*Od(7,1,7/2,Iz) + (0.4734*0.4420*Od(7,-3,7/2,Iz)
+ 0.2962*0.4740*Od(7,5,7/2,Iz))/sqrt(2));
end:
hfsdo:=proc(Iz)
       local result;
result:=evalf(0.8806*0.8355*Ou(7,0,7/2,Iz) + (0.4734*0.4420*Ou(7,-4,7/2,Iz)
+ 0.2962*0.4740*Ou(7,4,7/2,Iz))/sqrt(2));
end:
##############################################################################
```

Note that if the eigenvectors are real then it follows from Eq. (8.6) and (9.4) that for fixed J

$$\langle \mu = 0, I_z | \mathcal{H}_m | \mu = 1, I_z - 1 \rangle = \langle \mu = 1, I_z - 1 | \mathcal{H}_m | \mu = 0, I_z \rangle \tag{9.5a}$$

$$\langle \mu = 1, I_z | \mathcal{H}_m | \mu = 0, I_z + 1 \rangle = \langle \mu = 0, -I_z | \mathcal{H}_m | \mu = 1, -I_z - 1 \rangle \tag{9.5b}$$

Furthermore, the matrix elements will be zero unless

$$\mu + I_z = \mu' + I'_z \tag{9.6}$$

This is the crystal field analogue of the free ion restriction that

$$J_z + I_z = J'_z + I'_z \tag{9.7}$$

There are also the restrictions that

$$\Delta\mu = 0,\ \pm 1, \quad \Delta I_z = 0,\ \pm 1, \quad \Delta(\mu + I_z) = 0 \tag{9.8}$$

These various restrictions allow us to treat the case of Stark levels interacting via the magnetic hyperfine interaction without the need to construct large matrices or to resort to perturbation procedures.

■ 9.6 Some Group Theory

Our problem involves coupling the $I = 7/2$ angular momentum of the nucleus to the Γ_{34} and Γ_1 Stark levels. This will lead to pairs of irreducible representations that are complex conjugates and hence degenerate. We shall designate these as Γ_{56} and Γ_{78}. For $I = 7/2$ we obtain in S_4 symmetry the decomposition

$$[7/2] \Rightarrow 2\Gamma_{56} + 2\Gamma_{78} \tag{9.9}$$

Noting the Kronecker products

$$\Gamma_{34} \times (2\Gamma_{56} + 2\Gamma_{78}) = 4\Gamma_{56} + 4\Gamma_{78} \tag{9.10a}$$

$$\Gamma_1 \times (2\Gamma_{56} + 2\Gamma_{78}) = 2\Gamma_{56} + 2\Gamma_{78} \tag{9.10b}$$

$$\Gamma_2 \times (2\Gamma_{56} + 2\Gamma_{78}) = 2\Gamma_{56} + 2\Gamma_{78} \tag{9.10c}$$

which is consistent with the Γ_{34} Stark levels producing eight two-fold degenerate sub-levels and the Γ_1 and Γ_2 Stark levels each producing four two-fold degenerate sub-levels. This gives yet another method for distinguishing Γ_{34} Stark levels from those of Γ_1 and Γ_2 Stark levels.

■ 9.7 Some HFS Matrices

For the particular example we are pursuing the eigenvectors have been chosen as real and hence the hfs matrices are symmetric. There is one matrix for each value of $m = \mu + I_z$ with the matrices with $\pm m$ yielding the same eigenvalues and hence to calculate the hfs patterns it suffices to consider just the matrices associated with positive values of m. For the case under consideration this means three rank three matrices $m = 1/2,\ 3/2,\ 5/2$, a rank two matrix $m = 7/2$ and a rank one $m = 9/2$. These matrices can be expressed in terms of two parameters, Δ the energy separation of the two Stark levels and the magnetic hyperfine structure constant A. The matrices may be readily constructed using the Maple programme "hfs.cry" to give the matrices as

$$\begin{array}{lccc} m=1/2 & |0,1/2\rangle & |1,-1/2\rangle & |-1,3/2\rangle \\ \langle 0,1/2| & \Delta & 14.166A & 13.716A \\ \langle 1,-1/2| & 14.166A & -0.610A & 0 \\ \langle -1,3/2| & 13.716A & 0 & -1.830A \end{array} \qquad \begin{array}{lccc} m=3/2 & |0,3/2\rangle & |1,1/2\rangle & |-1,5/2\rangle \\ \langle 0,3/2| & \Delta & 13.716A & 12.268A \\ \langle 1,1/2| & 13.716A & 0.610A & 0 \\ \langle -1,5/2| & 12.268A & 0 & -3.050A \end{array}$$

$$\begin{array}{lccc} m=5/2 & |0,5/2\rangle & |1,3/2\rangle & |-1,7/2\rangle \\ \langle 0,5/2| & \Delta & 12.268A & 9.3697A \\ \langle 1,3/2| & 12.268A & 1.830A & 0 \\ \langle -1,7/2| & 9.3697A & 0 & -4.270A \end{array} \qquad \begin{array}{lcc} m=7/2 & |0,7/2\rangle & |1,5/2\rangle \\ \langle 0,7/2| & \Delta & 9.3697A \\ \langle 1,5/2| & 9.3697A & 3.050A \end{array} \qquad \begin{array}{lc} m=9/2 & |1,7/2\rangle \\ \langle 1,7/2| & (\,4.270A\,) \end{array}$$

Notice that in this case the off-diagonal hyperfine interaction matrix elements are significantly larger than those on the diagonal. This is partly associated with the expectation value $\langle J_z \rangle$ being of the order of unity. Unfortunately this hfs pattern has not been established experimentally, it probably being beyond the resolution currently available.

■ 9.8 Diagonalization of the HFS Matrices and Mixing

It is instructive to diagonalise the matrices for several values of Δ, the Stark level separation. In the first case we consider a value of $\Delta = 10cm^{-1}$ to obtain the following results

```
                Value chosen for Delta =  10
Value chosen for the Magnetic hfs constant A = .0275
                  Energy matrix for m = 1/2
                 10      .38956     .37718
                .38956  -.016775       0
                .37718       0     -.050325
                  Eigenvalues for m = 1/2
                [ -.070064, -.026497, 10.032 ]
                  Eigenvectors for m = 1/2
                .048787  -.022727    .99863
               -.35842     .93280    .03874
               -.93239    -.35976    .03736
```

```
Energy matrix for m = 3/2
10      .37718    .33737
.37718 .016775       0
.33737  0       -.08387
 Eigenvalues for m = 3/2
[ -.096699, .0043920, 10.025 ]
 Eigenvectors for m = 3/2
-.037817  .033135   .99872
 .12538  -.99138    .03764
 .99137   .12664    .03333
Energy matrix for m = 5/2
 10      .33737   .25767
 .33737 .05033    0
 .25767   0     -.11743
 Eigenvalues for m = 5/2
[ -.12446, .040016, 10.019 ]
 Eigenvectors for m = 5/2
-.027151  .03247   .99917
 .052261 -.99807   .03385
 .99832   .05313   .02542
Energy matrix for m = 7/2
      10     .25767
      .25767 .08388
 Eigenvalues for m = 7/2
    [ .0774, 10.007 ]
 Eigenvectors for m = 7/2
  .025959   -.99967
 -.99967    -.02596
 Eigenvalue for m = 9/2
    [ .11743 ]
 Eigenvector for m = 9/2
       1
```

Notice that even with a Stark level separation there are small admixtures of the $\mu = 0$ and $\mu = \pm 1$ states. The $\mu = 0$ level has acquired a small splitting into four sublevels (total width $0.025 cm^{-1}$ but quite beyond current resolution possibilities.

Let us now repeat the exercise but this time with the separation of the two Stark levels of $1 cm^{-1}$ to give the results now as

```
Value chosen for Delta = 1
Value chosen for the Magnetic hfs constant A = .0275
Energy matrix for m = 1/2
 1      .38956    .37718
.38956 -.01678      0
.37718     0     -.05033
```

```
  Eigenvalues for m = 1/2
[ -.26638, -.03310, 1.2326 ]
  Eigenvectors for m = 1/2
 .39272  .030852  .91918
-.61293  -.73630  .28662
-.68563   .67597  .27028
 Energy matrix for m = 3/2
  1     .37718   .33737
 .37718 .01678      0
 .33737     0   -.083876
  Eigenvalues for m = 3/2
[ -.24562, -.029050, 1.2078 ]
  Eigenvectors for m = 3/2
-.36718  .09685  .92503
 .52781 -.79725  .29295
 .76587  .59587  .24160
 Energy matrix for m = 5/2
   1     .33737   .25767
 .33737  .05033     0
 .25767     0    -.11743
  Eigenvalues for m = 5/2
[ -.20489, -.017401, 1.1552 ]
  Eigenvectors for m = 5/2
 .29588  -.17551  .93895
-.39111   .87457  .28669
-.87150  -.45209  .19012
 Energy matrix for m = 7/2
     1     .25767
   .25767  .08388
  Eigenvalues for m = 7/2
     [ .0164, 1.0675 ]
  Eigenvectors for m = 7/2
     .25341  -.96738
    -.96738  -.25341
  Eigenvalue for m = 9/2
      [ .11743 ]
  Eigenvector for m = 9/2
             1
```

Notice that modest mixing of the $\mu = 0$ and $\mu = \pm 1$ has occurred and that the total width of the sublevels of the $\mu = 0$ has increased to $0.165 cm^{-1}$ but the sublevel spacing is still beyond current resolution. Finally we give the case for a Stark level spacing of of just $0.2 cm^{-1}$

```
                Value chosen for Delta =  .2
Value chosen for the Magnetic hfs constant A = .0275
                 Energy matrix for m = 1/2
                 .2       .38956    .37718
                 .38956 -.01678       0
                 .37718       0    -.05033
                  Eigenvalues for m = 1/2
                [ -.47151, -.03378, .63835 ]
                  Eigenvectors for m = 1/2
                 .62798   .03094   .77768
                -.53795 -.70485   .46251
                -.56240   .70881   .42596
                 Energy matrix for m = 3/2
                 .2      .37718    .33737
                 .37718 .01678       0
                 .33737      0    -.08388
                  Eigenvalues for m = 3/2
                [ -.43654, -.03689, .60624 ]
                  Eigenvectors for m = 3/2
                 .61928   .09903   .77881
                -.51529 -.69717   .49831
                -.59241   .70990   .38072
                 Energy matrix for m = 5/2
                  .2      .33737    .25767
                  .33737 .05033      0
                  .25767      0     -.11743
                  Eigenvalues for m = 5/2
                [ -.35684, -.04622, .53599 ]
                  Eigenvectors for m = 5/2
                 .59290    .19501   .78131
                -.49124   -.68122   .54280
                -.63806    .70562   .30811
                 Energy matrix for m = 7/2
                     .2      .25767
                     .25767 .08388
                  Eigenvalues for m = 7/2
                    [ -.12221, .40605 ]
                  Eigenvectors for m = 7/2
                     .62453   -.78099
                    -.78099   -.62453
                  Eigenvalue for m = 9/2
                    [ .11743 ]
                  Eigenvector for m = 9/2
```

1

Now there is considerable mixing of the two Stark levels as indicated by the size of the eigenvector components. Only the $m = 9/2$ sublevel remains uncontaminated.

■ 9.9 Concluding remarks on HFS

The above exercise allows us to reach several conclusions regarding magnetic hyperfine structure in crystals. It is apparent that if the relevant Stark levels are well separated, say $> 10cm^{-1}$ then a first-order calculation suffices but for closely spaced Stark levels it is imperative to include the off-diagonal matrix elements of the magnetic hyperfine interaction and these will lead to mixing and considerable distortion of the first-order hyperfine patterns. Simple calculation of the quantity $\langle J_z \rangle (2 - g_{ic})A$ suffices to indicate, to a good approximation, the width of a hyperfine pattern and to establish its resolvability. Note we have as yet made no inclusion of electric-quadrupole hyperfine interaction and we should remember that ^{165}Ho does possess an electric-quadrupole moment.

■ 9.10 A Strategy for HFS Calculations

Throughout this course my emphasis has been on getting results by as simple and direct approach as possible. An improved strategy would be to do a complete "free ion" + Crystal Field calculation so as to give a complete account of $J-$mixing and intermediate coupling and then to use the resulting eigenvectors to calculate the hyperfine matrix elements as above. Note that we have not given the relevant formulae for the case of $J-$mixing but these follow trivially using the results of Lecture 3. Another problem untouched here is the *ab initio* calculation of the hyperfine structure constant A using the measured nuclear magnetic moment (directly measured by atomic beams rather than indirectly from analysis of hyperfine structure) and then a model for $\langle r^{-3} \rangle$. We have also ignored the effects of relativity. These will changed the values of the radial integrals for $\langle r^{-3} \rangle$ and lead to additional angular dependent terms. These corrections are likely to be small compared with approximations already made.

■ Appendix

Attached below is the Maple code used to calculate the diagonalisation results given above.

```
with(linalg):
read`hfs.cry`:
D:=.2:
A:=0.0275:
Digits:=5:
m1:=proc()
    local r1,S,result1;
    S:=array(sparse,1..3,1..3);
    r1:=array(symmetric,1..3,1..3);
    r1:=copyinto(S,r1,1,1);
    r1[1,1]:=D;
    r1[1,2]:=hfsdo(1/2);
    r1[1,3]:=hfsup(1/2);
    r1[2,2]:=1.22*(-.5)*A;
    r1[3,3]:=1.22*(-1.5)*A;
    result1:=r1;
    end:
m3:=proc()
    local r3,S,result3;
    S:=array(sparse,1..3,1..3);
    r3:=array(symmetric,1..3,1..3);
    copyinto(S,r3,1,1);
```

```
    r3[1,1]:=D;
    r3[1,2]:=hfsdo(3/2);
    r3[1,3]:=hfsup(3/2);
    r3[2,2]:=1.22*(.5)*A;
    r3[3,3]:=1.22*(-2.5)*A;
    result3:=r3;
    end:
m5:=proc()
    local r5,S,result5;
    S:=array(sparse,1..3,1..3);
    r5:=array(symmetric,1..3,1..3);
    copyinto(S,r5,1,1);
    r5[1,1]:=D;
    r5[1,2]:=hfsdo(5/2);
    r5[1,3]:=hfsup(5/2);
    r5[2,2]:=1.22*(1.5)*A;
    r5[3,3]:=1.22*(-3.5)*A;
    result5:=r5;
    end:
m7:=proc()
    local r7,S,result7;
    S:=array(sparse,1..2,1..2);
    r7:=array(symmetric,1..2,1..2);
    copyinto(S,r7,1,1);
    r7[1,1]:=D;
    r7[1,2]:=hfsdo(7/2);
    r7[2,2]:=1.22*(2.5)*A;
    result7:=r7;
    end:
m9:=proc()
    local result9;
    result9:=1.22*3.5*A;
    end:
print(`Value chosen for Delta = `,D);
print(`Value chosen for the Magnetic hfs constant A = `,A);
e1:=m1():
print(`Energy matrix for m = 1/2`);
print(e1);
print(`Eigenvalues for m = 1/2`);
evalf(Eigenvals(e1,V1));
print(`Eigenvectors for m = 1/2`);
print(V1);
e3:=m3():
```

```
print(‘Energy matrix for m = 3/2‘);
print(e3);
print(‘Eigenvalues for m = 3/2‘);
evalf(Eigenvals(e3,V3));
print(‘Eigenvectors for m = 3/2‘);
print(V3);
e5:=m5():
print(‘Energy matrix for m = 5/2‘);
print(e5);
print(‘Eigenvalues for m = 5/2‘);
evalf(Eigenvals(e5,V5));
print(‘Eigenvectors for m = 5/2‘);
print(V5);
e7:=m7():
print(‘Energy matrix for m = 7/2‘);
print(e7);
print(‘Eigenvalues for m = 7/2‘);
evalf(Eigenvals(e7,V7));
print(‘Eigenvectors for m = 7/2‘);
print(V7);
e9:=m9():
print(‘Eigenvalue for m = 9/2‘);
print(e9);
print(‘Eigenvector for m = 9/2‘);
print(‘1‘);
```

■ **The Groundstate of** $liYF_4 : Ho^{3+}$

As a final calculation we give the groundstate eigenvalues and eigenvectors for of $LiYF_4 : Ho^{3+}$ with no attempt to optimise the parameters. It will be noted that in this case there is very little mixing of the Stark crystal field levels.

```
                        Value chosen for Delta = , 6.85
              Value chosen for the Magnetic hfs constant A = , .0279
                           Energy matrix for m = 1/2
                6.85          .027014 - .17167 I   .026156 + .16622
           .027014 - .17167 I         .075609                0
           .026156 + .16622 I            0                .22683
                           Eigenvalues for m = 1/2
                        [ 6.8417 , .079724, .23103 ]
                           Eigenvectors for m = 1/2
    .99933                .02390 + .0073 I       .01255 - .02295 I
    .00399 - .02535 I     .13155 - .99183 I    - .02297 - .01798 I
    .00395 + .02511 I     .00429 - .02817 I      .79818 + .60334 I
```

```
                    Energy matrix for m = 3/2
          6.85          .026156 - .16622 I   .023394 + .14867 I
         .026156 - .16622 I       -.075609                0
         .023394 + .14867 I           0                .37805
                    Eigenvalues for m = 3/2
                 [ 6.8429 ,  - .071742 , .38141 ]
                    Eigenvectors for m = 3/2
.99943 - .0001 I    - .02304 - .00727 I     .01121 - .02065 I
.00378 - .0240 I    - .14686 + .99003 I   - .00687 - .00529 I
.00362 + .0230 I    - .00123 + .00797 I     .79639 + .60602 I
                    Energy matrix for m = 5/2
          6.85          .023394 - .14867 I   .017869 + .11355 I
         .02339 - .14867 I    -.22683                0
         .01787 + .11355 I          0        .52926
                    Eigenvalues for m = 5/2
                 [ 6.8450,  - .22377, .53125  ]
                    Eigenvectors for m = 5/2
 .99960 - .00016 I    - .02018 - .00660 I      .00874 - .01606 I
 .00330 - .02101 I    - .15873 + .98803 I    - .00291 - .00224 I
 .00283 + .01797 I    - .00052 + .00320 I      .79456 + .60805 I
                    Energy matrix for m = 7/2
                   6.85          .017869 - .11355 I
                  .017869 - .11355 I        -.37805
                    Eigenvalues for m = 7/2
                 [ 6.8483,  - .37630 ]
                    Eigenvectors for m = 7/2
          .99988 - .00008 I    .00489 - .01514 I
          .00247 - .01571 I  - .98817 - .15566 I
                     Eigenvalue for m = 9/2
                            -.52926
                    Eigenvector for m = 9/2
                              1
```

FINIS

Tomorrow is not an extrapolation of today